VNIVERSITAT DE VALÈNCIA

Facultad de Medicina y Odontología

Departamento de Medicina

Programa de doctorado: 3139 Medicina

Estudio de la deformidad del tejido cardiaco (*strain*) tras un infarto de miocardio con elevación del segmento ST mediante la técnica de resonancia magnética *tissue tracking*: dinámica, implicación estructural y valor pronóstico

Tesis Doctoral presentada por:

Josep Gavara Doñate

Dirigida por:

Dr. Vicente Bodí Peris

Dr. José Vicente Monmeneu Menadas

Valencia, Julio 2020

UNIVERSITAT DE VALÈNCIA

FACULTAT DE MEDICINA I ODONTOLOGIA

DEPARTAMENT DE MEDICINA

Dr. Vicente Bodí Peris, Catedrático de la Universitat de València y Jefe de la Sección de Hospitalización de la Sala de Cardiología del Hospital Clínico Universitario de Valencia.

Dr. José Vicente Monmeneu Menadas, Cardiólogo Especialista en Exploraciones Radiológicas Especiales S.A. ERESA en la Unidad de Resonancia Magnética Cardiaca del Hospital Clínico Universitario de Valencia.

CERTIFICAN:

Que la presente Tesis Doctoral titulada “Estudio de la deformidad del tejido cardiaco (*strain*) tras un infarto de miocardio con elevación del segmento ST mediante la técnica de resonancia magnética *tissue tracking*: dinámica, implicación estructural y valor pronóstico”, presentada por el Licenciado en Ingeniería de Telecomunicaciones **Josep Gavara Doñate**, ha sido realizada bajo nuestra dirección en el Departamento de Medicina de la Facultad de Medicina y Odontología de la Universitat de València.

Concluido el trabajo experimental y bibliográfico, autorizamos la presentación y defensa de esta Tesis Doctoral.

Para que así conste a los efectos oportunos, se expide la presente certificación en Valencia, a 19 de Junio de 2020.

Dr. Vicente Bodí Peris

Dr. José Vicente Monmeneu Menadas

If you want to go fast, go alone;

If you want to go far, go together

African Proverb

Agradecimientos

En primer lugar, me gustaría agradecerles a mis directores la posibilidad que me han dado para realizar esta tesis. A Vicente por introducirme en el mundo de la investigación y enseñarme que todo aquello que no se ha demostrado es susceptible de ser investigado, gracias por iniciarme en el mundo de la estadística, un mundo totalmente desconocido para mí, que tantos dolores de cabeza nos ha dado en estos últimos años pero que con constancia siempre hemos podido superar. A Jose Vicente por descubrirme el mundo de la resonancia magnética cardiaca, tu enorme conocimiento de este campo y tu facilidad para transmitir estos conocimientos siempre en un ambiente coloquial y agradable me han ayudado, sin duda, a que hoy pueda estar presentando esta tesis.

A mis compañeros del Hospital. Gracias Clara y Paolo por hacer que todo sea tan fácil y por todos esos momentos que hemos compartido.

A mis compañeros de laboratorio. A Nere y Elena, gracias por estar siempre dispuestas a ayudar con una sonrisa y por todos esos momentos que hemos compartido durante estos años. A Arantxa, por transmitirnos esa alegría que te caracteriza durante esos años que hemos podido compartir, no cambies nunca.

Gracias César, por convertirte en un pilar para mí, fuiste el último en llegar, pero te has convertido en un gran amigo y mejor compañero. Eres esa persona en la que siempre se puede confiar y que ameniza como nadie los días de duro trabajo.

A mi familia y amigos por convertirme en la persona que soy, no podría haberme rodeado de mejor compañía.

A mis padres, por ser el mejor ejemplo a seguir que se pueden tener, no puedo imaginarme un ambiente mejor en el que criarme que junto

a vosotros. Gracias por haber confiado siempre en mí, esa confianza ha sido la que me ha hecho llegar hasta aquí, sé que siempre podré confiar en vosotros.

A David, nunca podré agradecerte lo suficiente que desde pequeño hayas sido mi protector y disfrutar contigo toda una vida de momentos.

Por último, Mer… como olvidarme de ti, apareciste en mi vida durante la universidad y con la primera sonrisa me conquistaste. Durante estos años te has convertido en la persona más importante para mí, mi mujer y mi mejor amiga, juntos formamos un equipo imparable. Gracias por transmitirme tu alegría, tu risa contagiosa, tu cariño y tu apoyo incondicional durante estos años, siempre optimista, y gracias por los momentos que nos quedan por compartir.

ÍNDICE

ABREVIATURAS

ACD: Arteria coronaria derecha

ACTP: Angioplastia coronaria transluminal percutánea

ACX: Arteria circunfleja

ADA: Arteria descendente anterior

CS: *Circumferential strain*

ECVA: Eventos cardiovasculares adversos

FEVI: Fracción de eyección del ventrículo izquierdo

HR [IC 95%]: *Hazard ratio* [Intervalo de confianza del 95%]

IAMEST: Infarto agudo de miocardio con elevación del segmento ST

LS: *Longitudinal strain*

MRNI: Miocardio remoto no infartado

RAVI: Remodelado adverso del ventrículo izquierdo

RMC: Resonancia magnética cardíaca

RS: *Radial strain*

STIR: *Short time inversion recovery*

TIMI: *Thrombolysis in Myocardial Infarction*

TT: *Tissue tracking*

VI: Ventrículo izquierdo

VTDVI: Volumen telediastólico del ventrículo izquierdo

LISTA DE FIGURAS

LISTA DE TABLAS

ABSTRACT

The main objective of the present thesis was to evaluate the characterization, dynamics, and prognostic value of strain by tissue tracking (TT) cardiac magnetic resonance (CMR) after ST-segment elevation myocardial infarction (STEMI).

In last decade, CMR became the gold-standard technique for the study and characterization of cardiac tissue after STEMI. In recent years, TT has emerged as a novel CMR imaging technique that allows quantitative evaluation of deformation in all areas of the myocardium.

Although some studies performed in echocardiography explain the clinical relevance of strain, this is a relatively new technique. The clinical application of which is still under investigation. For this reason, given the lack of studies aimed at evaluating the risk reclassification of TT-CMR in STEMI patients, this was the main objective of this work.

In the first article, we evaluated the prognostic value of the three global strain indices (longitudinal strain [LS], circumferential strain [CS], and radial strain) in 323 patients after STEMI. TT-CMR provides systolic function information. The major adverse cardiovascular events (MACE) included were cardiovascular death, heart failure, and/or re-infarct. Global LS has emerged as the most powerful strain index for the risk stratification of MACE, showing a predictive value similar to traditional CMR indices such as the left ventricular ejection fraction (LVEF), infarct size, or microvascular obstruction. When these data were confirmed in an external validation cohort of 190 STEMI patients from a second University Hospital, although the predictive value of global LS was also demonstrated, it did not improve the risk stratification of traditional CMR indices.

In the second article, we focused on the association between strain and left ventricular adverse remodeling (LVAR) following STEMI. A combined registry made up of 374 STEMI patients from the

two University Hospitals was utilized. Firstly, we studied the prognostic value of strain in a combined MACE including events commonly associated with LVAR (cardiovascular death, heart failure and/or ventricular arrhythmias). Cardiac hypertrophy is an initially effective response to the overload of the myocardial tissue due to the loss of cardiomyocytes in the infarcted area leading to heart failure and ventricular arrhythmias. Both global LS and global CS presented a high association with these adverse events.

As a second objective, we hypothesized whether the combination of strain and left ventricular end-diastolic volume index (LVEDV) form the best definition of LVAR to predict MACE. LVAR usually causes an increase in LVEDV and, consequently, worse contractility and/or deformation. Global LS and CS presented more altered values in patients with LVAR (relative increase of LVEDV>15% from 1 week to 6 months). However, after evaluating relative differences between patients with and without MACE, only LVEF showed significant differences between both groups. Therefore, strain indices did not provide additional information to LVEDV for identifying LVAR and its association with this MACE. The new LVAR definition was obtained for the relative changes in both LVEDV and LVEF. It was observed that the remodeling index that best predicted MACE was a relative increase of more than 15% in VTDVI and a relative decrease of more than 3% in LVEF. However, this new definition of LVAR does not increase the prognostic value of strain and/or traditional CMR indexes in acute phase.

In the third article, we studied the characterization, dynamics, and structural and prognostic implications of LS in the different areas of myocardium (remote non-infarcted myocardium [RNM] and infarct area) in 271 STEMI patients. Since LS index has previously been demonstrated to be independently associated with patient prognosis,

only LS was exhaustively evaluated in both RNM and infarct area. In RNM, even though LS was affected in the acute phase after STEMI, this index tended to recover to normal values in chronic phase, causing a spontaneous recovery of LVEF. Altered RNM-LS was associated with more structural damage in acute and chronic phases. Furthermore, RNM-LS was an independent predictor of MACE (death, heart failure or re-infarction) after adjustment by clinical and traditional CMR indices and those patients with altered RNM-LS soon after STEMI had a greater probability of MACE.

Similarly, infarct area was also studied. Altered infarct-LS was detected in 75% of patients and 65% of infarcted segments. Although patients with altered infarct-LS displayed a higher probability of MACE, infarct-LS was not independently associated with MACE after adjusting for the rest of the clinical and CMR indices.

Therefore, RNM-LS was more decisive than infarct-LS in predicting MACE since RNM represents a larger portion than the infarcted area. Consequently, changes in this area would have a greater impact on systolic function. Furthermore, the fact that RNM supports a greater workload after STEMI due to cardiomyocytes loss in the infarcted region also seems to be decisive in having a more direct impact on recovery of function.

RESUMEN

El presente trabajo, que se dividió en tres partes, ha sido destinado al estudio de la deformación del tejido cardiaco (*strain*) mediante resonancia magnética cardiaca (RMC) tras un infarto agudo de miocardio con elevación del segmento ST (IAMEST). Para ello se realizó un estudio de la caracterización, dinámica, implicación estructural y valor pronóstico de los diferentes índices de *strain* derivados de la RMC.

La RMC se ha convertido en la última década en la técnica *gold-standard* para el estudio y la caracterización del tejido cardiaco después de sufrir un IAMEST. Durante los últimos años, el *tissue tracking* (TT) ha emergido cómo una técnica de imagen que permite evaluar de forma cuantitativa la deformación en todas las zonas del miocardio.

Aunque ya existían numerosos estudios en ecocardiografía sobre la importancia clínica del *strain*, se trata de una técnica relativamente novedosa, por lo que todavía se está investigando su utilidad. Es por ello, que frente a la falta de estudios destinados a evaluar la utilidad pronóstica del TT-RMC en pacientes IAMEST nos marcamos como primer objetivo estudiar su valor pronóstico.

En el primer artículo, decidimos evaluar el valor pronóstico de los diferentes índices de *strain* globales (*longitudinal strain* [LS], *circumferential strain* [CS] y *radial strain*) en 323 pacientes en la fase aguda tras un IAMEST. Estos índices globales, que tienen en cuenta la contractilidad del ventrículo izquierdo, aportan información sobre la función sistólica del corazón. Para ello, decidimos centrar el estudio en un evento combinado que recoge los principales eventos cardiovasculares adversos (ECVA: muerte cardiovascular, hospitalización por insuficiencia cardiaca y/o reinfarto). Frente a este evento combinado el LS global surgió como el índice de deformación

más potente, de los tres estudiados, para la estratificación de riesgo de ECVA, mostrando un valor predictivo a la altura de índices ya consolidados de RMC como la fracción de eyección del ventrículo izquierdo (FEVI), el tamaño de infarto o la obstrucción microvascular. Además, estos resultados fueron confirmados mediante una cohorte de validación externa de 190 pacientes IAMEST de un segundo Hospital Universitario. Aunque quedó demostrado el importante valor pronóstico de este novedoso índice, éste no mejoró significativamente el valor pronóstico de los índices ya establecidos de la RMC.

En el segundo artículo, pusimos el foco en estudiar la relación entre el *strain* y el remodelado adverso del ventrículo izquierdo (RAVI). Se empleó un registro combinado formado por 374 pacientes IAMEST de los dos Hospitales Universitarios involucrados en el anterior trabajo. Para ello, en primero lugar estudiamos el valor pronóstico del *strain* frente a un evento asociado comúnmente al RAVI tras un IAMEST. La hipertrofia cardiaca es una respuesta inicialmente eficaz a la sobrecarga de trabajo del músculo cardíaco debido a la pérdida de cardiomiocitos en la zona infartada, que puede acabar convirtiéndose en un problema, dificultando la función del corazón y causando insuficiencia cardiaca y arritmias ventriculares. Es por ello, que en este caso se decidió estudiar el papel del *strain* para la predicción del ECVA compuesto por la muerte cardiovascular, la hospitalización por insuficiencia cardiaca y/o las arritmias ventriculares. Tanto el LS global como el CS global presentaron una alta asociación con este ECVA.

Como segundo objetivo de este trabajo nos marcamos estudiar si el *strain* junto con el volumen telediastólico del ventrículo izquierdo (VTDVI) forman la mejor definición de RAVI para la predicción de ECVA. El remodelado ventricular provoca habitualmente un aumento del VTDVI y, por consiguiente, una peor contractilidad y/o

deformación. Pudimos observar que tanto el LS global como el CS global presentaban valores más alterados en los pacientes con un incremento relativo en el VTDVI>15% que en los que no presentaban esta dilatación tras 6 meses de seguimiento. Sin embargo, tras evaluar las diferencias relativas entre los pacientes con y sin ECVA de todos los índices de RMC que habían sido asociados en el análisis univariado con ECVA, únicamente la FEVI presentó diferencias significativas entre ambos grupos. Por tanto, ningún índice de *strain* (LS y CS globales) aportó cambios lo suficientemente significativos que permitieran identificar el RAVI y asociarlos con este ECVA, como si fue el caso de la FEVI. Debido a que estábamos buscando la definición de RAVI que mejor predijera los ECVA y este se encuentra estrechamente ligado al VTDVI, se obtuvo esta nueva definición de RAVI de los cambios relativos tanto en VTDVI como en la FEVI. Se observó que el índice de remodelado que mejor predice los ECVA era aquel caracterizado por un aumento superior al 15% del VTDVI y una disminución mayor del 3% de la FEVI. Sin embargo, esta nueva definición de RAVI no fue capaz de superar el valor pronóstico del *strain* ni de los índices tradicionales obtenidos mediante RMC en fase aguda.

Por último, y puesto que el papel exacto del *strain* sigue siendo incierto, en el tercer artículo decidimos estudiar la caracterización, la dinámica y las implicaciones estructurales y pronósticas del LS en las diferentes áreas del miocardio (en el miocardio remoto no infartado [MRNI] y en el área del infarto) en 271 pacientes con IAMEST, aunque pusimos el foco de la investigación en el área del MRNI. Se decidió estudiar únicamente el LS por ser el índice con más valor pronóstico. En este estudio, se pudo comprobar cómo el MRNI, que se encontraba alterado en una gran parte de los pacientes tras un IAMEST (48%), tendía a su recuperación de manera espontánea

hasta valores normales de LS-MRNI tras alcanzar la fase crónica, teniendo un efecto decisivo en la recuperación de la FEVI. Una alteración de LS-MRNI se asoció a un mayor daño estructural tanto en fase aguda como en fase crónica (volúmenes más dilatados, FEVI más deprimida, mayor tamaño de infarto). Además, el LS-MRNI se asoció de manera significativa e independiente con ECVA tras ajustarse por las variables clínicas y los índices de RMC tradicionales, mostrando que aquellos pacientes que presentaban una alteración del LS-MRNI en la fase aguda presentaban una mayor probabilidad de sufrir ECVA.

De manera similar se estudió el área infartada. Esta zona, como era de prever se encontraba más alterada que el MRNI. El 75% de los pacientes presentaron el LS-infarto alterado y el 65% de los segmentos de esta área se encontraba con valores alterados. Aunque, los pacientes con el LS-infarto alterado presentaron una mayor probabilidad de ECVA, el LS-infarto no resultó significativamente independiente tras ajustarlo por el resto de las variables clínicas y de RMC como sí lo fue el LS-MRNI.

El hecho de que la afectación del LS-MRNI sea más determinante que la afectación del LS-infarto puede ser debido principalmente a su extensión: el MRNI representa una porción más grande que el área infartada y, por tanto, una alteración de esta zona tan extensa repercutiría en mayor medida en la función sistólica. Además, el hecho de que esta zona tras el IAMEST debe de soportar una mayor carga de trabajo debido a la pérdida de cardiomiocitos en la zona infartada parece también ser determinante para que su afectación repercuta de manera más directa en la recuperación de la función.

I.- INTRODUCCIÓN

1. Enfermedades cardiovasculares

Según la Organización Mundial de la Salud, las enfermedades cardiovasculares constituyen la principal causa de muerte en el mundo. Millones de personas mueren cada año debido a enfermedades derivadas de la salud del corazón (*Atlas, 2014*).

El síndrome coronario agudo, y más concretamente, el infarto agudo de miocardio con elevación del segmento ST (IAMEST), es una de las principales causas de morbilidad y mortalidad de nuestro entorno. El aumento de la esperanza de vida hace prever que esta tendencia será más acusada en los próximos años (*OMS, 2014; TIMI Study Group, Engl J Med 1985*).

El infarto agudo de miocardio se produce principalmente debido a la aterosclerosis coronaria y, por lo general, por trombosis coronaria añadida (*Boersma et al. Lancet 2003; Aguilar et al. Revista Paceña Medicina Familiar 2008*). El electrocardiograma es una pieza clave para identificar la gravedad del proceso isquémico. Dado que en el electrocardiograma se registran varias derivaciones que corresponden a la actividad eléctrica del corazón permite conocer de forma rápida cuál es el segmento del corazón afectado por el infarto e inferir cuál de las arterias coronarias se ha ocluido bruscamente y ha provocado el evento isquémico. La elevación del segmento ST se produce debido a la oclusión permanente de la arteria coronaria (*Lorenzo. Rev Urug Cardiol 2013*).

2 El IAMEST

2.1 Fisiopatología

La ateroesclerosis es una afección que se presenta mayoritariamente en personas de edad avanzada debido a una acumulación de grasa, colesterol y células inflamatorias en las

paredes de las arterias. Esta acumulación en las paredes de las arterias se conoce comúnmente como placas de ateroma. Con el tiempo, estas placas pueden crecer y endurecerse haciendo que se reduzca la luz de las arterias y limitando la cantidad de sangre que llega al miocardio. Esta disminución del volumen de sangre puede provocar que los nutrientes y el oxígeno que alcanzan el miocardio sea insuficiente, hecho que provoca la aparición de isquemia (Figura 1) (*Hansson et al. Nat Rev Immunol 2006; van 't Hof et al. Circulation 1998*).

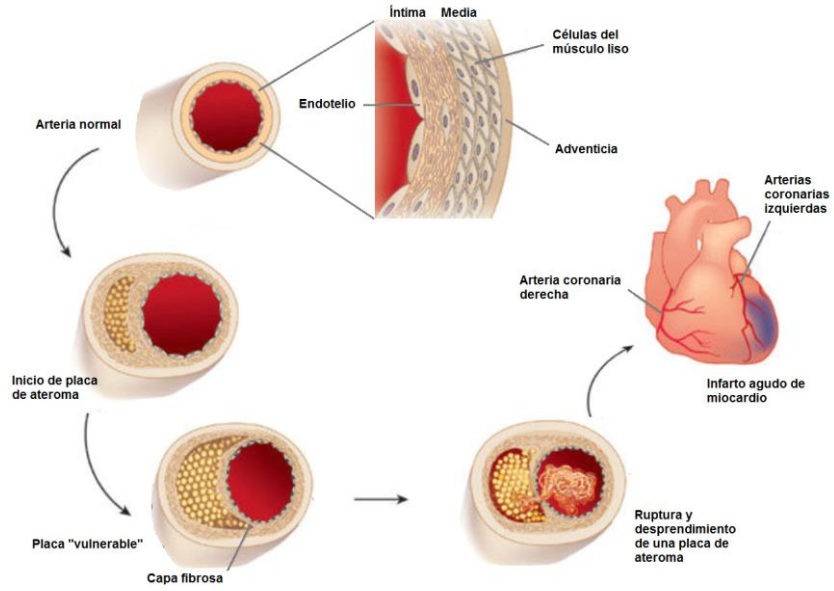

Figura 1. Etiología del síndrome isquémico agudo. Adaptado de *Libby. Nature 2002*.

El IAMEST se produce por la oclusión trombótica de una arteria coronaria epicárdica debido al desprendimiento de una de estas placas de ateroma. La falta de riego sanguíneo provoca una falta de oxígeno y de nutrientes que conduce a una situación de isquemia que

puede desencadenar en una necrosis del miocardio irrigado por dicha arteria (*Boersma et al. Lancet 2003; Aguilar et al. Revista Paceña Medicina Familiar 2008*).

2.2 Tratamiento del IAMEST

Según las guías clínicas, tras la oclusión trombótica de una arteria coronaria, la principal terapia es restablecer cuanto antes el flujo sanguíneo y así evitar la isquemia y la correspondiente muerte celular. Para ello existen tanto procedimientos farmacológicos como mecánicos que permiten restablecer de manera correcta el riego sanguíneo (Figura 2) (*Ibáñez et al. J Am Coll Cardiol 2015, Niccoli et al. Eur Heart J 2016*).

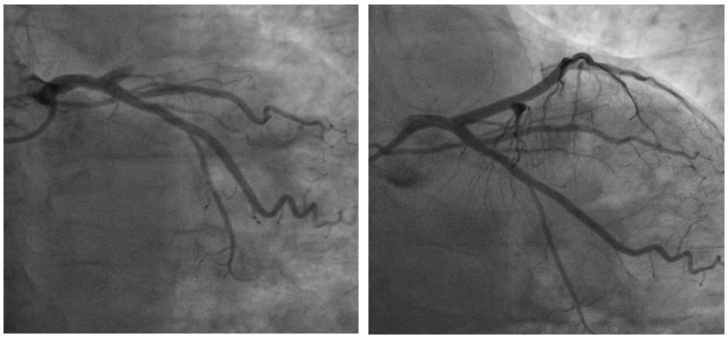

Figura 2. Coronariografía de un paciente con una arteria ocluida (**izquierda**) y reperfundida (**derecha**) después de practicar una angioplastia coronaria transluminal percutánea.

La angioplastia coronaria transluminal percutánea (ACTP) se ha convertido en los últimos años en la técnica de elección para la apertura de la arteria ocluida. La ACTP es un procedimiento mecánico mediante el cual se accede a la lesión con un catéter. El inflado de un balón de angiografía permite la apertura de la arteria ocluida (*TIMI Study Group. N Engl J Med 1985; Weaver et al. JAMA 1997; GUSTO investigators. N Engl J Med 1993*).

2.3 Fibrosis miocárdica

Tras un IAMEST es inevitable, en la mayoría de los casos, que se produzca una muerte de cardiomiocitos debido al tiempo de hipoxia al que han sido sometidos hasta la revascularización.

La fibrosis miocárdica es una entidad patológica del remodelado de la matriz extracelular y aparece tan pronto como la integridad de los miocitos se ve afectada (*Karamitsos et al. J Am Coll Cardiol 2009; Mahrholdt et al. Eur Heart J 2005; Karamitsos et al. J Cardiovasc Magn Reson 2007*).

El miofibroblasto tiene una posición central en este proceso mediante el aumento de la producción de colágeno y otros componentes de la matriz extracelular bajo la influencia de diversos factores (sistema renina-angiotensina, la apoptosis de los miocitos, las citoquinas proinflamatorias, especies reactivas de oxígeno) (Figura 3) (*Mewton et al. J Am Coll Cardiol 2011*).

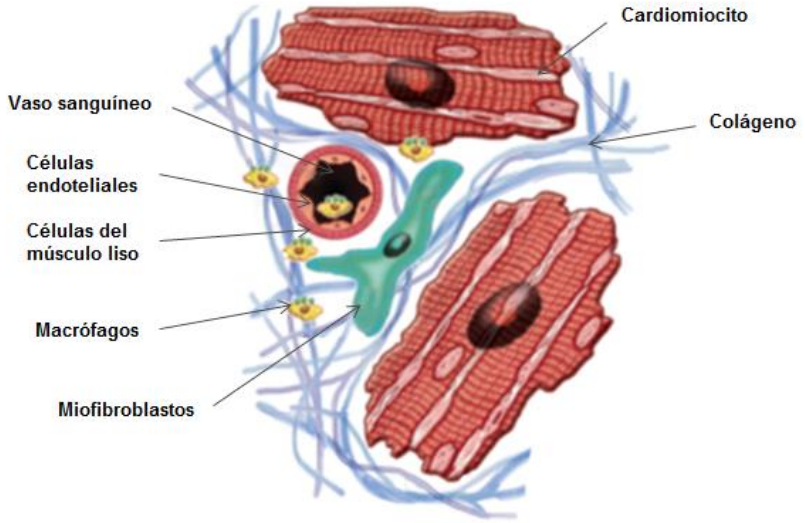

Figura 3. Fisiopatología de la fibrosis miocárdica. La fibrosis miocárdica es un proceso complejo que implica a cada componente celular del tejido miocárdico. Adaptado de *Mewton et al. J Am Coll Cardiol 2011*.

Múltiples factores contribuyen a la remodelación ventricular en diferentes etapas post-IAMEST. El remodelado cardíaco estructural está asociado con una respuesta inflamatoria, seguido de la formación de una cicatriz en la localización del infarto. El tejido fibroso que se forma en el lugar donde se produce la pérdida de cardiomiocitos preserva la integridad estructural y forma parte de la recuperación del corazón (*Sun. Cardiovasc Res 2009*). Sin embargo, una acumulación excesiva de colágeno o una remodelación estructural del miocardio viable puede afectar el comportamiento de los tejidos.

La acumulación progresiva de colágeno a menudo conduce a un aumento de la rigidez del miocardio y puede promover anormalidades de la función cardíaca (*Conrad et al. Circulation 1995*).

3 Remodelado ventricular

La insuficiencia cardíaca es un problema global de salud, que aparece más comúnmente en pacientes que han sufrido previamente un infarto de miocardio (*Bueno et al. Int J Cardiol 2017; Schiele et al. Eur Heart J Acute Cardiovasc Care 2017*). La remodelación cardíaca, particularmente la fibrosis, es reconocida por ser el mayor determinante del empeoramiento de la función ventricular (*Sun. Cardiovasc Res 2009; Conrad et al. Circulation 1995*).

La principal causa de insuficiencia cardíaca tras un IAMEST es el remodelado adverso del ventrículo izquierdo (RAVI) (*Carrick et al. J Am Coll Cardiol Img 2015*) como respuesta al aumento de trabajo de la pared del ventrículo izquierdo (VI) debido a la pérdida de cardiomiocitos y a una distensión en la zona infartada (Figura 4) (*Pfeffer et al. Circulation 1990*).

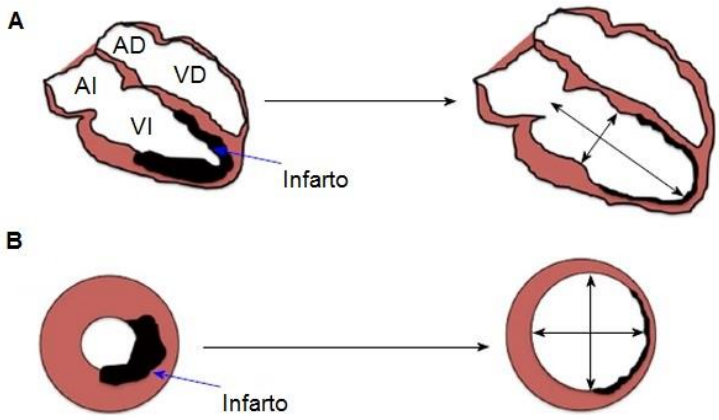

Figura 4. Desarrollo del RAVI tras un infarto agudo de miocardio en vista de eje largo (A) y de eje corto (B). En las vistas de la derecha las flechas indican las nuevas dimensiones adquiridas por el VI. Adaptado de *Shetye et al. World J Cardiol 2015.*

AD = Aurícula derecha. AI = Aurícula izquierda. RAVI = Remodelado adverso del ventrículo izquierdo. VD = Ventrículo derecho. VI = Ventrículo izquierdo.

El RAVI es normalmente definido como un incremento del 20% del volumen telediastólico del VI (VTDVI), o lo que es lo mismo, un aumento del 20% en el volumen del VI cuando el miocardio se encuentra relajado (*Bolognese et al. Circulation 2002; Bulluck et al. J Cardiovasc Magn Reson 2017*). Sin embargo, existe cierta controversia con respecto a esta definición de RAVI, ya que un aumento del VTDVI no tiene por qué implicar un peor desarrollo de la enfermedad y, por tanto, un peor pronóstico (*Brooks et al. J Am Coll Cardiol 2016*).

4 La resonancia magnética cardiaca

Anteriormente, la única manera de evaluar la fibrosis miocárdica era mediante la técnica de la biopsia de tejido endomiocárdico. Esta metodología permite la evaluación de la cantidad de colágeno. Los principales problemas de esta técnica residen en que se trata de una

técnica invasiva y en que no se puede determinar la fibrosis de todo el ventrículo (*Martos et al. Circulation 2007*).

Es por ello que la resonancia magnética cardiaca (RMC) se ha establecido en las últimas décadas como la técnica de imagen *gold standard* para caracterizar de manera no invasiva la morfología, la función, la anatomía coronaria, la perfusión y la viabilidad con niveles muy altos de precisión y reproducibilidad. El uso de contrastes ha elevado todavía más la exactitud y la precisión con la que se analiza la composición del tejido miocárdico y especialmente la fibrosis. Su principal problema radica en que anula la señal en el miocardio sano y, por tanto, no permite evaluar la fibrosis reactiva en el miocardio remoto no infartado (MRNI). El aumento de la concentración de contraste dentro del tejido fibrótico genera una intensidad de señal brillante en la imagen de RMC. Por tanto, la discriminación entre miocardio fibrótico y MRNI se basa en las diferencias de concentración de contraste combinadas con el ajuste elegido de los parámetros de la secuencia de adquisición. Estos parámetros se establecen para que la señal sea nula en el MRNI que aparecerá oscura en la imagen final en relación con la señal brillante del miocardio fibrótico. (*Mewton et al. J Am Coll Cardiol 2011*).

En la actualidad existen diferentes secuencias de adquisición de RMC que permiten obtener a través del procesado de imagen la información necesaria en un solo estudio (Figura 5):

- Las secuencias de cine permiten evaluar la morfología y la función cardiaca.
- Las secuencias STIR (*short time inversion recovery*) permiten identificar la zona del miocardio con edema en la fase aguda del infarto de miocardio.

- Las secuencias de realce tardío permiten evaluar la viabilidad del miocardio después de la administración de un medio de contraste, localizando la zona infartada y, la presencia o no de obstrucción microvascular.
- Por último, las secuencias T2* permiten identificar la hemorragia intramiocárdica.

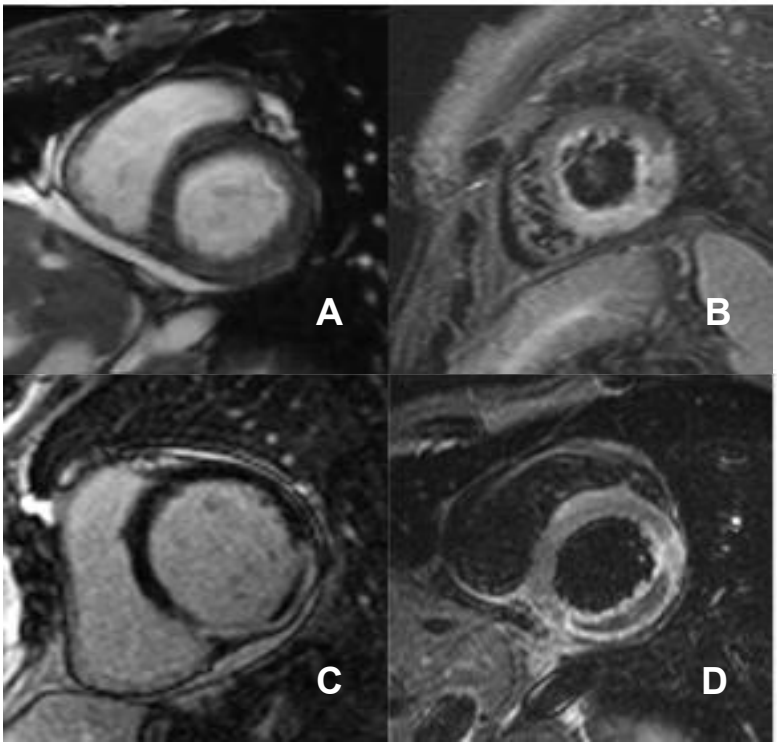

Figura 5. Diferentes tipos de imágenes de eje corto adquiridas mediante un escáner de resonancia magnética de 1,5 teslas asociados a cada una de las secuencias de adquisición que permiten identificar cada uno de los procesos fisiológicos. A) Imagen de cine. B) Imagen STIR: la zona con mayor intensidad se corresponde la zona con edema. C) Imagen de realce tardío: la zona infartada se corresponde a la zona del miocardio con mayor intensidad. Dentro de esta zona se encuentra la obstrucción microvascular con una intensidad similar a la del resto del miocardio. D) Imagen T2*: se aprecia tanto el edema como la hemorragia intramiocárdica en el interior del mismo.

5 El *strain*

El *strain* es un nuevo índice de imagen cardíaca que describe la deformación miocárdica como cambios relativos en la longitud de cada segmento del VI en cada instante. De forma que permite caracterizar el tejido cardiaco a nivel segmentario, regional o global (*Buckberg et al. Circulation 2008*).

5.1 Definición

La deformación viene dada como cambios en la longitud del tejido y se expresa como porcentajes de acortamiento o alargamiento con respecto a su longitud en reposo (fórmula de Lagrangian) (*Buckberg et al. Circulation 2008*):

$$\varepsilon = (L - L_0)/L_0$$

Dónde ε representa el *strain* o deformación (acortamiento/alargamiento)*;* L la longitud de la fibra en cada instante y, L_0 la longitud de la fibra en reposo. Así pues, valores negativos de ε representarán un acortamiento de las fibras del tejido (contracción muscular) mientras que un valor positivo representaría un alargamiento (elongación o engrosamiento). Es por ello por lo que, en un ciclo cardíaco la máxima deformación corresponderá al momento de sístole mientras que en diástole el miocardio estará en reposo.

5.2 Tipos de *strain*

Debido a que el corazón se deforma (contrae/elonga) en todos los ejes del espacio se han determinado tres índices ortogonales diferentes para poder caracterizar correctamente esta deformación (*Cuberas-Borrós et al. Rev Esp Cardiol 2010*). Por tanto, en función de la dirección en la que se deforma el miocardio encontramos:

- El *circumferential strain* (CS) mide el acortamiento/alargamiento circunferencial debido al movimiento hacia dentro de la pared media.
- El *longitudinal strain* (LS) es el medido a lo largo de una línea recta en cada segmento en el eje longitudinal.
- El *radial strain* (RS) mide el engrosamiento de la pared del ventrículo en dirección radial.

Por tanto, los vectores que determinan la deformación están descompuestos en direcciones ortogonales con respecto al VI como se muestra en la figura 6.

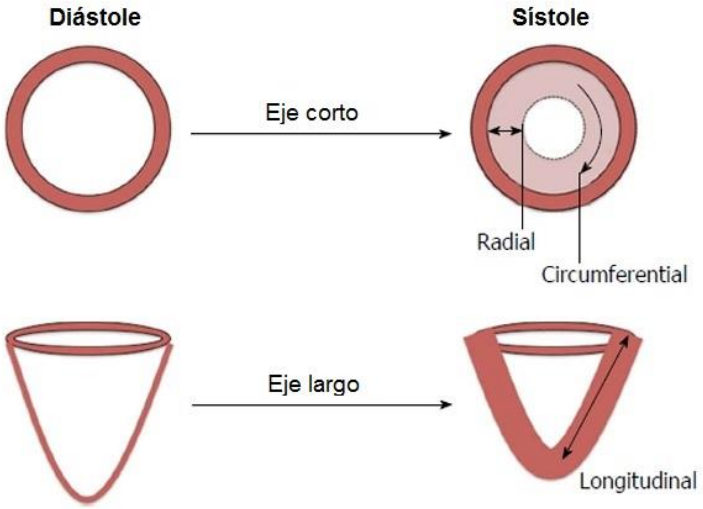

Figura 6. Direcciones de la deformación ventricular. Adaptado de *Shetye et al. World J Cardiol 2015.*

5.3 Cuantificación del *strain*

En la actualidad existen diferentes técnicas de imagen para valorar la deformación miocárdica. La ecocardiografía fue la primera

prueba diagnóstica que incorporó técnicas de imagen para la cuantificación del *strain* (Doppler Tisular y *speckle tracking*). Pero debido a las diferentes limitaciones que presentaban se empezó a trabajar con la RMC (*tagging* y *tissue tracking* [TT]).

5.3.1 Técnicas basadas en ecocardiografía

La ecocardiografía Doppler Tisular fue la primera capaz de obtener el *strain* mediante el procesado de la imagen. Esta técnica permite medir velocidades, desplazamientos y deformaciones (*strain* y *strain rate*) (Figura 7). Además, los nuevos equipos permiten marcar la región miocárdica de la imagen que queremos explorar y de esta manera obtener el desplazamiento desde su punto inicial. La principal limitación que presenta es que es ángulo dependiente y, por tanto, debido a que el miocardio está formado por fibras orientadas en 3 direcciones: longitudinal, circunferencial y radial, no permite valorar simultáneamente los diferentes componentes de deformación en todos los segmentos miocárdicos (*Amzulescu et al. Eur Heart J Cardiovasc Imaging 2019*).

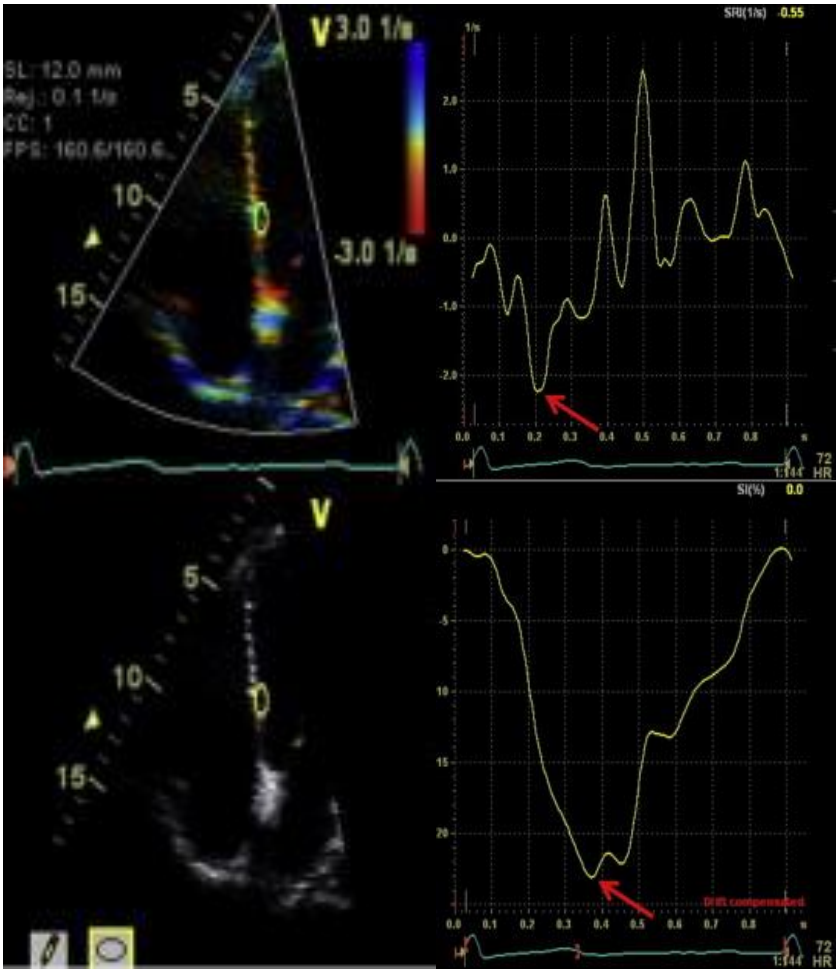

Figura 7. Doppler Tisular. Imagen Doppler Tisular del tabique interventricular (**izquierda**) y la región de interés (**óvalo amarillo**) de donde se obtuvieron los valores de *strain* y *strain rate*. Curva de *strain rate* (**derecha, arriba**); y *longitudinal strain* (**derecha, abajo**) en la región marcada. Las flechas indican los picos máximos del *strain rate* y el *longitudinal strain.* Adaptado de *Thavendiranathan et al. J Am Coll Cardiol 2014*.

Más tarde surgió el *speckle tracking*, está técnica dejó de basarse en los principios del Doppler Tisular para basarse en el seguimiento de marcadores acústicos. Cada región del miocardio posee un patrón único el cual puede ser rastreado y posteriormente

procesado para estudiar el movimiento (Figura 8). De esta manera es capaz de corregir la dependencia del ángulo y permite analizar el comportamiento en las tres direcciones de forma simultánea en todos los segmentos miocárdicos. Ambas técnicas presentan limitaciones de resolución de imagen. Sin embargo, la principal desventaja del *speckle tracking* frente al Doppler Tisular es su menor resolución temporal (*Amzulescu et al. Eur Heart J Cardiovasc Imaging 2019*).

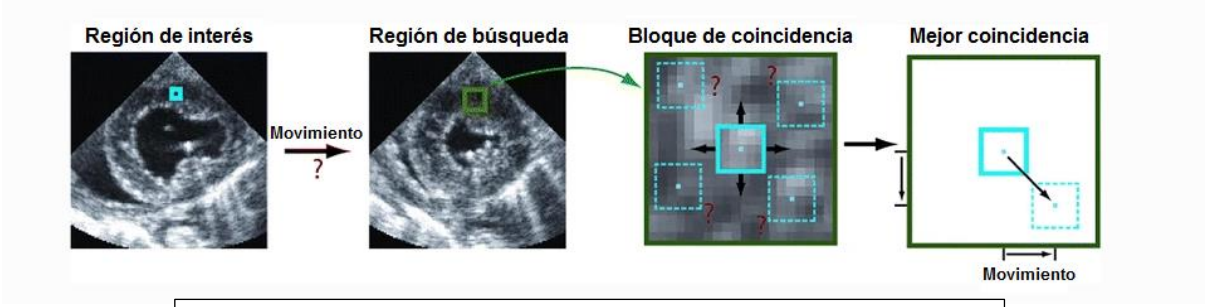

Figura 8. *Speckle tracking*. Se identifica una región de interés (bloque) y se rastrea dentro de la región de búsqueda del *frame* siguiente. Después de comparar este bloque de interés con todas las posibles regiones de coincidencia, la posición de la mejor coincidencia determina el movimiento del tejido. Adaptado de *Jasaityte et al. J Am Soc Echocardiogr 2013*.

5.3.2 Técnicas basadas en RMC: tagging y TT

Posteriormente se empezaron a desarrollar técnicas de imagen para cuantificar el *strain* en RMC. La primera técnica que surgió fue el *tagging*. Esta técnica está basada en la creación de unos marcadores, previamente a la adquisición de la imagen, que marcan magnéticamente en forma de cuadrícula diferentes regiones del miocardio. El seguimiento de la deformación de esta cuadrícula permite la evaluación directa de la deformación miocárdica (Figura 9). Las principales ventajas que presenta esta técnica son que se puede realizar un análisis transmural, se realiza de forma automática y es una técnica reproducible. Sin embargo, sus principales desventajas son el alto tiempo de procesamiento de imágenes y la necesidad de

emplear secuencias de adquisición adicionales a las que se realizan en la práctica clínica habitual (*Amzulescu et al. Eur Heart J Cardiovasc Imaging 2019*).

Figura 9. *Tagging*. Imágenes de *tagging* para la cuantificación del *longitudinal strain* (**arriba**) y el *circumferential strain* (**abajo**). Adaptado de *Amzulescu et al. Eur Heart J Cardiovasc Imaging 2019*.

El último en aparecer y en el que se ha basado el desarrollo de esta Tesis ha sido el TT. Esta técnica se basa en el marcado de los contornos endocárdicos y epicárdicos al final de la diástole y de la sístole en las imágenes de cine de eje corto y de eje largo. El rastreo de estos contornos permite la obtención de los 3 *strains* en todo el ciclo cardíaco (Figura 10). Las principales ventajas que presenta frente al *tagging* son la reproducibilidad y que no necesita de secuencias ni codificaciones adicionales para su posterior procesado, ya que utiliza las imágenes de cine que se adquieren en la mayoría de los protocolos cardíacos (*Amzulescu et al. Eur Heart J Cardiovasc Imaging 2019*).

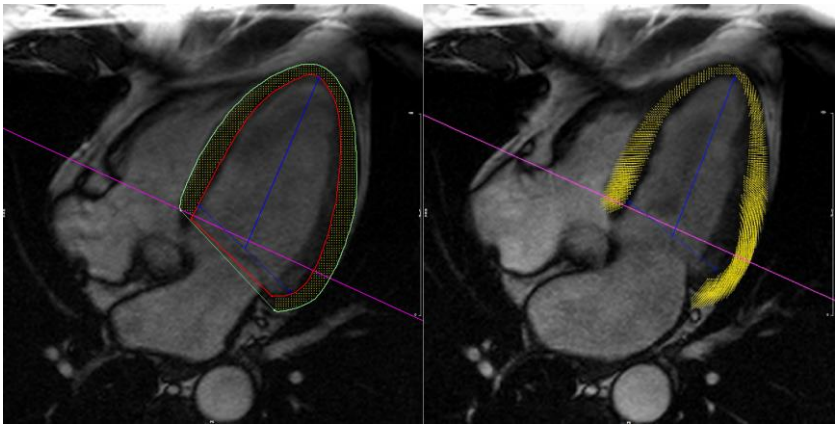

Figura 10. *Tissue Tracking***.** En la figura se puede observar el marcado de los bordes endocárdicos y epicárdicos en una imagen de cuatro cámaras (**izquierda)** y el seguimiento del movimiento que es capaz de realizar esta técnica (**derecha**).

5.4 Estado del arte

Hasta la fecha, el *strain* únicamente había sido estudiado en profundidad mediante ecocardiografía. Muchos eran los estudios que habían estudiado la relación entre la zona infartada y una alteración del *strain* mediante ecocardiografía. Zhang et al. observaron que el RS se encontraba alterado en las zonas con infarto transmural (*Zhang et al. J Am Coll Cardiol 2005*), mientras que Loutfi et al. determinaron que el LS era un buen predictor de infartos extensos (*Loutfi et al Clin Med Insights Cardiol 2016*). En cuanto al valor pronóstico, algunos estudios como el de Wang et al. vieron como el LS estaba asociado con diferentes eventos cardiovasculares adversos (ECVA) (*Wang et al. Eur Heart J 2016*).

El *strain* mediante RMC no había sido abordado con profundidad. Los primeros estudios con *strain* mediante RMC se centraron en el CS. Buss et al. y Shetye et al. vieron como existía una buena correlación entre el CS y el tamaño del infarto (*Buss et al. Int J Cardiol 2015; Shetye et al. BMC Cardiovasc Disord 2017*). Además,

no existían estudios mediante TT-RMC que evaluaran la caracterización, la dinámica y las implicaciones pronósticas de los diferentes índices de *strain* (LS, CS y RS) en pacientes IAMEST.

6. Contribución original del autor

El autor de este trabajo ha llevado a cabo la adquisición y análisis de los datos estudiados. Las tres partes de esta Tesis, formada por un compendio de 3 artículos, han sido publicadas en revistas científicas internacionales indexadas dentro de Journal of Citation Report. El autor de este trabajo ha escrito todos los artículos y ha desempañado las funciones necesarias como primer autor.

II.- HIPÓTESIS

El *strain* miocárdico global del ventrículo izquierdo cuantificado mediante la técnica *tissue tracking* permite la estratificación de riesgo en pacientes IAMEST.

La definición de remodelado adverso que mejor predice los eventos cardiovasculares es la compuesta por una combinación del *strain* miocárdico global del ventrículo izquierdo y el volumen telediastólico del ventrículo izquierdo.

El *tissue tracking* es una técnica de imagen que puede proporcionar información relevante para la caracterización de la función sistólica del miocardio tanto en el área infartada como en el área del miocardio remoto no infartado. Además, permite monitorizar sus respectivas dinámicas y sus implicaciones pronósticas y estructurales en cuanto al remodelado adverso tras un IAMEST.

III.- OBJETIVOS

El objetivo principal de esta Tesis es el estudio del *strain* miocárdico mediante la técnica de imagen *tissue tracking* en pacientes que han sufrido previamente un IAMEST.

Para ello se han determinado los siguientes objetivos específicos:

1. Determinar el valor pronóstico del *strain* miocárdico global del ventrículo izquierdo (LS, CS y RS globales) obtenido mediante *tissue tracking* en un registro de pacientes IAMEST de un Hospital Universitario.

2. Realizar una validación externa del valor pronóstico del *strain* en una cohorte de pacientes de un segundo Hospital Universitario.

3. Evaluar en un registro formado por pacientes IAMEST de dos Hospitales Universitarios si una combinación entre el *strain* miocárdico global del ventrículo izquierdo y el volumen telediastólico del ventrículo izquierdo forman la mejor definición de remodelado adverso para predecir eventos.

4. Analizar la caracterización y la dinámica del LS en el área del miocardio remoto no infartado durante los primeros meses tras un IAMEST.

5. Estudiar las implicaciones estructurales y pronósticas del LS en el área del miocardio remoto no infartado tras un IAMEST.

IV.- MÉTODOS

1 Pacientes y protocolo de RMC

La metodología empleada en este trabajo y la caracterización de los pacientes debe de consultarse con más detalle en cada uno de los manuscritos adjuntos. Aquí se muestra brevemente los materiales y métodos generales empleados en todas las partes del trabajo.

Este proyecto fue aprobado por el Comité Ético de Investigación Clínica de nuestro centro (Anexo VI).

Nuestro registro de IAMEST incluye pacientes consecutivos que acudieron a nuestro Hospital Universitario con un primer IAMEST, tratados con ACTP y remitidos para realizarse una RMC previamente al alta hospitalaria.

A todos los pacientes se les realizó una prueba de RMC de 1.5T (Sonata Magnetom; Siemens, Erlangen, Germany) y, a parte de ellos se les remitió por protocolo para la realización de una segunda prueba de RMC a los 6 meses.

Las imágenes se obtuvieron con la ayuda de una bobina de superficie *phased-array*, mediante la contención de la respiración y activación electrocardiográfica.

Todas las secuencias de imagen fueron lanzadas en los mismos planos de adquisición. Adquiriéndose imágenes de eje largo de dos, tres y cuatro cámaras y de eje corto (Figura 11).

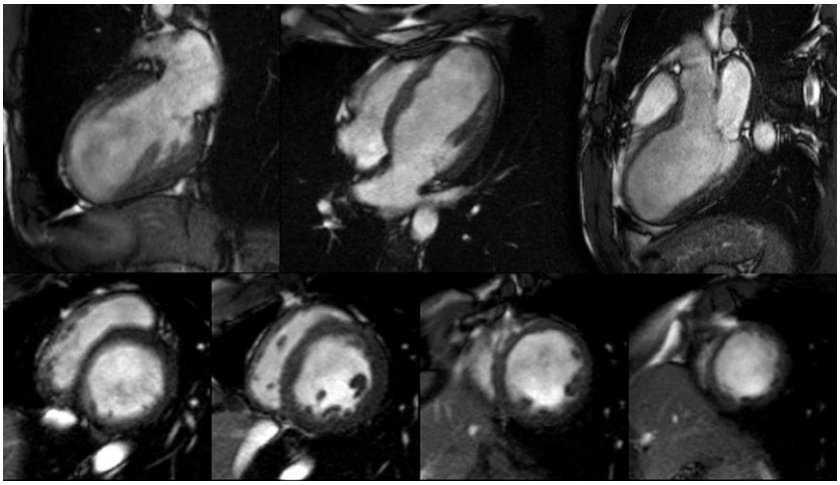

Figura 11. Imágenes de cine de dos, tres y cuatro cámaras (**panel superior**) y de eje corto (**panel inferior**).

Las imágenes de cine se obtuvieron mediante el uso de una secuencia *steady state free precession* (tiempo de repetición / tiempo de eco: 2,8ms/1,2ms; ángulo de giro: 58º; matriz: 256x300, campo de visión: 320x270mm; grosor del corte: 7mm).

Entre 10-15 minutos después de la administración del contraste ácido gadolinio dietilentriaminopentaacético a 0.1mmol/kg (Magnograf, Juste S.A.Q.F., Madrid, España), con una velocidad de flujo de 3 ml/s, se adquirieron las imágenes de captación tardía de gadolinio utilizando una secuencia de inversión-recuperación segmentada *steady state free precession* (tiempo de repetición/ tiempo de eco: 2,5ms/1,26ms; ángulo de inclinación: 45º; matriz: 256x184; campo de visión: 340x235mm; grosor del corte: 7mm). El tiempo de inversión fue ajustado para que la señal fuera nula en el miocardio sano.

También se emplearon secuencias STIR (de sangre negra), secuencias de recuperación de la inversión de T1 cortas ponderadas en T2 en mitad de la diástole. Se utilizó una secuencia *half Fourier acquisition single shot turbo spin echo* (tiempo de recuperación, 2 intervalos RR; tiempo de eco: 33ms; tiempo de inversión: 170ms; grosor del corte: 8 mm; intervalo de sección: 2 mm; ángulo de giro: 180º; matriz: 256x146; ancho de banda: 235 Hz/píxel).

1.1 Análisis de RMC

Posteriormente, los estudios fueron cuantificados de manera *off-line,* por un experimentado observador desconocedor de los datos del paciente, utilizando un software certificado (QMASS MR 6.1.5; *Medis, Laiden*, Holanda).

La fracción de eyección del VI (FEVI) (%), el VTDVI (ml/m²), el volumen telesistólico del VI (ml/m²) y la masa de las paredes del VI (g/m²) se calcularon mediante planimetría manual de los bordes endocárdicos y epicárdicos en las imágenes de cine de eje corto.

Se consideró que existía presencia de realce tardío de gadolinio cuando la intensidad de señal era >5 desviaciones estándar con respecto al área del MRNI en las imágenes de realce tardío. El tamaño de infarto (% de la masa del VI) se cuantificó mediante planimetría manual como el porcentaje de masa del VI que mostraba realce tardío de gadolinio.

La obstrucción microvascular (% de la masa del VI) se cuantificó mediante planimetría manual y se definió como el porcentaje de masa del VI que mostró falta de captación del contraste en el núcleo de un segmento rodeado por tejido que mostrara realce tardío.

Se consideró como edema miocárdico las áreas hiperintensas en T2 con una desviación estándar >2 con respecto al MRNI. La

presencia de edema se visualizó mediante planimetría manual y expresada como porcentaje de VI.

El miocardio salvado fue calculado restando la masa infartada al miocardio con edema, y expresado como porcentaje de masa de VI con edema miocárdico.

1.2 Análisis del *strain*

El *strain* no se cuantificó hasta 2016 cuando se dispuso del software necesario *(*CMR42*, Circle Cardiovascular Imaging Inc., Calgary, Alberta,* Canadá*)*. El *strain* se cuantificó de manera *off-line* mediante planimetría manual de los bordes endocárdicos y epicárdicos en las imágenes de cine de eje corto y de eje largo.

Los contornos endocárdicos y epicárdicos del VI fueron marcados al final de la diástole y de la sístole en las imágenes de eje corto y de eje largo. El final de la diástole se definió por la apertura de la válvula aórtica, mientras que el final de la sístole se definió por el cierre de la válvula aórtica. El corte más basal de eje corto se identificó como el primer corte basal que contenía el 100% de miocardio circunferencial en todo el ciclo cardíaco. Además, en las imágenes de eje largo se dibujaron marcadores perpendiculares para identificar la posición de los planos de eje corto basales y apicales. Posteriormente, el software decidió la inclusión o no de cada uno de los cortes de acuerdo con estos marcadores perpendiculares (Figura 12). Los músculos papilares y las trabeculaciones se excluyeron en los cálculos del *strain*.

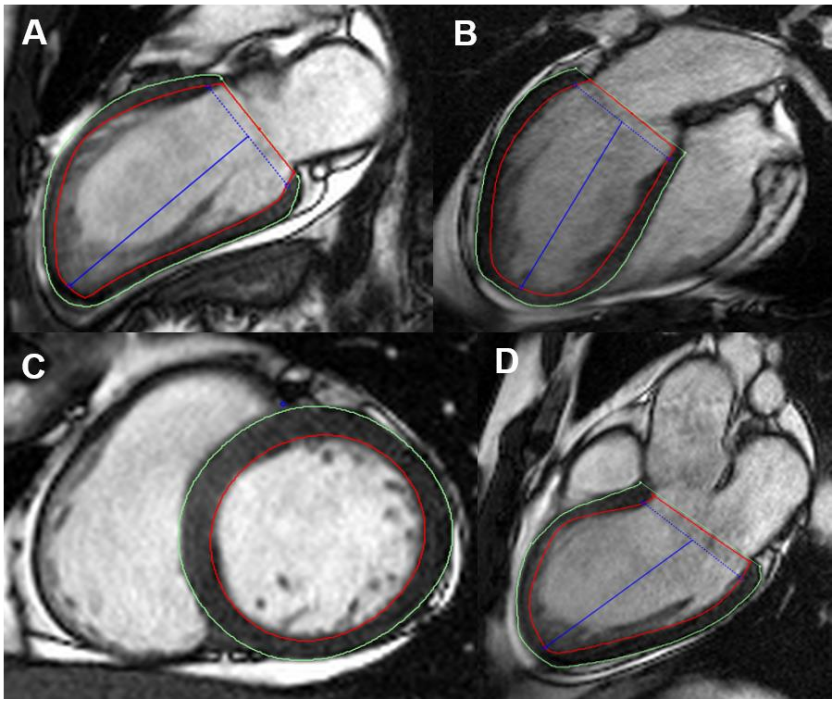

Figura 12. En la figura se pueden observar imágenes de eje largo (**A, B y D**) y de eje corto (**C**) con el borde endocárdico y epicárdico dibujado y con los marcadores perpendiculares en todas las imágenes eje largo.

El software utilizado necesitó para una correcta cuantificación al menos dos imágenes de eje largo para obtener el LS, y las imágenes de eje corto y al menos una imagen de eje largo para calcular el CS y RS. De esta manera se consiguió un correcto rastreo de los pixeles de cada uno de los segmentos del VI y, por tanto, el cálculo de su deformación en cada instante.

El software obtuvo cada uno de los diferentes *strains* (LS, CS y RS) en cada segmento del VI en todo el ciclo cardíaco según un modelo de 16 segmentos (Figura 13).

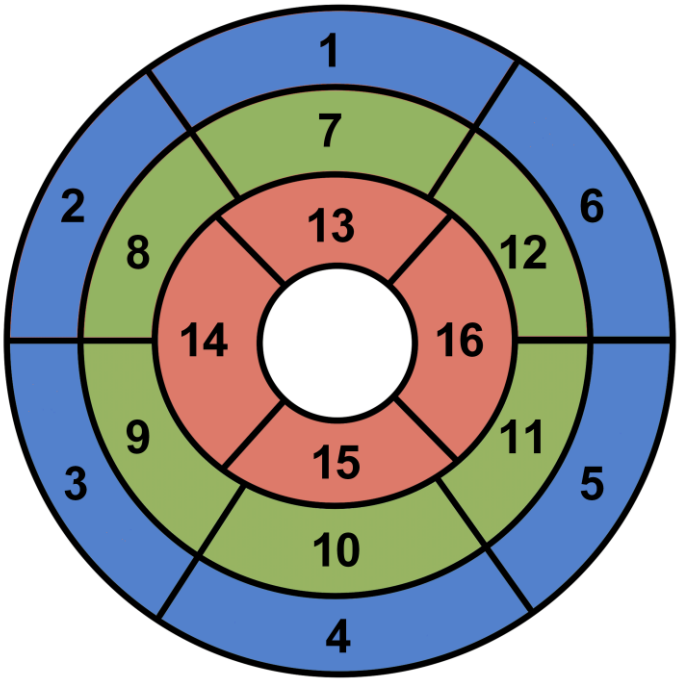

Figura 13. Diagrama de distribución de segmentos en el ventrículo izquierdo. Adaptado de *Cuberas-Borrós et al. Rev Esp Cardiol 2010*.

Tras el análisis y con los datos en crudo de todos los pacientes se desarrolló un *script* en Matlab R2012b (*Mathworks Inc, Natick*, EEUU) para la recogida de los valores de pico de cada segmento de cada uno de los tres *strains* (LS, CS y RS) (Figura 14). Estos valores fueron los utilizados para obtener los índices estudiados en los 3 trabajos presentados (globales y regionales). El cálculo de los diferentes índices se detalla en cada uno de los 3 trabajos adjuntos.

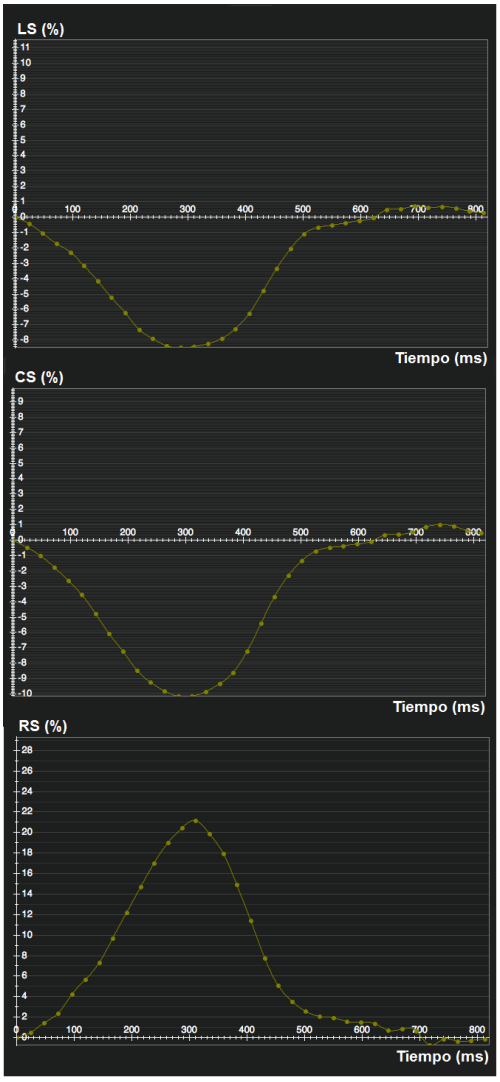

Figura 14. Representación del LS, CS y RS de un segmento de un paciente IAMEST a lo largo del ciclo cardíaco.

CS = Circumferential strain. IAMEST = Infarto agudo de miocardio con elevación del segmento ST. LS = Longitudinal strain. RS = Radial strain.

V.- RESUMEN DE MANUSCRITOS

1. Prognostic value of strain by tissue tracking cardiac magnetic resonance after ST-segment elevation myocardial infarction (Anexo I)

Gavara J*, Rodríguez-Palomares JF**, Valente F, et al. Prognostic value of strain by tissue tracking cardiac magnetic resonance after ST-segment elevation myocardial infarction. J Am Coll Cardiol Img 2018; 11:1448-57.

Objetivo: El objetivo principal de este estudio fue evaluar el valor pronóstico del *strain* obtenido mediante TT-RMC en la fase aguda del IAMEST.

Métodos: En este trabajo se evaluó el valor pronóstico del TT-RMC mediante un amplio registro de 323 pacientes de un Hospital Universitario que habían sido remitidos para realizarse una prueba de RMC una semana después de haber sufrido un IAMEST.

Siguiendo el modelo de 16 segmentos (*Cuberas-Borrós et al. Rev Esp Cardiol 2010*), se obtuvo el valor de pico máximo de cada uno de los tres *strains* (LS, CS y RS) para cada segmento a lo largo del ciclo cardiaco (Figura 15, panel superior). Este valor se sitúa en el momento de máxima deformación del miocardio. Los valores globales de cada *strain* (LS, CS y RS globales) se calcularon como la media de estos valores de pico.

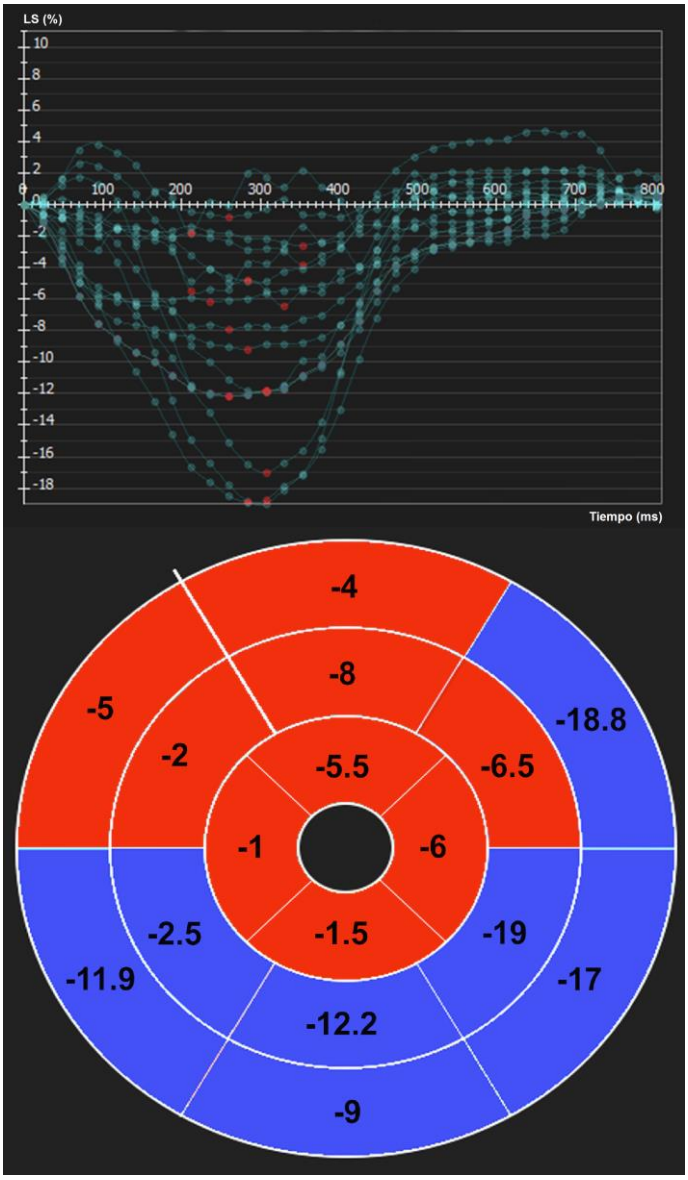

Figura 15. LS durante todo el ciclo cardiaco en los 16 segmentos del VI de un paciente con un infarto anterior extenso. **Los puntos rojos** indican el valor de pico de LS de cada segmento (**panel superior**). El **panel inferior** muestra en rojo los segmentos que se encuentran alterados en comparación con los segmentos de los pacientes control.

LS = Longitudinal strain. VI = Ventrículo izquierdo.

Para el análisis categórico, los valores de corte se obtuvieron de un grupo control de 32 pacientes que habían sido remitidos para realizarse una RMC, pero que no presentaban evidencias estructurales de ninguna enfermedad cardiovascular.

Basándonos en la literatura reciente se establecieron las siguientes variables: 1) LS, CS y RS globales: media de los valores de pico de los segmentos de cada paciente según el modelo de 16 segmentos. 2) Número de segmentos de cada paciente con el LS, CS y RS alterados: número de segmentos con el LS y CS por encima de su valor de corte y número de segmentos con el RS por debajo de su valor de corte. 3) Se consideró que un paciente tenía el LS global alterado si era ≥-11%, tenía el CS global alterado si era ≥-14% y tenía el RS global alterado si era <32%. Además de estos índices también se calcularon los principales parámetros de RMC: FEVI, volúmenes, tamaño de infarto y obstrucción microvascular.

Los resultados obtenidos en este estudio fueron validados por una cohorte de validación externa de 190 pacientes IAMEST de un segundo Hospital Universitario.

Resultados: Durante una mediana de seguimiento de 1.085 días, se registraron 54 ECVA (10 muertes cardiacas, 25 hospitalizaciones por insuficiencia cardiaca y 19 reinfartos). El ECVA fue asociado con anormalidades más severas en todos los índices de *strain* según la prueba *t-student* (p-valor<0,001). Como se observa en las curvas Kaplan-Meier mediante la prueba *log-rank* (Figura 16), los pacientes con el LS global≥-11%, el CS global≥-14% y el RS global≤32% mostraron un mayor riesgo de ECVA durante el seguimiento (p-valor<0,05 para todas las comparaciones). Lo mismo ocurrió en la cohorte de validación externa.

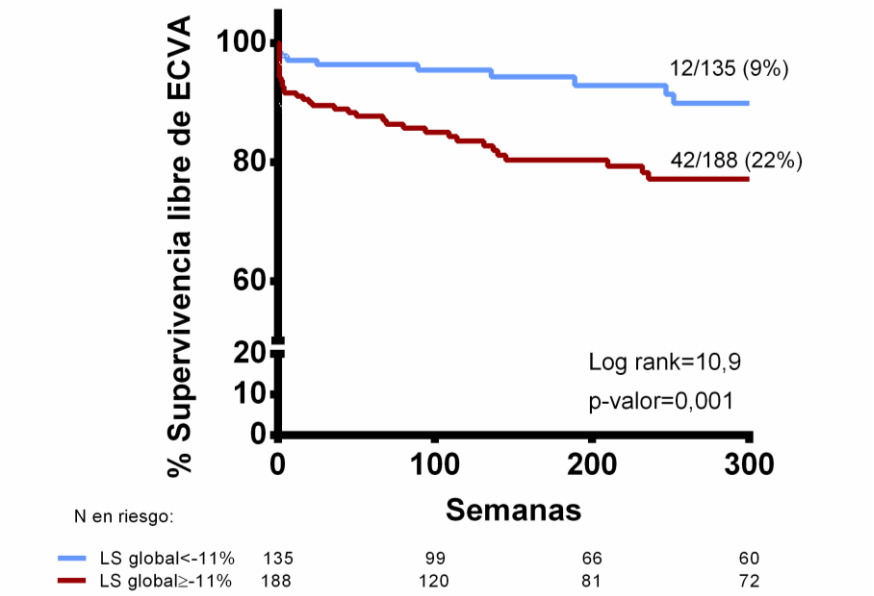
% Supervivencia libre de ECVA
100
80
60
20
10
0
12/135 (9%)
42/188 (22%)
Log rank=10,9
p-valor=0,001
0
100
200
300
Semanas
N en riesgo:
LS global<-11% 135 99 66 60
LS global≥-11% 188 120 81 72

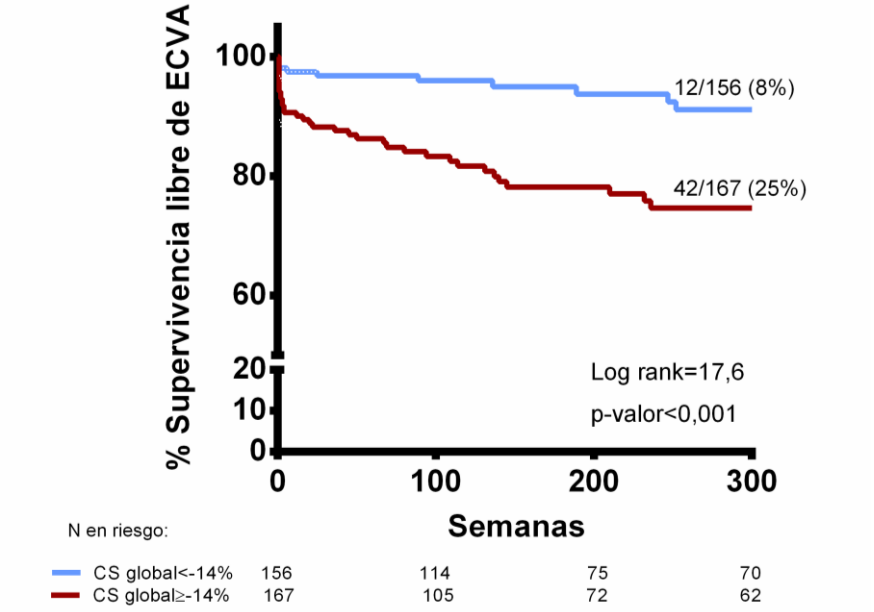
% Supervivencia libre de ECVA
100
80
60
20
10
0
12/156 (8%)
42/167 (25%)
Log rank=17,6
p-valor<0,001
0
100
200
300
Semanas
N en riesgo:
CS global<-14% 156 114 75 70
CS global≥-14% 167 105 72 62

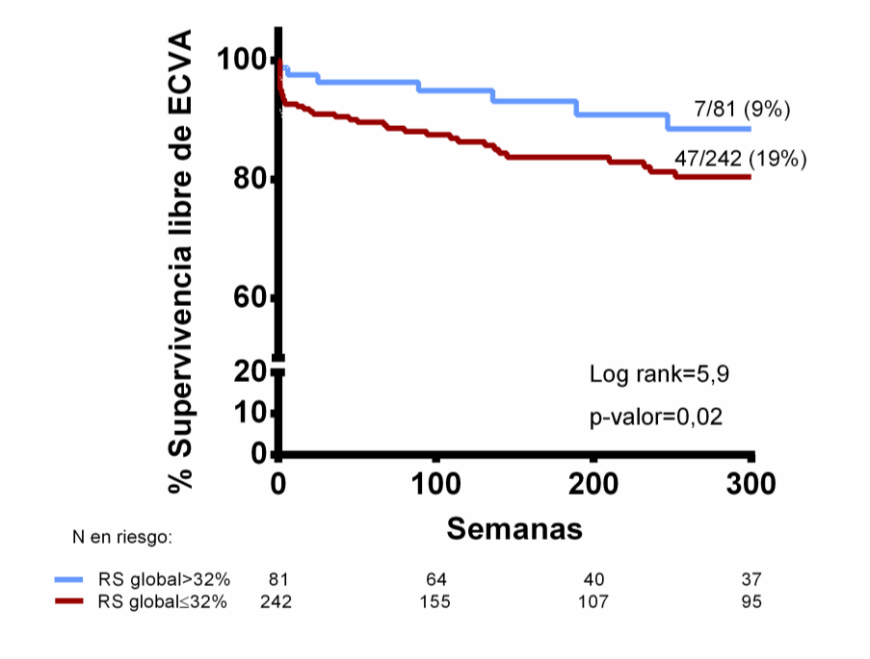

Figura 16. Curvas de supervivencia Kaplan-Meier. Los pacientes con el LS global≥-11%, el CS global≥-14% y el RS global≤32% mostraron un riesgo significativamente superior de ECVA.

CS = Circumferential strain. ECVA = Eventos cardiovasculares adversos. LS = Longitudinal strain. RS = Radial strain.

Sin embargo, sólo el LS global surgió como predictor independiente de ECVA (p-valor<0,001) (Tabla 1).

Tabla 1. Predictores de ECVA: Análisis multivariado de los índices de *strain.*

	OR (IC 95%)	**p-valor**
Número de segmentos con el LS alterado	1,14 (0,91-1,41)	0,3
Número de segmentos con el CS alterado	0,88 (0,56-1,38)	0,6
Número de segmentos con el RS alterado	1,12 (0,73-1,71)	0,7
LS global (%)	1,25 (1,14-1,36)	<0,001
CS global (%)	1,25 (0,89-1,77)	0,9
RS global (%)	1,08 (0,96-1,22)	0,5

CS = Circumferential strain. ECVA = Eventos cardiovasculares adversos. LS = Longitudinal strain. OR (IC 95%) = Odds Ratio (Intervalo de confianza del 95%). RS = Radial strain.

Con el fin de evitar el sobreajuste, se realizaron tres modelos multivariados diferentes. El modelo 1 incluyó únicamente variables clínicas asociadas con ECVA en el análisis univariado (p-valor<0,1). El modelo 2 incluyó las variables clínicas que habían salido significativamente independientes en el modelo 1 (p-valor<0,05) más las variables tradicionales de RMC que habían sido asociadas con ECVA en el análisis univariado (p-valor<0,1). Por último, en el modelo 3 se incluyó el LS global a las que habían salido significativamente independientes en el modelo 2. En este caso, el tiempo hasta la reperfusión, la escala de riesgo TIMI (de las siglas en inglés, *Thrombolysis in Myocardial Infarction*) y el LS global fueron las únicas variables asociadas de manera independiente con ECVA (Tabla 2).

Tabla 2. Predictores de ECVA: Análisis multivariado.

	HR (IC 95%)	p-valor
Modelo 3: Características clínicas + índices RMC + LS global		
Tiempo hasta la reperfusión (min)	1,001 (1,0004-1,001)	<0,001
Escala de riesgo TIMI	1,17 (1,04-1,31)	0,008
FEVI (%)	0,99 (0,96-1,02)	0,4
LS global (%)	1,21 (1,11-1,32)	<0,001

ECVA = Eventos cardiovasculares adversos. FEVI = Fracción de eyección del ventrículo izquierdo. LS = Longitudinal strain. HR (IC 95%) = Hazard Ratio (Intervalo de confianza del 95%). RMC = Resonancia magnética cardíaca. TIMI = Thrombolysis in Myocardial Infarction.

En la cohorte de validación externa, el LS global también fue predictor independiente de ECVA después de ajustar con las características clínicas y de RMC: Hazard ratio [Intervalo de confianza del 95%] (HR [IC 95%]): 1,18 [1,04-1,33]; p-valor=0,008.

Sin embargo, la inclusión del LS global en los modelos multivariados que incluían las características clínicas y los índices tradicionales de RMC, no mejoró significativamente ni la precisión de discriminación según el estadístico C (Modelo 2 vs. Modelo 3: 0,69 vs. 0,70, p-valor=0,7) ni la estratificación de riesgo comparada mediante el *continuous net reclassification improvement index* (-0,015; p-valor=0,7). Tampoco mejoró el estadístico C (0,70 vs. 0,70, p-valor=0,8) ni la estratificación de riesgo (-0,019, p-valor=0,9) en la cohorte de validación externa.

2. Prognostic value of initial left ventricular remodeling in patients with reperfused STEMI (Anexo II)

Rodríguez-Palomares JF*****, ***Gavara J****, Ferreira-González I, et al. Prognostic value of initial left ventricular remodeling in patients with reperfused STEMI. J Am Coll Cardiol Img 2019; 12:2445-56.

Objetivo: Este estudio se centró en estudiar el valor pronóstico del *strain* frente a un ECVA compuesto por aquellos eventos más relacionados con el RAVI y en establecer la mejor definición de RAVI, mediante índices de RMC, que mayor valor pronóstico tuviera frente a este ECVA.

Métodos: El grupo de pacientes del estudio estuvo compuesto por aquellos con un primer IAMEST provenientes de dos Hospitales Universitarios que habían recibido una ACTP dentro de las primeras 6h desde la aparición de los primeros síntomas (n=498), a los que se les realizó una primera RMC durante la hospitalización y otra después de 6 meses. Los *strains* globales (LS, CS y RS globales) fueron obtenidos mediante la media de los valores de pico de cada uno de los segmentos del VI. Además, se obtuvieron los índices tradicionales de RMC (volúmenes, FEVI, tamaño de infarto y obstrucción microvascular). El ECVA se definió por la muerte cardiovascular, la hospitalización por insuficiencia cardiaca y la arritmia ventricular, el que ocurriera primero.

Resultados: El estudio fue llevado a cabo finalmente con 374 pacientes. Durante un seguimiento medio de 72,9±42,8 meses, se registraron un total de 49 ECVA. El LS global, el CS global y la mayoría de los índices tradicionales de RMC presentaron una mayor afectación tanto a la semana como a los 6 meses en los pacientes con ECVA (Tabla 3). Además, el LS global (HR [IC 95%]: 1,34 [1,17-

1,54], p-valor<0,001) y el CS global (HR [IC 95%]: 1,25 [1,13-1,40], p-valor<0,001) se asociaron de manera significativa con ECVA.

Tabla 3. Predictores de ECVA.

	No ECVA	**ECVA**	**p-valor**
FEVI (%)			
1ª semana	53±12	46±13	0,001
6º mes	56±11	46±14	<0,001
Diferencia relativa (%)	8,3±18,6	3,4±27,2	0,02
VTDVI (ml)			
1ª semana	79±21	84±28	0,4
6º mes	80±24	90±37	0,3
Diferencia relativa (%)	3,4±22,7	8,3±26,6	0,2
VTSVI (ml)			
1ª semana	38±18	48±24	0,02
6º mes	37±20	52±32	0,005
Diferencia relativa (%)	0,1±33	12,1±41,8	0,03
TI (% del VI)			
1ª semana	21±14	29±16	<0,001
6º mes	21,7±13,1	28,7±15,8	0,001
Diferencia relativa (%)	-10,9±18,7	10,9±21	0,9

LS global (%)			
1ª semana	-10,7±3,1	-8,5±2,5	<0.001
6º mes	-11,5±3,1	-9,5±3,2	0,003
Diferencia relativa (%)	-16,8±34,6	-38,8±46,5	0,06
CS global (%)			
1ª semana	-16,8±3,8	-14,3±4,2	0,001
6º mes	-18,7±4,2	-16,9±4,4	0,003
Diferencia relativa (%)	-14,1±26,3	-31,9±41,2	0,07

CS = Circumferential strain. ECVA = Evento cardiovascular adverso. FEVI = Fracción de eyección del ventrículo izquierdo. LS = Longitudinal strain. TI = Tamaño de infarto. VI = Ventrículo izquierdo. VTDVI = Volumen telediastólico del ventrículo izquierdo. VTSVI = Volumen telesistólico del ventrículo izquierdo.

Tanto el LS global (-8,9±3,6% vs. -10,3±3,3%, p-valor=0,04) como el CS global (-12,2±4,3% vs. -13,9±4,2%, p-valor=0,03) mostraron una afectación mayor en los pacientes con un incremento relativo del VTDVI>15% desde la 1ª semana a los 6 meses frente a los que no habían sufrido esa dilatación.

Sin embargo, tras comprobar las diferencias relativas en ambos índices (LS y CS globales) (Tabla 3), entre los grupos de ECVA y no ECVA, estas diferencias no fueron significativas (p-valor=0,06 y 0,07, respectivamente). Por ello ninguno se empleó para realizar una nueva definición de RAVI. Si que lo fueron las de la FEVI (p-valor=0,02).

Aunque el volumen telesistólico del VI sí que presentó diferencias significativas en las diferencias relativas entre ambos

grupos, se escogió igualmente el VTDVI junto a la FEVI por ser el índice que tradicionalmente se ha asociado con el RAVI.

Por ello la nueva definición de RAVI que pretendía maximizar el valor pronóstico fue la formada por el VTDVI y la FEVI. Los valores que maximizaron la habilidad para detectar pacientes con o sin ECVA fueron un aumento relativo del VTDVI del 15% (HR: 2,1, p-valor=0,007) y un descenso relativo del 3% en la FEVI (HR: 2,5, p-valor=0,001). Sin embargo, el modelo predictivo (usando el análisis estadístico *C*) no pudo demostrar que la observación directa del RAVI a los 6 meses añadiera información pronóstica a los datos del *strain* (LS global y CS global) en fase aguda (estadístico C: 0,714 vs. 0,750), ni a los datos tradicionales de la RMC temprana (estadístico *C*: 0,714 vs. 0,770) en la predicción de ECVA (Figura 17).

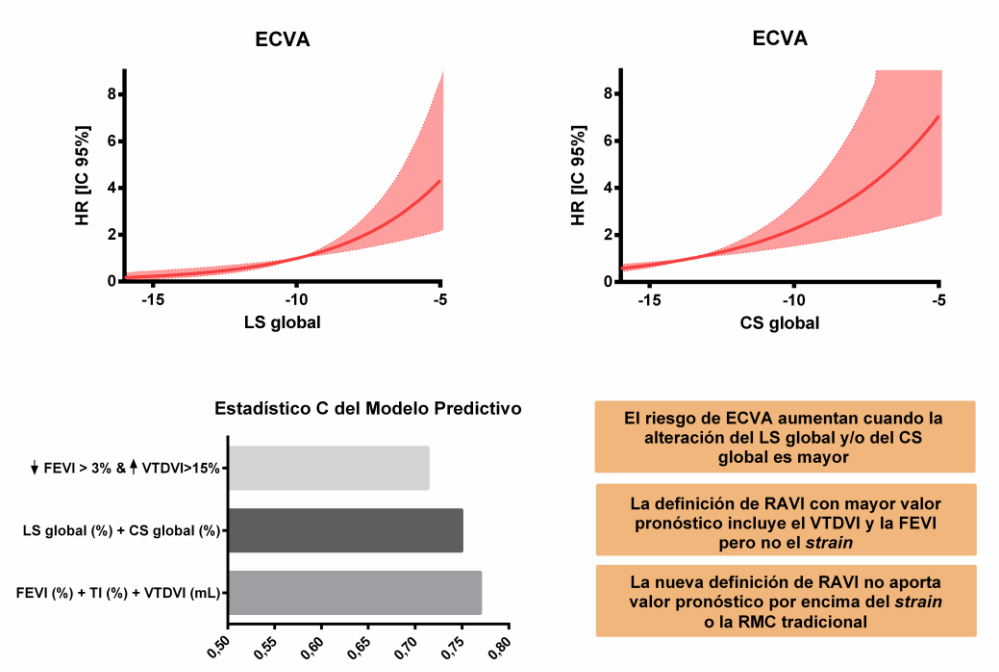

Figura 17. El riesgo de ECVA aumenta de forma paralela al aumento del LS y el CS globales (intervalo de confianza del 95%) (**paneles superiores**). Sin embargo, la definición de RAVI con mayores implicaciones pronosticas no incluye ningún *strain*. La nueva definición de RAVI no aporta información pronóstica por encima del *strain* ni de la RMC tradicional (**panel inferior**).

CS = Circumferential strain. ECVA = Evento cardiovascular adverso. FEVI = Fracción de eyección del ventrículo izquierdo. HR [IC] = Hazard ratio [Intervalo de confianza del 95%]. LS = Longitudinal strain. RAVI = Remodelado adverso del ventrículo izquierdo. RMC = Resonancia magnética cardiaca. TI = Tamaño del infarto. VTDVI = Volumen telediastólico del ventrículo izquierdo.

3. Longitudinal strain in remote non-infarcted myocardium by tissue tracking CMR: characterization, dynamics, structural and prognostic implications (Anexo III)

Gavara J*, Rodríguez-Palomares JF*, Ríos-Navarro C, et al. Longitudinal strain in remote non-infarcted myocardium by tissue tracking CMR: characterization, dynamics, structural and prognostic implications. Int J Cardiovasc Imaging 2020; Doi: 10.1007/s10554-020-01890-w.

Objetivo: El LS en MRNI no había sido caracterizado hasta el momento mediante TT-RMC en pacientes IAMEST. Por ello, nos marcamos los siguientes objetivos: 1) Caracterizar la dinámica del LS-MRNI dentro de los 6 primeros meses tras el IAMEST. 2) Analizar las implicaciones estructurales del LS-MRNI a corto y largo plazo. 3) Evaluar el impacto de la dinámica del LS-MRNI en la recuperación de la FEVI.

Como objetivo secundario decidimos estudiar las implicaciones pronósticas resultado de una alteración del LS-MRNI en la fase aguda tras el IAMEST.

Métodos: Se reclutaron un total de 271 pacientes con un primer IAMEST en un Hospital Universitario entre 2011 y 2014 que habían sido derivados para la realización de una RMC durante la primera semana tras el infarto. De ellos, 145 fueron sometidos a una segunda RMC a los 6 meses tras el IAMEST. Debido a que durante la realización del primer trabajo se observó que el LS fue el índice que más información pronóstica aportaba en los pacientes IAMEST, únicamente se empleó el valor del LS en cada región del VI, los otros dos índices fueron descartados (CS y RS).

En base a datos previamente validados (*Ortiz-Perez et al. J Am Coll Cardiol Img 2008*), las áreas de MRNI se definieron para cada paciente en función de la arteria coronaria culpable del infarto: arteria descendente anterior izquierda (ADA), arteria circunfleja izquierda (ACX) y arteria coronaria derecha (ACD). La Figura 18 muestra dentro del modelo de 16 segmentos (*Cerqueira et al. Circulation 2002*) qué segmentos se clasificaron como infarto o MRNI dependiendo de la arteria coronaria culpable.

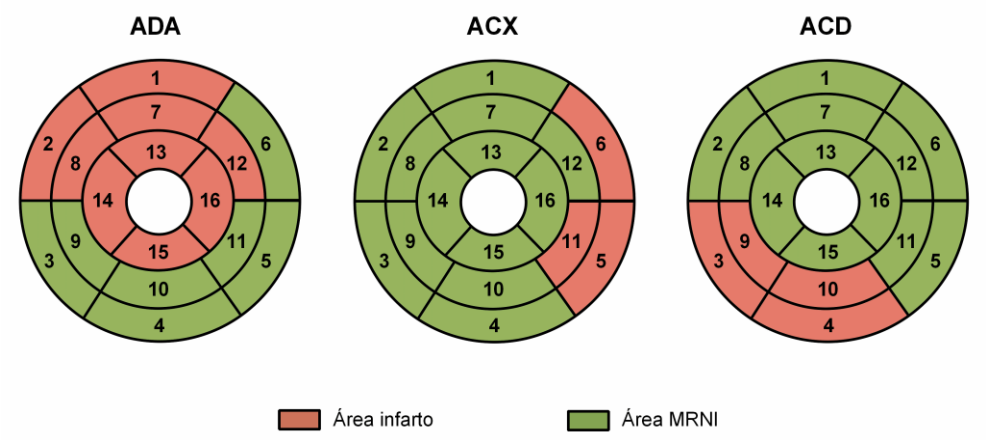

Figura 18. Clasificación de los segmentos del VI de acuerdo con la arteria coronaria culpable del infarto.

ACD = Arteria coronaria derecha. ACX = Arteria circunfleja. ADA = Arteria descendente anterior. MRNI = Miocardio remoto no infartado. VI = Ventrículo izquierdo.

El LS-MRNI y el LS-infarto se calcularon individualmente para cada paciente como la media de los valores absolutos máximos de los segmentos incluidos en el área MRNI o en el área del infarto dependiendo de la arteria coronaria culpable (Figura 18).

Con respecto a los valores de corte utilizados para definir si el LS estaba alterado en el área del infarto o en el área MRNI, se calcularon seis valores de corte diferentes en relación con el área (infarto o

MRNI) y la arteria coronaria culpable (ADA, ACX o ACD). Para calcular estos valores, se utilizó un grupo control de 32 pacientes.

De acuerdo con las tres principales arterias coronarias relacionadas con el infarto, los valores de corte utilizados para definir LS-infarto o LS-MRNI alterado se calcularon como el percentil 95% inferior del valor absoluto medio de LS de aquellos segmentos clasificados como infarto o MRNI en la Figura 18.

En consecuencia, dependiendo de la arteria coronaria culpable, se obtuvieron los siguientes valores de corte para definir LS alterado (tanto en MRNI como en el área del infarto): ADA (LS-MRNI≤11,2%, y LS-infarto≤11,1%); ACX (LS-MRNI≤10,8%, y LS-infarto≤12,9%), y ACD (LS-MRNI≤12,1%, y LS-infarto≤8,9%).

Resultados: Para el estudio de la dinámica y de las implicaciones estructurales del LS-MRNI se emplearon un total de 145 pacientes (2.320 segmentos) que habían sido remitidos a una segunda RMC a los 6 meses. La alteración del LS-MRNI en la primera semana (n=70, 48%) (Figura 19A) se asoció con un tamaño de infarto mayor y una FEVI más deprimida tanto a la semana como a los 6 meses tras el IAMEST (Tabla 4, p-valor<0,001).

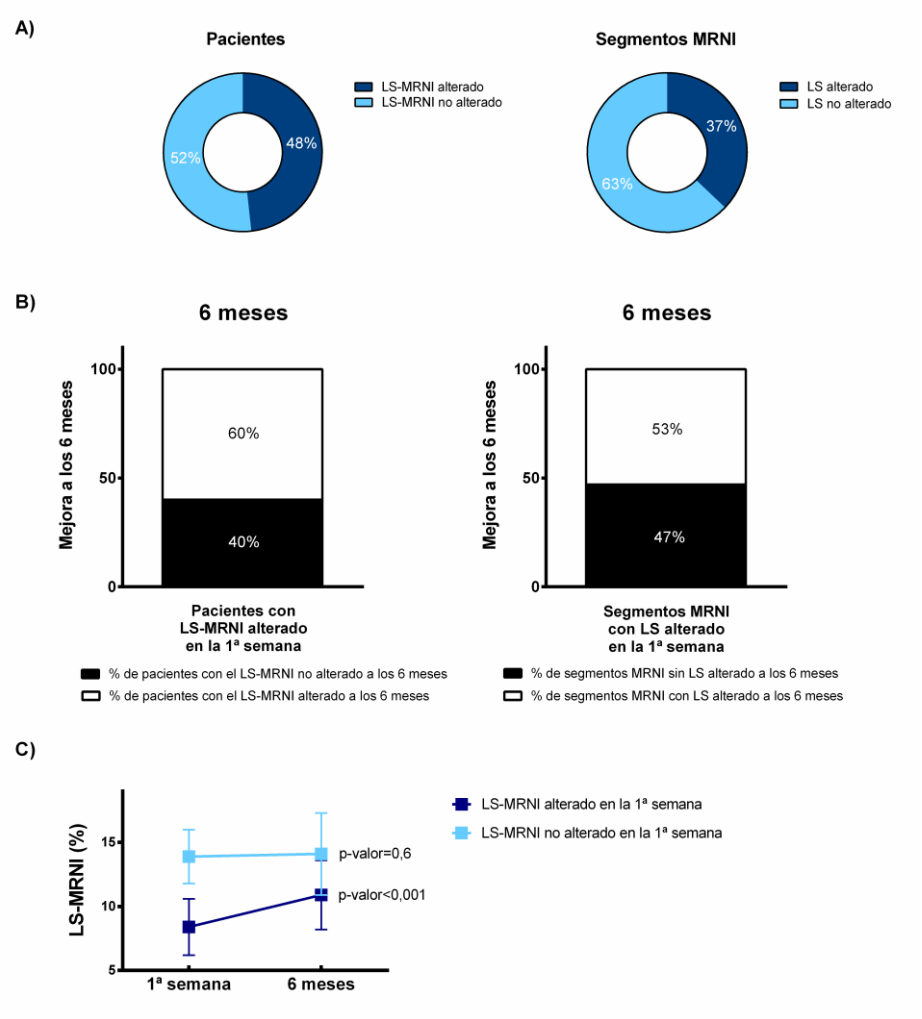

Figura 19. Caracterización y dinámica del LS-MRNI en base a los pacientes y a los segmentos.

A) Porcentaje de pacientes con y sin el LS-MRNI alterado, y de segmentos localizados en el MRNI con y sin el LS alterado.

B) Porcentaje de pacientes y segmentos que mejoran el LS-MRNI y el LS, respectivamente, cuando este se encontraba alterado en la 1ª semana.

C) Dinámica del LS-MRNI (desde la 1ª semana a los 6 meses) en función de si este estaba alterado o no en la 1ª semana.

LS = Longitudinal strain. MRNI = Miocardio remoto no infartado.

Tabla 4. Índices tradicionales de RMC en la 1ª semana y a los 6 meses de los pacientes con y sin el LS-MRNI alterado en la 1ª semana. Grupo de pacientes reestudiados a los 6 meses.

		LS-MRNI no alterado	LS-MRNI alterado	p-valor
Número de pacientes		75	70	
FEVI (%)	**1ª semana**	59±10	45±12	<0,001
	6 meses	62±11	51±12	<0,001
	p-valor	0,001	<0,001	
TI (% masa del VI)	**1ª semana**	16±12	30±15	<0,001
	6 meses	14±10	23±12	<0,001
	p-valor	0,002	<0,001	

FEVI = Fracción de eyección del ventrículo izquierdo. LS = Longitudinal strain. MRNI = Miocardio remoto no infartado. RMC = Resonancia magnética cardíaca. TI = Tamaño de infarto. VI = Ventrículo izquierdo.

Casi la mitad de los pacientes con el LS-MRNI alcanzaron valores normales de LS-MRNI a los 6 meses (28/70, 40%) (Figura 19B).

Se observó una mejora significativa de la 1ª semana a los 6 meses en el LS-MRNI (11,2±3,5% vs. 12,5±3,4%, p-valor<0,001). Sin embargo, esto fue debido principalmente a la evolución de los pacientes que presentaban el LS-MRNI alterado en la 1ª semana (8,4±2,2% vs. 10,9±2,7%, p-valor<0,001) que mejoraron más que los que ya se encontraban con valores por encima del umbral (13,9±2,1% vs. 14,1±3,2%, p-valor=0,6) (Figura 19C).

En base a los segmentos, 1.348 segmentos de los 2.320 incluidos en el estudio se localizaron en el MRNI. De ellos, 500 (37%) presentaron un LS alterado en la 1ª semana. Alrededor de un 47% (234/500) alcanzó valores normales a los 6 meses (Figura 19).

Una vez ajustado por todos los índices de RMC, el ΔLS-MRNI mostró una relación lineal y positiva con el ΔFEVI (Figura 20).

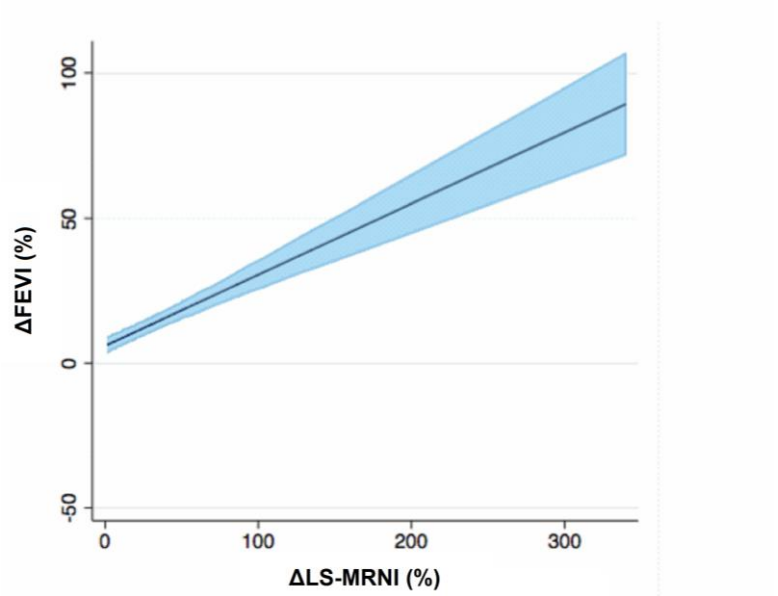

Figura 20. Asociación entre ΔLS-MRNI y ΔFEVI de la 1ª semana a los 6 meses (intervalo de confianza del 95%).

FEVI = Fracción de eyección del ventrículo izquierdo. LS = Longitudinal strain. MRNI = Miocardio remoto no infartado. ΔFEVI = Cambio relativo (%) en la FEVI de la 1ª semana a los 6 meses. ΔLS-MRNI = Cambio relativo (%) en el LS-MRNI de la

En el registro completo (n=271 pacientes) se registraron un total de 52 primeros ECVA (18 muertes, 16 hospitalizaciones por insuficiencia cardiaca y 18 reinfartos). Los pacientes con un LS-MRNI alterado durante la 1ª semana tras el IAMEST tuvieron mayor porcentaje de ECVA tanto en el grupo de estudio (26% vs. 11%, p-valor=0,002) (Figura 21, panel superior) como en la cohorte de validación externa, que estaba formada por 177 pacientes IAMEST de otro Hospital Universitario y dónde se registraron un total de 29 ECVA (57% vs. 13%, p-valor<0,001) (Figura 21, panel inferior).

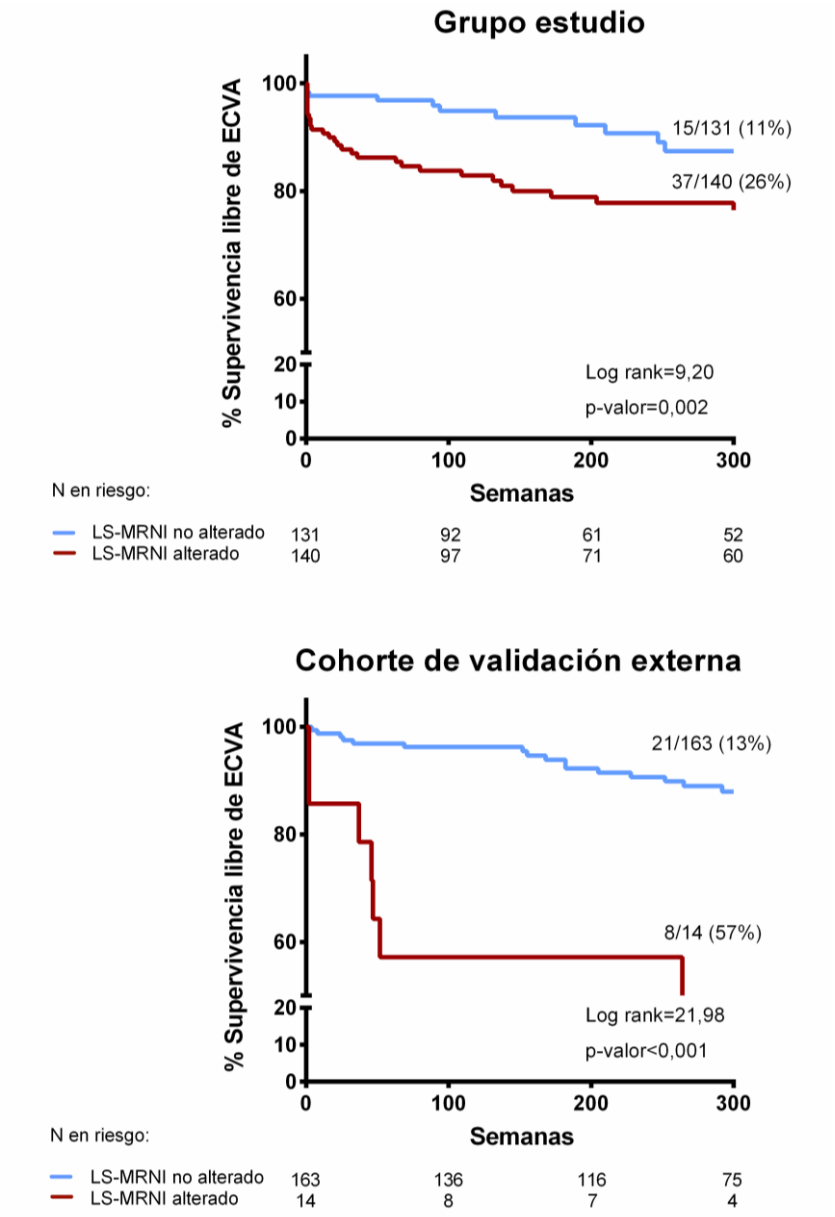

Figura 21. Curvas de supervivencia Kaplan-Meier. Los pacientes del grupo de estudio cuyo LS-MRNI se encuentra alterado muestran un riesgo significativamente superior de sufrir ECVA que los que presentan un LS-MRNI normal (**panel superior**). En la cohorte externa de validación se observan resultados similares (**panel inferior**).

ECVA = Eventos cardiovasculares adversos. LS = Longitudinal strain. MRNI = Miocardio remoto no infartado.

VI.- DISCUSIÓN

El infarto agudo de miocardio constituye una de las principales causas de morbilidad y mortalidad en nuestro entorno. Como consecuencia del aumento de la esperanza de vida, esta tendencia será más acusada en los próximos años. En consecuencia, esta patología se encuentra entre las entidades que demandan una mayor atención en nuestro sistema sanitario (*OMS, 2014*).

Técnicas de imagen como el *speckle tracking* mediante ecocardiografía se han empleado para observar el estado de la deformación del tejido cardíaco poco después del IAMEST y se ha observado que la afectación de la deformación puede predecir la recuperación local de la función cardiaca y los ECVA (*Wang et al. Eur Heart J 2016; Ersbøll et al. J Am Coll Cardiol 2013*). La resolución, la precisión y la accesibilidad de la RMC para los pacientes en fases tempranas tras un IAMEST hacen que las técnicas de imagen mediante RMC sean el futuro y/o presente para la cuantificación precisa del *strain*.

1. Strain miocárdico mediante TT-RMC y su valor pronóstico tras un IAMEST

El *tissue tagging* medido mediante RMC ha sido considerado el mejor método para determinar la deformación miocárdica y la función sistólica. Sin embargo, algunas de sus limitaciones como la necesidad de realizar secuencias de adquisición adicionales o su costoso procesamiento hacen que se hayan seguido desarrollando nuevas técnicas de imagen (*Khan et al. Eur J Radiol 2015*).

Una de las técnicas que ha surgido con más fuerza ha sido el TT-RMC, que está llamado a convertirse en el mejor método para la cuantificación del *strain*. Debido a la excelente resolución espacial de la RMC, las limitaciones relacionadas con la calidad de imagen son casi inexistentes. Algunos estudios han observado que el TT-RMC es

capaz de predecir la recuperación sistólica tardía poco después del infarto (*Buss et al. Int J Cardiol 2015*) y que, en comparación con el *tagging*, proporciona un mejor seguimiento del miocardio, una menor variabilidad interobservador, un análisis más rápido y una correlación más fuerte con índices tradicionales de RMC referentes como el tamaño del infarto (*Khan et al. Eur J Radiol 2015*).

En el primer trabajo, se observó que los pacientes con ECVA presentaban una mayor alteración de todos los índices de *strain* cuantificados (LS, CS y RS globales). Sin embargo, el LS global fue el único de todos ellos relacionado independientemente con ECVA. Estudios anteriores de ecocardiografía también habían determinado que el LS global era el índice más apropiado en pacientes isquémicos para predecir ECVA como la muerte o la insuficiencia cardiaca (*Wang et al. Eur Heart J 2016; Ersbøll et al. J Am Coll Cardiol 2013; Biering-Sørensen et al. PLoS One 2016*). En base a estas observaciones y a nuestros propios resultados, sólo fue incluido el LS global en el análisis multivariado posterior, en el que se incluyeron tanto las variables clínicas basales como los índices tradicionales de RMC. Después de un ajuste mediante todos estos índices, sólo 3 variables surgieron como significativamente independientes, aportando información pronóstica significativa para predecir ECVA: el tiempo transcurrido desde que empieza el dolor hasta la reperfusión, la puntuación de riesgo TIMI y el LS global.

Este estudio demostró el valor pronóstico del LS global por TT-RMC en una población IAMEST homogénea. Además, dichos resultados fueron confirmados por una cohorte de validación externa.

Aunque el LS global fue seleccionado como un predictor independiente por el modelo multivariado final tanto en el grupo de estudio como en la cohorte de validación externa, estos modelos no

mejoraron significativamente la precisión de la discriminación y la reclasificación del riesgo en comparación con los modelos que incluían únicamente características clínicas basales y variables tradicionales de RMC. Creemos que los principales factores que pudieron contribuir a esta observación fueron: 1) la robustez de las puntuaciones clínicas y la tecnología actual (en este caso, los índices RMC tradicionales) para fines pronósticos hace que cada vez sea más difícil lograr mejoras sustanciales en la predicción del riesgo mediante la adición de nuevos índices (*Wang et al. N Engl J Med 2006*); y 2) la presencia de colinealidad entre LS global y la FEVI podría haber obstaculizado el poder discriminatorio adicional del LS global.

Los datos presentados indicaron que TT-RMC podría usarse en mediciones rutinarias de RMC con fines pronósticos en pacientes post-IAMEST. Sin embargo, al observar la falta de mejora en la discriminación, junto con la gran evidencia científica que respalda el valor pronóstico de la FEVI, el tamaño del infarto y la obstrucción microvascular derivada de la RMC después de un IAMEST (*van Kranenburg et al. J Am Coll Cardiol Img 2014; Bodí et al. J Am Coll Cardiol Img 2009*), nuestra interpretación fue que el TT-RMC podría complementar, pero no sustituir, el uso de estos índices consolidados.

Durante las semanas posteriores a un IAMEST, el VI puede sufrir cambios en el volumen, la geometría y la función asociados con el desarrollo de insuficiencia cardíaca, un proceso conocido como remodelación adversa (*Bolognese et al. Circulation 2002; Gheorghiade et al. Circulation 1998; Goldberg et al. Arch Intern Med 1999*). Aunque no existe una definición universalmente aceptada de la remodelación adversa, el criterio más utilizado para definirla ha sido el de un aumento relativo del 15% al 20% en el VTDVI (*Bolognese et al. Circulation 2002; Gaudron et al. Circulation 1993*). La incidencia y

el alcance del RAVI tras un IAMEST han disminuido tras el descubrimiento de la ACTP y el uso casi sistemático de medicamentos "antirremodelación" (como inhibidores de la enzima convertidora de angiotensina y betabloqueantes). Sin embargo, estas mejoras no han sido suficientes para evitar el RAVI, que sigue siendo un evento relativamente frecuente después de un IAMEST (*Cung et al. N Engl J Med 2015; Savoye et al. Am J Cardiol 2006*).

2. El valor pronóstico del remodelado ventricular en pacientes IAMEST

Durante la realización de esta Tesis hemos podido comprobar que la incidencia de ECVA en pacientes tratados con ACTP después de un IAMEST no es trivial. En la realización de nuestro segundo trabajo descubrimos como tanto el LS global como el CS global se encontraban altamente relacionados con los eventos relacionados con el RAVI y, también mostraron una asociación con el aumento del VTDVI tras 6 meses. Esto confirma los resultados obtenidos por Na et al., Bonios et al. y Park et al. que ya vieron, mediante *speckle tracking* en pacientes IAMEST con infarto anterior, que tanto el LS global como el CS global eran unos excelentes predictores del RAVI (Na et al. J Cardiovasc Ultrasound 2016; *Bonios et al. Hellenic J Cardiol 2014; Park et al. J Am Soc Echocardiogr 2008*). Sin embargo, contrasta con Shetye et al. que con una cohorte pequeña concluyeron que el *strain* era incapaz de predecir la remodelación (*Shetye et al. BMC Cardiovasc Disord 2017*).

Tras el análisis descubrimos que la definición de RAVI que mayor valor pronóstico tenía es la que tiene en cuenta tanto los cambios en el VTDVI como los cambios en la FEVI, por tanto, no incluye ningún índice de *strain*. El aumento aislado del VTDVI no se asoció estadísticamente con un resultado adverso. Sin embargo, el

aumento del VTDVI en presencia de una disminución de FEVI sí que implicó un peor pronóstico. Los criterios que mejor identificaron a los pacientes según su riesgo de ECVA en los años posteriores fueron un aumento relativo en el VTDVI del 15% o más y una reducción del 3% o más en la FEVI durante los 6 meses posteriores a un IAMEST.

Sin embargo, estos cambios en el VTDVI y la FEVI durante los primeros 6 meses después de un IAMEST no aumentó el valor pronóstico del *strain* ni de las principales variables derivadas de la RMC obtenidas durante la hospitalización.

Dada la importancia pronóstica de la información obtenida de la RMC temprana, no es sorprendente que la información obtenida de la RMC de seguimiento no aumente su valor pronóstico. En nuestro estudio, la RMC temprana se realizó tras una semana aproximadamente del IAMEST, cuando la mayoría de los cambios dinámicos en el área infartada (por ejemplo, edema, obstrucción microvascular) habían ocurrido y la necrosis era más estable *(Bulluck et al. J Am Coll Cardiol Img 2017*). Esto también podría influir potencialmente en la ausencia de un aumento en el valor pronóstico de la RMC de seguimiento.

Estos resultados son consistentes con la idea de que los cambios tempranos en el VI en la fase aguda de IAMEST, según lo evaluado por RMC, resume los efectos de la reperfusión y son importantes para determinar el RAVI y los ECVA.

Después de un IAMEST, la pérdida de actividad contráctil en los segmentos del infarto y su expansión pueden aumentar la tensión en los segmentos distantes. En el área del infarto, la infiltración temprana de neutrófilos y la liberación de citocinas proinflamatorias reclutan otras células inflamatorias que participan en la eliminación de los cardiomiocitos necróticos y en la diferenciación de fibroblastos en

miofibroblastos que juegan un papel esencial en el proceso de reparación (*Frangogiannis. Nat Rev Cardiol 2014*). La fase reparadora se asocia con una reducción en las células proinflamatorias y un aumento de los macrófagos antiinflamatorios. El aumento del estrés de la pared en el miocardio sano y distante puede conducir a hipertrofia excéntrica progresiva, dilatación del VI, insuficiencia cardíaca y RAVI (*Shah et al. Eur J Heart Fail 2010*). Es importante tener en cuenta que el miocardio salvado y distante también está infiltrado por células inflamatorias que modulan la hipertrofia y la fibrosis (*Inserte et al. Cardiovasc Res 2012; Frangogiannis. Circ Res 2012*).

Por ello, después de la realización de estos dos estudios se decidió evaluar el estado del MRNI tras un primer infarto. El TT-RMC es una herramienta que podría proporcionar información valiosa para caracterizar la movilidad del MRNI y monitorizar su dinámica y sus implicaciones estructurales, independientemente del área infartada. Además, este estudio permitiría determinar el significado pronóstico de esta región del miocardio, sin tener en cuenta el resto del miocardio más deteriorado por el infarto.

El TT-RMC se ha convertido en una excelente técnica para cuantificar el *strain* en pacientes IAMEST (*Khan et al. Eur J Radiol 2015; Buss et al. Int J Cardiol 2015*). Además, recientemente ha confirmado su valor pronóstico y su utilidad en la guía hacia nuevas terapias en pacientes IAMEST (*Bodí. J Am Coll Cardiol Img 2018; Podlesnikar et al. J Am Coll Cardiol Img 2019*).

3. Dinámica e implicaciones estructurales del LS-MRNI

Durante los últimos años ha existido cierta controversia sobre la contractilidad en el área del MRNI: mientras algunos estudios sugieren la presencia de una movilidad realzada compensatoria en

esta región (*Ito et al. Jpn Heart J 1999*), otros indican un deterioro de la función y anormalidades estructurales (*Bodí et al. Int J Cardiol 1999; Husser et al. Int J Cardiol Img 2012*).

Sin embargo, hasta el momento la dinámica y las implicaciones estructurales del LS-MRNI medido mediante TT o *speckle-tracking* no había sido todavía estudiado.

Durante el presente trabajo hemos observado que casi la mitad (48%) de los pacientes y el 37% de los segmentos ubicados en MRNI tenían un LS-MRNI alterado. La presencia del LS-MRNI alterado en la primera semana se asoció con anomalías graves de los parámetros tradicionales de RMC. Es de destacar que este subgrupo mostró una FEVI mucho más deprimida y un tamaño de infarto más grande que los pacientes con el LS-MRNI preservado en la primera semana (tanto en fase aguda como en fase crónica).

Los mecanismos fisiopatológicos subyacentes a estas asociaciones no se han dilucidado completamente. Aunque no se puede descartar un cierto grado de fibrosis remota o pérdida de células en la fase crónica en pacientes con infartos muy grandes, nuestros datos actuales y anteriores parecen sugerir que en estos pacientes hay anormalidades en el movimiento de la pared del área no infartada debido principalmente a una sobrecarga hemodinámica. De hecho, se podría especular que la eficacia de las diferentes terapias recomendadas en este entorno (es decir, betabloqueantes, inhibición del sistema renina-angiotensina-aldosterona o sacubitril-valsartán) podría verse parcialmente afectada por la reducción de la sobrecarga en MRNI (*Ibáñez et al. Eur Heart J 2018; Ponikowski et al. Eur Heart J 2016*).

Se detectó una tendencia hacia la recuperación espontánea del LS-MRNI. Esta tendencia refleja la conocida trayectoria del área

infartada en el contexto del aturdimiento miocárdico (*Bodí et al. J Am Coll Cardiol 2005*). Dicha mejoría se produjo principalmente en pacientes con un LS-MRNI alterado en la primera semana, de tal manera que las diferencias con respecto a los pacientes con el LS-MRNI conservado se acortaron significativamente en la fase crónica después del infarto.

La FEVI representa la variable más consolidada en la estratificación del riesgo después de un IAMEST (*Ibáñez et al. Eur Heart J 2018; Gavara et al. J Am Coll Cardiol Img 2018*) y la dinámica de LS-MRNI parece crucial para explicar el estado de la FEVI en fase crónica. La mejora tardía del LS-MRNI se asoció con una FEVI más preservada a los 6 meses. Beneficiando principalmente a aquellos pacientes que más lo necesitaban, es decir, los pacientes con una FEVI deprimida en la fase aguda del infarto mostraron una mayor mejoría relativa (ΔFEVI), lo que se correlacionó con una mayor mejora del LS-MRNI (ΔLS-MRNI).

Implicaciones pronósticas del LS-MRNI

Este es el primer estudio que demuestra una relación entre el LS-MRNI tras un IAMEST y los ECVA. Se detectó una asociación significativa entre el LS-MRNI y la tasa de ECVA, tanto a nivel continuo como categórico. Aunque, tanto en el grupo de estudio como en el de validación los pacientes con el LS-MRNI alterado presentaron una mayor tendencia a padecer ECVA, existieron diferencias entre ambos grupos en los resultados. Esto fue debido a que el número de pacientes del grupo de validación fue más pequeño y que en este grupo el número de pacientes con el LS-MRNI alterado y no alterado no estaba tan equilibrado. Además, en el análisis multivariado en el que se incluyeron las variables clínicas basales y los índices tradicionales de RMC, el LS-MRNI surgió como una

variable independiente asociada con ECVA. Estos resultados están en línea con los obtenidos en el primer trabajo de esta Tesis (*Gavara et al. J Am Coll Cardiol Img 2018*) dónde demostramos el valor pronóstico de LS global en este mismo registro de pacientes.

Con este estudio no pretendemos sugerir el uso rutinario del LS-MRNI para la estratificación del riesgo más allá del amplio abanico de índices clínicos, biomarcadores y parámetros estructurales potentes que se encuentran bien establecidos en la actualidad y que permiten una estratificación precisa del riesgo de pacientes con IAMEST (*Ibáñez et al. Eur Heart J 2018*). Sin embargo, nuestros datos pueden ser útiles para ilustrar el posible impacto clínico perjudicial de una reducción de la deformación en el MRNI, y la necesidad de prestar más atención al MRNI después de un IAMEST.

El hecho de que el área infartada comprenda miocardio disfuncional y ya necrótico probablemente motivó el hallazgo de que sus cambios dinámicos fueran menos sorprendentes que los observados en el MRNI viable. Además, en general, el MRNI representa una proporción mayor del VI que el área infartada. Esto probablemente explica por qué el LS-MRNI fue más determinante en la recuperación tardía de la FEVI y en la aparición de ECVA que el LS-infarto.

VII.- CONCLUSIONS

1. In ST-segment elevation myocardial infarction (STEMI) patients, global strain (global longitudinal strain [LS], global circumferential strain [CS] and global radial strain) evaluated by tissue tracking cardiovascular magnetic resonance is associated with worse prognosis. However, global LS is the only strain index significantly and independently associated with major adverse cardiac events after adjustment by clinical and traditional cardiovascular magnetic resonance indices.

2. In an external validation cohort from a second University Hospital, all strain indices were associated with major adverse cardiac events. In this cohort, global LS was also the only strain index independently associated with major adverse cardiac events after adjustment by clinical and traditional cardiovascular magnetic resonance indices. However, global LS did not substantially improve risk reclassification in either of the two cohorts beyond traditional cardiovascular magnetic resonance indices.

3. In a large series comprising STEMI patients from two University Hospitals, global LS and global CS strain indices were associated with worse prognostic. However, the best definition of left ventricular adverse remodeling for major adverse cardiac events prediction is a more than 15% relative increase in left ventricular end diastolic volume and a more than 3% relative decrease in left ventricular ejection fraction. Therefore, none of the strain indices significantly explain left ventricular adverse remodeling for major adverse cardiac event prediction.

4. LS by tissue tracking represents an excellent tool to characterize remote non-infarcted myocardium in STEMI patients. Although remote-LS was altered in nearly half the cases, altered remote-LS tends to recover to normal values of LS in chronic phase, causing a spontaneous recovery of left ventricular ejection fraction.

5. In STEMI patients, altered remote-LS by tissue tracking is associated with more severe short- and long-term structural consequences in the left ventricle and with a higher risk of clinical events.

VIII.- CONCLUSIONES

1. En pacientes IAMEST, los tres índices de *strain* globales del ventrículo izquierdo cuantificados mediante *tissue tracking* (LS, CS y RS globales) se asociaron con un peor pronóstico. Sin embargo, el LS global fue el índice de *strain* que más información pronóstica proporcionaba, ya que fue el único de los tres que se asoció de manera significativa e independiente con los eventos adversos tras ajustarse con las características clínicas e índices tradicionales de resonancia magnética cardíaca.

2. Se confirmó mediante una cohorte de validación externa de un segundo Hospital Universitario que el LS global es el índice de *strain* que más información pronóstica aportaba para la predicción de eventos en pacientes IAMEST, a la altura de índices tradicionales de resonancia magnética cardíaca como la fracción de eyección o el tamaño de infarto. Sin embargo, en ninguno de los dos casos el *strain* fue capaz de incrementar de manera significativa la estratificación de riesgo aportada por los índices tradicionales de resonancia magnética cardíaca.

3. En una serie amplia compuesta por pacientes IAMEST de dos Hospitales Universitarios el *strain* (LS global y CS global) se asoció con un peor pronóstico. Sin embargo, la mejor definición de remodelado adverso para la predicción de eventos fue la compuesta por un incremento relativo del volumen telediastólico superior al 15% y un descenso relativo en la fracción de eyección del 3%. Por tanto, el *strain* no formó parte de esta nueva definición de remodelado adverso.

4. El *tissue tracking* es una excelente técnica de imagen que permite caracterizar el LS en el área del miocardio remoto no infartado. En pacientes IAMEST, el LS se encontraba alterado en una gran proporción de los segmentos del miocardio remoto tras el infarto. Sin embargo, existe una tendencia a la recuperación espontánea del

LS en esa zona, lo que ejerce un efecto decisivo en la recuperación de la fracción de eyección.

5. Una alteración del LS en el miocardio remoto en la fase aguda tras el IAMEST se asoció con consecuencias estructurales más graves a corto y largo plazo en el ventrículo izquierdo y se relacionó de manera significativa e independiente con un peor pronóstico.

IX.- BIBLIOGRAFÍA

Aguilar J, Garabito RD. Infarto agudo de miocardio. Revista Paceña Medicina Familiar 2008;5:102–114.

Amzulescu MS, De Craene M, Langet H, Pasquet A, Vancraeynest D, Pouleur AC, et al. Myocardial strain imaging: review of general principles, validation, and sources of discrepancies. Eur Heart J Cardiovasc Imaging 2019;20:605–19.

Atlas 2014. World Health Organization WHO. Global atlas on cardiovascular disease prevention and control: Policies, strategies and interventions. 2011.

Biering-Sørensen T, Jensen JS, Pedersen SH, Galatius S, Fritz-Hansen T, Bech J, et al. Regional longitudinal myocardial deformation provides incremental prognostic information in patients with ST-segment elevation myocardial infarction. PLoS One 2016;11:e0158280.

Bodí V, Sanchís J, Berenguer A, Insa LD, Chorro FJ, Llácer A, et al. Wall motion of noninfarcted myocardium. Relationship to regional and global systolic function and to early and late left ventricular dilation. Int J Cardiol 1999;71:157–65.

Bodí V, Sanchís J, López-Lereu MP, Losada A, Núñez J, Pellicer M, et al. Usefulness of a comprehensive cardiovascular magnetic resonance imaging assessment for predicting recovery of left ventricular wall motion in the setting of myocardial stunning. J Am Coll Cardiol 2005;46:1747–52.

Bodí V, Sanchís J, Núñez J, Mainar L, López-Lereu MP, Monmeneu JV, et al. Prognostic value of a comprehensive cardiac magnetic resonance assessment soon after a first ST-segment elevation myocardial infarction. J Am Coll Cardiol Img 2009;2:835–42.

Bodí V. Strain by feature tracking: a short summary of the journey of CMR in STEMI. J Am Coll Cardiol Img 2018. pii:S1936-878X(18)30731-9.

Boersma E, Mercado N, Poldermans D, Gardien M, Vos J, Simoons ML. Acute myocardial infarction. Lancet 2003;361:847–58.

Bolognese L, Neskovic AN, Parodi G, Cerisano G, Buonamici P, Santoro GM, et al. Left ventricular remodeling after primary coronary angioplasty: patterns of left ventricular dilation and long-term prognostic implications. Circulation 2002;106:2351–7.

Bonios MJ, Kaladaridou A, Tasoulis A, Papadopoulou E, Pamboukas C, Ntalianis A, et al. Value of apical circumferential strain in the early post-myocardial infarction period for prediction of left ventricular remodeling. Hellenic J Cardiol 2014;55:305–12.

Brooks GC, Lee BK, Rao R, Lin F, Morin DP, Zweibel SL, et al. Predicting persistent left ventricular dysfunction following myocardial infarction: the PREDICTS study. J Am Coll Cardiol 2016;67:1186–96.

Buckberg G, Hoffman JI, Mahajan A, Saleh S, Coghlan C. Cardiac mechanics revisited: the relationship of cardiac architecture to ventricular function. Circulation 2008;118:2571–87.

Bueno H, Martín-Asenjo R. Acute heart failure after STEMI. Still a problem, still an opportunity for improving care quality. Int J Cardiol 2017;248:274–5.

Bulluck H, Go YY, Crimi G, Ludman AJ, Rosmini S, Abdel-Gadir A, et al. Defining left ventricular remodeling following acute ST-segment elevation myocardial infarction using cardiovascular magnetic resonance. J Cardiovasc Magn Reson 2017;19:26.

Bulluck H, Hammond-Haley M, Weinmann S, Martinez-Macias R, Hausenloy DJ. Myocardial infarct size by CMR in clinical cardioprotection studies: insights from randomized controlled trials. J Am Coll Cardiol Img 2017;10:230–40.

Buss SJ, Krautz B, Hofmann N, Sander Y, Rust L, Giusca S, et al. Prediction of functional recovery by cardiac magnetic resonance feature tracking imaging in first time ST-elevation myocardial infarction. Comparison to infarct size and transmurality by late gadolinium enhancement. Int J Cardiol 2015;183:162–70.

Carrick D, Haig C, Rauhalammi S, Ahmed N, Mordi I, McEntegart M, et al. Pathophysiology of LV remodeling in survivors of STEMI: inflammation, remote myocardium, and prognosis. J Am Coll Cardiol Img 2015;8:779–89.

Cerqueira MD, Weissman NJ, Dilsizian V, Jacobs AK, Kaul S, Laskey WK, et al. Standardized myocardial segmentation and nomenclature for tomographic imaging of the heart. A statement for healthcare professionals from the Cardiac Imaging Committee of the Council on Clinical Cardiology of the American Heart Association. Circulation 2002;105:539–42.

Conrad CH, Brooks WW, Hayes JA, Sen S, Robinson KG, Bing OH. Myocardial fibrosis and stiffness with hypertrophy and heart failure in the spontaneously hypertensive rat. Circulation 1995;91:161–70.

Cuberas-Borrós G, Aguadé-Bruix S, Boronat-de Ferrater M, Muxí-Pradas MA, Romero-Farina G, Castell-Conesa J, et al. Base de datos de normalidad de la SPECT de perfusión miocárdica en la población española. Rev Esp Cardiol 2010;63:934–42.

Cung TT, Morel O, Cayla G, Rioufol G, Garcia-Dorado D, Angoulvant D, et al. Cyclosporine before PCI in patients with acute myocardial infarction. N Engl J Med 2015;373:1021–31.

Ersbøll M, Valeur N, Mogensen UM, Andersen MJ, Møller JE, Velazquez EJ, et al. Prediction of all-cause mortality and heart failure admissions from global left ventricular longitudinal strain in patients with acute myocardial infarction and preserved left ventricular ejection fraction. J Am Coll Cardiol 2013;61:2365–73.

Frangogiannis NG. Regulation of the inflammatory response in cardiac repair. Circ Res 2012;110:159–73.

Frangogiannis NG. The inflammatory response in myocardial injury, repair, and remodeling. Nat Rev Cardiol 2014;11:255–65.

Gaudron P, Eilles C, Kugler I, Ertl G. Progressive left ventricular dysfunction and remodeling after myocardial infarction. Potential mechanisms and early predictors. Circulation 1993;87:755–63.

Gavara J, Rodríguez-Palomares JF, Valente F, Monmeneu JV, López-Lereu MP, Bonanad C, et al. Prognostic value of strain by tissue tracking cardiovascular magnetic resonance after ST-segment elevation myocardial infarction. J Am Coll Cardiol Img 2018;11:1448–57.

Gheorghiade M, Bonow RO. Chronic heart failure in the United States: a manifestation of coronary artery disease. Circulation 1998;97:282–9.

Goldberg RJ, Konstam MA. Assessing the population burden from heart failure: need for sentinel population-based surveillance systems. Arch Intern Med 1999;159:15–7.

GUSTO investigators. An international randomized trial comparing four thrombolytic strategies for acute myocardial infarction. N Engl J Med 1993;329:673–82.

Hansson GK, Libby P. The immune response in atherosclerosis: a double-edged sword. Nat Rev Immunol 2006;6:508–19.

Husser O, Chaustre F, Sanchis J, Nunez J, Monmeneu JV, Lopez-Lereu MP, et al. Function of remote non-infarcted myocardium after STEMI: analysis with cardiovascular magnetic resonance. Int J Cardiol Img 2012;28:2057–64.

Ibáñez B, Heusch G, Ovize M, Van de Werf F. Evolving therapies for myocardial ischemia/reperfusion injury. J Am Coll Cardiol 2015;65:1454–71.

Ibáñez B, James S, Agewall S, Antunes MJ, Bucciarelli-Ducci C, Bueno H, et al. 2017 ESC Guidelines for the management of acute myocardial infarction in patients presenting with ST-segment elevation: The Task Force for the management of acute myocardial infarction in patients presenting with ST-segment elevation of the European Society of Cardiology (ESC). Eur Heart J 2018;39:119–77.

Inserte J, Hernando V, Garcia-Dorado D. Contribution of calpains to myocardial ischaemia/reperfusion injury. Cardiovasc Res 2012;96:23–31.

Ito S, Suzuki T, Hosokawa H, Inada T, Takeda Y, Suzumura H, et al. Increased hyperkinesis in noninfarcted areas during short-term

follow-up in patients with first anterior acute myocardial infarction treated by direct percutaneous transluminal coronary angioplasty. Jpn Heart J 1999;40:549–60.

Jasaityte R, Heyde B, D'hooge J, et al. Current state of three-dimensional myocardial strain estimation using echocardiography. J Am Soc Echocardiogr 2013;26:15–28.

Karamitsos TD, Francis JM, Myerson S, Selvanayagam JB, Neubauer S. The role of cardiovascular magnetic resonance imaging in heart failure. J Am Coll Cardiol 2009;54:1407–24.

Karamitsos TD, Hudsmith LE, Selvanayagam JB, Neubauer S, Francis M. Operator induced variability in left ventricular measurements with cardiovascular magnetic resonance is improved after training. J Cardiovasc Magn Reson 2007;9:777–83.

Khan JN, Singh A, Nazir SA, Kanagala P, Gershlick AH, McCann GP. Comparison of cardiovascular magnetic resonance feature tracking and tagging for the assessment of left ventricular systolic strain in acute myocardial infarction. Eur J Radiol 2015;84:840–8.

Libby P. Inflammation in atherosclerosis. Nature 2002;420:868–74.

Loutfi M, Ashour S, El-Sharkawy E, El-Fawal S, El-Touny K. Identification of high-risk patients with non-ST segment elevation myocardial infarction using strain Doppler echocardiography: correlation with cardiac magnetic resonance imaging. Clin Med Insights Cardiol 2016;10:51–9.

Mahrholdt H, Wagner A, Judd RM, Sechtem U, Kim RJ. Delayed enhancement cardiovascular magnetic resonance assessment

of non-ischaemic cardiomyopathies. Eur Heart J 2005;26:1461–74.

Martos R, Baugh J, Ledwidge M, O'Loughlin C, Conlon C, Patle A, et al. Diastolic heart failure: evidence of increased myocardial collagen turnover linked to diastolic dysfunction. Circulation 2007;115:888–95.

Mewton N, Liu CY, Croisille P, Bluemke D, Lima JA. Assessment of myocardial fibrosis with cardiac magnetic resonance. J Am Coll Cardiol 2011;57:891–903.

Na HM, Cho GY, Lee JM, Cha MJ, Yoon YE, Lee SP, et al. Echocardiographic predictors for left ventricular remodeling after acute ST elevation myocardial infarction with low risk group: speckle tracking analysis. J Cardiovasc Ultrasound 2016;24:128–34.

Niccoli G, Scalone G, Lerman A, Crea F. Coronary microvascular obstruction in acute myocardial infarction. Eur Heart J 2016;37:1024–33.

OMS: The World Health Report 2004–Changing History. Edited by Salud OMdl:2014:120-4.

Ortiz-Perez JT, Rodríguez J, Meyers SN, Lee DC, Davidson C, Wu E. Correspondence between the 17-segment model and coronary arterial anatomy using contrast-enhanced cardiac magnetic resonance imaging. J Am Coll Cardiol Img 2008;1:282–93.

Park YH, Kang SJ, Song JK, Lee EY, Song JM, Kang DH, et al. Prognostic value of longitudinal strain after primary reperfusion therapy in patients with anterior-wall acute myocardial infarction. J Am Soc Echocardiogr 2008;21:262–7.

Pfeffer MA, Braunwald E. Ventricular remodeling after myocardial infarction. Experimental observations and clinical implications. Circulation 1990;81:1161–72.

Podlesnikar T, Pizarro G, Fernández-Jiménez R, Montero-Cabezas JM, Sánchez-González J, Bucciarelli-Ducci C, et al. Effect of early metoprolol during ST-segment elevation myocardial infarction on left ventricular strain: feature-tracking cardiovascular magnetic resonance substudy from the METOCARD-CNIC trial. J Am Coll Cardiol Img 2019;12:1188–98.

Ponikowski P, Voors AA, Anker SD, Bueno H, Cleland JGF, Coats AJS, et al. 2016 ESC guidelines for the diagnosis and treatment of acute and chronic heart failure: The Task Force for the diagnosis and treatment of acute and chronic heart failure of the European Society of Cardiology (ESC). Eur Heart J 2016;37:2129–200.

Lorenzo R. El electrocardiograma en el infarto agudo de miocardio. Rev Urug Cardiol 2013;28:419–429.

Savoye C, Equine O, Tricot O, Nugue O, Segrestin B, Sautière K, et al. Left ventricular remodeling after anterior wall acute myocardial infarction in modern clinical practice (from the REmodelage VEntriculaire [REVE] study group). Am J Cardiol 2006;98:1144–9.

Schiele F, Gale CP, Bonnefoy E, Capuano F, Claeys MJ, Danchin N, et al. Quality indicators for acute myocardial infarction: a position paper of the Acute Cardiovascular Care Association. Eur Heart J Acute Cardiovasc Care 2017;6:34–59.

Shah AM, Solomon SD. A unified view of ventricular remodeling. Eur J Heart Fail 2010;12:779–81.

Shetye A, Nazir SA, Razvi NA, Price N, Khan JN, Lai FY, et al. Comparison of global myocardial strain assessed by cardiovascular magnetic resonance tagging and feature tracking to infarct size at predicting remodelling following STEMI. BMC Cardiovasc Disord 2017;17:7.

Shetye A, Nazir SA, Squire IB, McCann GP. Global myocardial strain assessment by different imaging modalities to predict outcomes after ST-elevation myocardial infarction: A systematic review. World J Cardiol 2015;7:948–60.

Sun Y. Myocardial repair/remodelling following infarction: roles of local factors. Cardiovasc Res 2009;81:482–90.

Thavendiranathan P, Poulin F, Lim KD, Plana JC, Woo A, Marwick TH. Use of myocardial strain imaging by echocardiography for the early detection of cardiotoxicity in patients during and after cancer chemotherapy: a systematic review. J Am Coll Cardiol 2014;63:2751-68.

TIMI Study Group. The Thrombolysis in Myocardial Infarction (TIMI) trial. Phase I findings. N Engl J Med 1985;312:932–6.

van Kranenburg M, Magro M, Thiele H, de Waha S, Eitel I, Cochet A, et al. Prognostic value of microvascular obstruction and infarct size, as measured by CMR in STEMI patients. J Am Coll Cardiol Img 2014;7:930–9.

van 't Hof AW, Liem A, Suryapranata H, Hoorntje JC, de Boer MJ, Zijlstra F. Angiographic assessment of myocardial reperfusion in patients treated with primary angioplasty for acute myocardial

infarction: myocardial blush grade. Zwolle Myocardial Infarction Study Group. Circulation 1998;97:2302–6.

Wang N, Hung CL, Shin SH, Claggett B, Skali H, Thune JJ, et al. Regional cardiac dysfunction and outcome in patients with left ventricular dysfunction, heart failure, or both after myocardial infarction. Eur Heart J 2016;37:466–72.

Wang TJ, Gona P, Larson MG, Tofler GH, Levy D, Newton-Cheh C, et al. Multiple biomarkers for the prediction of first major cardiovascular events and death. N Engl J Med 2006;355:2631–9.

Weaver WD, Simes RJ, Betriu A, Grines CL, Zijlstra F, Garcia E, et al. Comparison of primary coronary angioplasty and intravenous thrombolytic therapy for acute myocardial infarction: a quantitative review. JAMA 1997;278:2093–8.

Zhang Y, Chan AK, Yu CM, Yip GW, Fung JW, Lam WW, et al. Strain rate imaging differentiates transmural from non-transmural myocardial infarction: a validation study using delayed-enhancement magnetic resonance imaging. J Am Coll Cardiol 2005;46:864–71.

X.- ANEXOS

ANEXO I: Gavara J*, Rodríguez-Palomares JF*, Valente F, et al. J Am Coll Cardiol Img 2018;11:1448–57

JACC: CARDIOVASCULAR IMAGING
© 2018 BY THE AMERICAN COLLEGE OF CARDIOLOGY FOUNDATION
PUBLISHED BY ELSEVIER

VOL. 11, NO. 10, 2018

Prognostic Value of Strain by Tissue Tracking Cardiac Magnetic Resonance After ST-Segment Elevation Myocardial Infarction

Jose Gavara, MSc,[a,*] Jose F. Rodriguez-Palomares, MD, PhD,[b,*] Filipa Valente, MD,[b] Jose V. Monmeneu, MD, PhD,[c] Maria P. Lopez-Lereu, MD, PhD,[c] Clara Bonanad, MD, PhD,[a] Ignacio Ferreira-Gonzalez, MD, PhD,[b,d] Bruno Garcia del Blanco, MD, PhD,[b] Julian Rodriguez-Garcia, MD,[b] Maria Mutuberria, MD, PhD,[b] Elena de Dios, MSc,[a] Cesar Rios-Navarro, MSc,[a] Nerea Perez-Sole, BSc,[a] Paolo Racugno, MD,[a] Ana Paya, MD,[a] Gema Minana, MD, PhD,[a] Joaquim Canoves, MD, PhD,[a,e] Mauricio Pellicer, MD,[a] Francisco J. Lopez-Fornas, MD, PhD,[a] Jose Barrabes, MD, PhD,[b] Arturo Evangelista, MD, PhD,[b] Julio Nunez, MD, PhD,[a] Francisco J. Chorro, MD, PhD,[a,e] David Garcia-Dorado, MD, PhD,[b,e] Vicente Bodi, MD, PhD[a,e]

ABSTRACT

OBJECTIVES The aim of this study was to evaluate the prognostic value of strain as assessed by tissue tracking (TT) cardiac magnetic resonance (CMR) soon after ST-segment elevation myocardial infarction (STEMI).

BACKGROUND The prognostic value of myocardial strain as assessed post-STEMI by TT-CMR is unknown.

METHODS The authors studied the prognostic value of TT-CMR in 323 patients who underwent CMR 1 week post-STEMI. Global (average of peak segmental values [%]) and segmental (number of altered segments) longitudinal (LS), circumferential, and radial strain were assessed using TT-CMR. Global and segmental strain cutoff values were derived from 32 control patients. CMR-derived left ventricular ejection fraction, microvascular obstruction, and infarct size were determined. Results were validated in an external cohort of 190 STEMI patients.

RESULTS During a median follow-up of 1,085 days, 54 first major adverse cardiac events (MACE), which included 10 cardiac deaths, 25 readmissions for heart failure, and 19 readmissions for reinfarction were documented. MACE was associated with more severe abnormalities in all strain indexes ($p < 0.001$), although only global LS was an independent predictor ($p < 0.001$). The MACE rate was higher in patients with a global LS of $\geq -11\%$ (22% vs. 9%; $p = 0.001$). After adjustment for baseline and CMR variables, global LS (hazard ratio [HR]: 1.21; 95% confidence interval [CI]: 1.11 to 1.32; $p < 0.001$) was associated with MACE. In the external validation cohort, a global LS $\geq -11\%$ was seen in a higher proportion of patients with MACE (34% vs. 9%; $p < 0.001$). Global LS predicted MACE after adjustment for baseline and CMR variables (HR: 1.18; 95% CI: 1.04 to 1.33; $p = 0.008$). The addition of global LS to the multivariate models, including baseline and CMR variables, did not significantly improve the categorical net reclassification improvement index in either the study group (−0.015; $p = 0.7$) or in the external validation cohort (−0.019; $p = 0.9$).

CONCLUSIONS TT-CMR provided prognostic information soon after STEMI. However, it did not substantially improve risk reclassification beyond traditional CMR indexes. (J Am Coll Cardiol Img 2018;11:1448-57)
© 2018 by the American College of Cardiology Foundation.

From the [a]Department of Cardiology, Hospital Clínico Universitario, INCLIVA, University of Valencia, Valencia, Spain; [b]Hospital Universitari Vall d'Hebron, Department of Cardiology, Vall d'Hebron Institut de Recerca (VHIR), Universitat Autònoma de Barcelona, Barcelona, Spain; [c]Cardiovascular Magnetic Resonance Unit, ERESA, Valencia, Spain; [d]Centro de Investigación Biomédica en Red-ESP, Madrid, Spain; and the [e]Centro de Investigación Biomédica en Red-CV, Madrid, Spain. This work was supported by the Instituto de Salud Carlos III and co-funded by FEDER (grant numbers PI14/00271, PIE15/00013, CIBERCV16/11/00486, CIBERCV16/11/00479) and the Generalitat Valenciana (grant number PROMETEO/2013/007). The authors have reported that they have no relationships relevant to the contents of this paper to disclose. *Drs. Gavara and Rodriguez-Palomares contributed equally to this work.

Manuscript received April 20, 2017; revised manuscript received September 18, 2017, accepted September 25, 2017.

ISSN 1936-878X/$36.00 https://doi.org/10.1016/j.jcmg.2017.09.017

JACC: CARDIOVASCULAR IMAGING, VOL. 11, NO. 10, 2018
OCTOBER 2018:1448–57

Recent studies have shown that myocardial deformation imaging by speckle tracking echocardiography soon after ST-segment elevation myocardial infarction (STEMI) predicts regional cardiac function recovery (1) and patient outcomes (2,3). Tissue tracking (TT) cardiac magnetic resonance (CMR) is feasible in acute STEMI and promises to be a more accurate method for strain quantification (4,5).

After STEMI, CMR allows for a comprehensive state-of-the-art analysis of the structural consequences of myocardial infarction (6), and CMR indexes have emerged as potent predictors of patient outcomes (7,8). Currently, the prognostic value of the assessment of myocardial strain by TT-CMR soon after STEMI has not been validated. We hypothesized that myocardial strain assessed by TT-CMR permits risk stratification of patients soon after STEMI.

SEE PAGE 1458

METHODS

STUDY GROUP. This is a retrospective study based on a large registry of STEMI patients in a tertiary university hospital (6,8). All patients gave written informed consent. The study protocol was approved by the local ethics committee on human research and complies with the 1975 Declaration of Helsinki guidelines. TT-CMR indexes were retrospectively quantified using currently available software.

Criteria for the study group included patients admitted for a first STEMI, which was defined according to current definitions (9), patients treated with percutaneous coronary intervention, and patients who underwent CMR pre-discharge. From 2002 to 2014, we enrolled 542 patients with these characteristics.

Exclusion criteria were death (n = 22), re-infarction (n = 24), severe clinical instability (n = 36) during admission, and any contraindications to CMR, including claustrophobia (n = 19), previous pacemaker (n = 10), the decision of the patient (n = 7), and a history of adverse reactions to gadolinium contrast (n = 3). TT-CMR measurements were performed retrospectively and were not planned when the registry was started. As a consequence, 98 patients had to be excluded because of incomplete or insufficient image acquisition for an accurate offline assessment of all TT-CMR indexes; the number of phases acquired for short- and long-axis images was different in 81 patients, and in 17 patients 1 of the long-axis images needed for calculations was not available. Thus, the final study group consisted of 323 patients.

Baseline characteristics, including the global registry of acute coronary events (10) and Thrombolysis In Myocardial Infarction (TIMI) (11) risk scores, were prospectively registered in all cases. The percutaneous coronary intervention technique was left at the discretion of the interventional operator. TIMI flow grade in the culprit artery (before and after percutaneous coronary intervention) was analyzed in all cases (12). Patients were managed both in-hospital and after discharge by a specific STEMI unit, and current recommendations were strictly followed (9). Further details on patient characteristics are provided in Table 1.

CARDIAC MAGNETIC RESONANCE. All patients included in the study group were examined with a 1.5-T System (Sonata Magnetom, Siemens, Erlangen, Germany) 7 ± 2 days after STEMI in accordance with our previously validated study protocol (6,8). CMR studies were analyzed offline by an experienced observer blinded to all patient data using customized software (QMASS MR 6.1.5, Medis, Leiden, the Netherlands). CMR data were prospectively incorporated into the database.

Left ventricular ejection fraction (LVEF) (%), LV end-diastolic volume index (ml/m^2), LV end-systolic volume index (ml/m^2), LV mass index (g/m^2), infarct size (% of LV mass), microvascular obstruction (% of LV mass), myocardial edema (% of LV mass), and myocardial salvage index (% of LV mass with myocardial edema not showing delayed enhancement) were calculated.

Further details on the technical aspects of CMR acquisition, sequences, and quantification can be found in the Online Appendix. Interobserver and intraobserver variability for all CMR indexes used in the present study are shown in Online Tables 1A and 1B, and in Online Figure 1.

TISSUE TRACKING CMR. All strain parameters were quantified offline by an experienced observer blinded to all patient data. These analyses were carried out retrospectively using currently available certified software (CMR42, Circle Cardiovascular Imaging Inc., Calgary, Alberta, Canada).

On a segmental basis, the 16-segment model was used for calculation of the peak longitudinal strain (LS), circumferential strain (CS), and radial strain (RS) in each segment (13). On a per-patient basis, the global LS, CS, and RS were calculated as the mean of the respective peak values in the 16 segments (Figure 1).

ABBREVIATIONS AND ACRONYMS

CMR = cardiac magnetic resonance
CS = circumferential strain
EF = ejection fraction
LS = longitudinal strain
LV = left ventricular
MACE = major adverse cardiac event(s)
RS = radial strain
STEMI = ST-segment elevation myocardial infarction
TIMI = Thrombolysis In Myocardial Infarction
TT = tissue tracking

TABLE 1 Baseline Characteristics of the Entire Study Group and of Patients With and Without MACE

	All Patients (N = 323)	MACE (n = 54)	No MACE (n = 269)	p Value
Age, yrs	59 ± 11	63 ± 14	59 ± 11	0.01
Male	268 (83)	43 (80)	225 (84)	0.6
Diabetes mellitus	68 (21)	9 (17)	59 (22)	0.4
Hypertension	154 (48)	30 (56)	124 (46)	0.2
Hypercholesterolemia	147 (46)	25 (46)	122 (45)	0.9
Smoker	182 (56)	32 (59)	150 (56)	0.6
Heart rate on admission, beats/min	79 ± 21	88 ± 25	78 ± 20	<0.001
Systolic pressure, mm Hg	128 ± 30	129 ± 32	128 ± 29	0.9
Killip class				0.009
I	273 (85)	43 (80)	230 (85)	
II	40 (12)	6 (11)	34 (13)	
III	6 (2)	4 (7)	2 (1)	
IV	4 (1)	1 (2)	3 (1)	
Time to reperfusion, min	180 (120-300)	280 (178-424)	210 (120-280)	0.005
Peak creatine kinase MB mass, ng/ml	177 (66-300)	254 (79-423)	161 (60-295)	0.04
Anterior infarction	167 (52)	38 (70)	129 (48)	0.003
Multivessel disease	85 (26)	15 (28)	70 (26)	0.8
TIMI flow grade before PCI				0.9
0	169 (52)	28 (52)	141 (53)	
1	24 (7)	5 (9)	19 (7)	
2	35 (11)	5 (9)	30 (11)	
3	95 (30)	16 (30)	79 (29)	
TIMI flow grade after PCI				0.8
0	4 (1)	0 (0)	4 (1)	
1	1 (1)	0 (0)	1 (1)	
2	26 (8)	5 (9)	21 (8)	
3	292 (90)	49 (91)	243 (90)	
GRACE risk score	136 ± 30	148 ± 31	133 ± 29	0.001
TIMI risk score	2.8 ± 2.2	3.8 ± 2.5	2.6 ± 2.1	<0.001

Values are mean ± SD, n (%), or median (25th to 75th percentile).

GRACE = Global Registry of Acute Coronary Events; MACE = major adverse cardiac event(s); MB = myocardial band; PCI = percutaneous coronary intervention; TIMI = Thrombolysis In Myocardial Infarction.

For categorical analyses, cutoff values were derived from a control group of 32 patients who underwent CMR for a cardiovascular checkup and who had no evidence of structural cardiac disease.

In summary and based on recent literature (2,3), we used the following sets of strain variables: 1) global LS, CS, and RS: mean of the respective peak values in the 16 segments for each patient (3); 2) number of segments in each patient with altered LS, CS, and RS: number of segments with LS and CS above the respective segmental cutoff values and number of segments with RS below the respective segmental cutoff values (2); and 3) patients were considered to have altered global LS if LS was ≥−11%, altered global CS if CS was ≥−14%, and altered global RS if RS was ≤32%.

Further details on the acquisition of strain indexes and definition of cutoff values can be found in the Online Appendix and in Online Table 2.

EXTERNAL VALIDATION COHORT. Although the operator measuring TT-CMR parameters in the study group was blinded to all patient data, and it was improbable that the retrospective quantification of TT-CMR could exert an influence on the association between strain data with patient outcomes, we decided to confirm our results in an external validation cohort.

The external validation cohort included 190 patients admitted for STEMI in a different tertiary hospital; we used the same inclusion and exclusion criteria as the study group. Patient management, CMR scanner characteristics, CMR studies protocol, and CMR software were the same used in the study group, but studies and quantification were carried out by local personnel. In the external validation cohort, all data, including TT-CMR indexes, were prospectively and immediately incorporated into the database. A local experienced observer blinded to all patient data quantified CMR studies of patients included in the external validation cohort. Further details on the external validation cohort are listed in Online Tables 3 and 4. The association of TT-CMR indexes with the occurrence of major adverse cardiac events (MACE) was explored using the same sets of strain indexes and cutoff values tested in the study group.

ENDPOINT AND FOLLOW-UP. The endpoint was time to first MACE and included a composite of cardiac death, readmission for heart failure, or readmission for reinfarction, whichever occurred first. Current definitions were applied (14,15).

As secondary endpoints, we examined the association of altered TT-CMR indexes with: 1) time to the occurrence of cardiac death, readmission for heart failure, and readmission for reinfarction separately in the whole study group; and 2) time to the occurrence of the first MACE in patients with TIMI flow grade 3 after percutaneous coronary intervention (after 31 patients with TIMI flow grade <3 after percutaneous coronary intervention were excluded from the study group).

All MACE were systematically reviewed, and consensus among 3 cardiologists was required to classify a cardiac event.

STATISTICAL ANALYSIS. Data were tested for normal distribution using the Kolmogorov-Smirnov test. Continuous normally distributed data were expressed as the mean ± SD and compared using the unpaired Student's *t* test. Nonparametric data were expressed as the median (interquartile range) and

JACC: CARDIOVASCULAR IMAGING, VOL. 11, NO. 10, 2018
OCTOBER 2018:1448–57

FIGURE 1 Tissue Tracking–Cardiac Magnetic Resonance Assessment

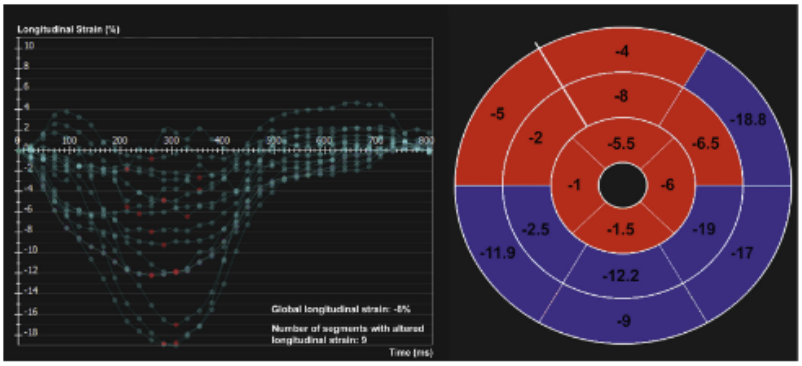

Longitudinal strain throughout the cardiac cycle in the 16 segments of a patient with a large anterior infarction. **Red points** indicate the peak strain values in the respective segments. On a per patient basis, global strain (% deformation) was calculated as the mean of the respective peak values in the 16 segments **(left panel)**. The number of segments displaying abnormal strain (in comparison with segmental values in control patients) was also determined **(right panel)**.

compared using the Mann-Whitney *U* test. Group percentages were compared using the chi-square test or Fisher exact test, where appropriate. In the univariate analyses, the associations of global strain variables with time to the first MACE, time to cardiac death, time to readmission for heart failure, and time to readmission for reinfarction were assessed using Kaplan-Meier curves and the log-rank test.

We performed a first multivariable analysis to test the association of the 6 strain indexes with time to MACE using a multivariable Cox proportional hazard regression model. In this model, the only strain index independently associated with the time to MACE was global LS. To avoid variable overfitting, for subsequent multivariable analyses, global LS was the only strain parameter tested.

The association of global LS with time to MACE adjusted for baseline and CMR variables was assessed using multivariable Cox proportional hazard regression models. The variables adjusted for in the multivariable models to predict time to MACE were identified by comparing patients who did and who did not exhibit MACE during follow-up; variables with a p value < 0.1 were included in the regression models as cofactors. Hazard ratios with the corresponding 95% confidence intervals were computed. The proportional hazards assumption based on Schoenfeld's residuals was considered to be accomplished if the p value was >0.05.

From a clinical point of view and to avoid variable overfitting of the final multivariable model, we carried out the following steps: 1) first, a multivariable model (Model 1: baseline characteristics) was tested, including those baseline variables that showed an association ($p < 0.1$ in Table 1) with the occurrence of MACE; 2) a second multivariable model (Model 2: baseline characteristics plus CMR indexes) included variables from Model 1 independently related to the occurrence of MACEs plus CMR indexes that showed an association with MACE ($p < 0.1$ in Table 2); and 3) the final multivariable model (Model 3: baseline characteristics plus CMR indexes plus global LS) included variables from Model 2 that were independently related to the occurrence of MACE plus global LS. Colinearity of variables tested in the final multivariate Model 3 (independent variables selected in Model 2 plus global LS) was assessed using the tolerance statistic (excessive if <0.20) and the variance inflation factor (excessive if >5) (16). The correlation matrix, including global LS, all CMR indexes, and independent variables in Model 3, was also obtained.

Changes in the discrimination accuracy (c-statistic) and in risk reclassification (using the categorical net reclassification improvement index and the respective frequency data) when global LS was included in the final multivariable model (Model 3 vs. Model 2)

TABLE 2 Cardiac Magnetic Resonance Characteristics of the Entire Study Group and of Patients With and Without MACE

	All Patients (N = 323)	MACE (n = 54)	No MACE (n = 269)	p Values
LVEF, %	53 ± 13	45 ± 15	54 ± 12	<0.001
LV end-diastolic volume index, ml/m^2	80 ± 24	84 ± 28	79 ± 23	0.2
LV end-systolic volume index, ml/m^2	39 ± 22	49 ± 26	37 ± 20	0.005
LV mass, g/m^2	74 ± 19	76 ± 18	74 ± 19	0.4
Edema, % of LV mass	30 ± 17	37 ± 18	28 ± 17	0.001
Microvascular obstruction, % of LV mass	0 (0.0–2.4)	0.2 (0.0–2.7)	0 (0.0–2.4)	0.05
Infarct size, % of LV mass	22 ± 15	28 ± 18	20 ± 14	0.003
Myocardial salvage index, %	22 (2.5–46.0)	15.5 (1.5–40.0)	23 (2.9–48.0)	0.4

Values are mean ± SD or median (25th to 75th percentile).
LV = left ventricular; LVEF = left ventricular ejection fraction; MACE = major adverse cardiac event(s).

were computed both for the study group and for the external validation cohort.

Statistical significance was considered a 2-tailed $p < 0.05$. The SPSS statistical package version 15.0 (SPSS Inc., Chicago, Illinois) and STATA version 9.0 (StataCorp, College Station, Texas) were used.

RESULTS

From the initial study group of 323 patients with a median follow-up of 1,085 days (range 14 to 4,711 days), we documented 54 patients with first MACE, including 10 cardiac deaths, 25 readmissions for heart failure, and 19 readmissions for reinfarction.

Baseline characteristics and cardiac catheterization variables associated with the occurrence of MACE are displayed in Table 1.

Table 2 depicts the state of traditional CMR parameters in the whole study group and in patients with and without MACE during follow-up.

TISSUE TRACKING CMR AND MACE. Table 3 shows the characteristics of the 6 strain indexes determined in the whole study group and in patients with and without MACE during follow-up. Patients with MACE displayed a higher number of segments with abnormal LS, CS, and RS ($p < 0.001$ for all comparisons). Similarly, patients with MACE during follow-up exhibited higher values of global LS and global CS, and lower values of global RS ($p < 0.001$ for all comparisons).

TABLE 3 Strain Characteristics of the Entire Study Group and of Patients With and Without MACE

	All Patients (N = 323)	MACE (n = 54)	No MACE (n = 269)	p Value
Segments with altered CS, n	9.7 ± 3.7	11.3 ± 3.6	9.4 ± 3.6	<0.001
Segments with altered LS, n	9.3 ± 3.7	11.5 ± 3.6	8.8 ± 3.6	<0.001
Segments with altered RS, n	9.7 ± 3.6	11.2 ± 3.6	9.3 ± 3.6	<0.001
Global CS, %	−13.7 ± 4.3	−11.4 ± 4.4	−14.2 ± 4.2	<0.001
Global LS, %	−10.1 ± 3.4	−8.1 ± 3.2	−10.5 ± 3.3	<0.001
Global RS, %	24.9 ± 10.1	20.4 ± 9.8	25.9 ± 10.0	<0.001

Values are mean ± SD. Cutoff values for considering the presence of abnormal segmental strain are listed in Online Table 2.
CS = circumferential strain; LS = longitudinal strain; MACE = major adverse cardiac event(s); RS = radial strain(s).

Figure 2 shows the MACE-free survival curves. Patients with global LS ≥−11%, global CS ≥−14%, and global RS ≤32% displayed a significantly higher risk of MACE during follow-up ($p < 0.05$ for all comparisons).

A similar tendency was observed when these same analyses were carried out separately for cardiac death, readmission for heart failure, and readmission for reinfarction (Online Figures 2A to 2C).

Similar to results in the whole study group, in patients with TIMI flow 3 after percutaneous coronary intervention (n = 292), those with global LS ≥−11%, global CS ≥−14%, and global RS ≤32% displayed a significantly higher risk of MACE during follow-up ($p < 0.05$ for all comparisons) (Online Figure 3).

MULTIVARIABLE ANALYSES. To simplify data management and to select the strain index with the highest prognostic value, we carried out a preliminary multivariable analysis that included only the 6 TT-CMR indexes determined in the present study. Of these, global LS was the only one found to be independently associated with MACEs (Table 4).

We aimed to determine whether global LS was significantly associated with MACE once adjusted for baseline characteristics and for those CMR indexes that were independently related to the occurrence of MACE (Table 5). In the final multivariable model (Table 5), the variables associated with MACE were time to reperfusion, the TIMI risk score, and global LS. The proportional hazards assumption of the final multivariate model was not violated ($p = 0.8$).

Regarding colinearity, all variables tested in the final multivariate model (LVEF, time to reperfusion, the TIMI risk score, and global LS) showed a tolerance statistic of >0.20 and a variance inflation factor of <5 (Table 5 footnote). A negative correlation ($r = -0.7$) existed between global LS and LVEF. The correlation matrix is provided in Online Table 5.

EXTERNAL VALIDATION COHORT. Baseline and CMR characteristics of patients with (n = 28) and without MACE (n = 162) in the external validation cohort are listed in Online Tables 3 and 4.

As with the study group, patients with MACE in the external validation cohort also displayed higher global LS and CS values, and lower RS values ($p < 0.05$ for all comparisons) (Table 6).

JACC: CARDIOVASCULAR IMAGING, VOL. 11, NO. 10, 2018
OCTOBER 2018:1448–57

As shown in Figure 3, patients in the external validation cohort with global LS ≥−11% displayed a significantly higher risk of MACE during follow-up (34% vs. 9%; p < 0.001).

Finally, as with the study group, global LS was significantly associated with the occurrence of MACE in the external validation cohort after adjustment for baseline characteristics and CMR indexes (1.18; 95% CI: 1.04 to 1.33; p = 0.008) (Online Table 6). The proportional hazards assumption of the final multivariate model was not violated (p = 0.2). All variables tested in the final multivariate model showed a tolerance statistic of >0.20 and a variance inflation factor of <5 (Online Table 6 footnote).

CHANGES IN DISCRIMINATION ACCURACY AND IN RISK RECLASSIFICATION. In the study group, when compared with the multivariate model that tested baseline and traditional CMR indexes without global LS (Model 2 in Table 5), the final multivariate model that included global LS (Model 3 in Table 5) did not significantly improve the discrimination accuracy as derived from the c-statistics (Model 2: 0.69; 95% CI: 0.59 to 0.79; Model 3: 0.70; 95% CI: 0.60 to 0.79; p = 0.7) nor the risk reclassification as derived from the categorical net reclassification improvement index (−0.015; p = 0.7) (Table 7).

Similar results were detected in the external validation cohort (Online Table 7).

DISCUSSION

The main finding of the present study was that myocardial strain as derived from TT-CMR contributes significant prognostic information to stratify risk soon after STEMI. However, it did not substantially improve the risk reclassification of patients compared with the information provided by the baseline characteristics of patients and traditional CMR indexes.

MYOCARDIAL STRAIN BY ECHOCARDIOGRAPHY AND PROGNOSIS AFTER STEMI. Echo-derived myocardial strain has been shown to be a good predictor of outcome in a variety of clinical settings (3). In patients with a recent myocardial infarction (either with or without ST-segment elevation), Wang et al. (2) and Ersboll et al. (3) showed that a more severely altered global LS was associated with cardiovascular death or heart failure hospitalization. In a group of 391 STEMI patients, Biering-Sørensen et al. (17) demonstrated that regional longitudinal myocardial deformation appeared to be a paramount marker of adverse outcome.

The prognostic value of TT-CMR in STEMI patients has not yet been analyzed. Moreover, whether

FIGURE 2 Kaplan-Meier Curves With 95% CIs Representing the Survival Free of MACEs in Patients of the Study Group With and Without Altered Global LS, CS, and RS

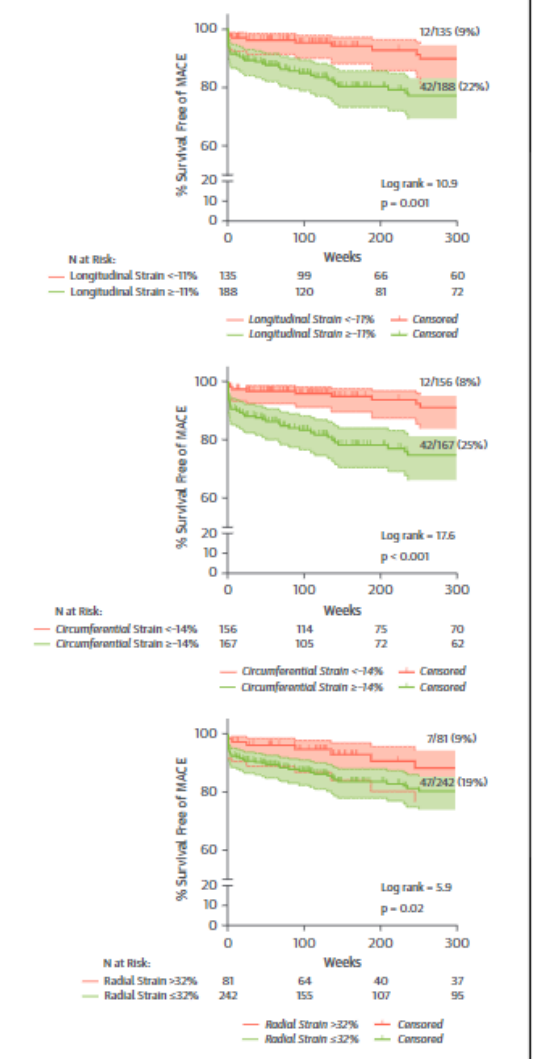

Patients with altered global longitudinal strain (LS), circumferential strain (CS), and radial strain (RS) displayed a significantly higher risk of a first major adverse cardiac event (MACE). **Solid lines** represent the survival curves and the **upper and lower lines of the colored areas** correspond to the 95% confidence intervals (CIs).

JACC: CARDIOVASCULAR IMAGING, VOL. 11, NO. 10, 2018
OCTOBER 2018:1448–57

TABLE 4 Predictors of MACE: Multivariable Study of Strain Variables

	Odds Ratio (95% CI)	p Value
Segments with altered CS, n	0.88 (0.56–1.38)	0.60
Segments with altered LS, n	1.14 (0.91–1.41)	0.30
Segments with altered RS, n	1.12 (0.73–1.71)	0.70
Global CS, %	1.25 (0.89–1.77)	0.90
Global LS, %	1.25 (1.14–1.36)	<0.001
Global RS, %	1.08 (0.96–1.22)	0.50

To avoid variable overfitting and to select the strain variable with the highest prognostic value, the first multivariable analysis included only strain indexes.
CI = confidence interval; other abbreviations as in Tables 1 and 3.

TABLE 6 Strain Characteristics of Patients With and Without MACE in the External Validation Cohort

	MACE (n = 28)	No MACE (n = 162)	p Values
Segments with altered CS, n	6.8 ± 2.7	5.7 ± 2.7	0.05
Segments with altered LS, n	6.0 ± 3.6	3.5 ± 2.7	0.001
Segments with altered RS, n	6.8 ± 3.0	5.6 ± 2.7	0.03
Global CS, %	15.5 ± 4.8	18.2 ± 3.9	0.002
Global LS, %	11.3 ± 4.0	14.2 ± 3.0	0.001
Global RS, %	36.0 ± 14.8	42.1 ± 12.5	0.02

Values are mean ± SD. Cutoff values for considering the presence of abnormal segmental strain are listed in Online Table 2.
Abbreviations as in Table 3.

myocardial strain (either by echocardiography or by CMR) provides information once adjusted for potent CMR markers remains uncertain.

TABLE 5 Predictors of MACE: Multivariable Study

	Hazard Ratio (95% CI)	p Value
Model 1: baseline characteristics		
Age, yrs	1.03 (0.99–1.07)	0.30
Heart rate on admission, beats/min	1.020 (1.002–1.030)	0.10
Killip class I	–	–
Killip class II vs. I	0.15 (0.01–1.77)	0.10
Killip class III vs. I	0.12 (0.01–1.35)	0.09
Killip class IV vs. I	2.47 (0.24–25.05)	0.40
Time to reperfusion, min	1.001 (1.0004–1.001)	<0.001
Peak creatine kinase MB mass, ng/ml	1.000 (1.000–1.001)	0.40
Anterior infarction	2.02 (1.10–3.70)	0.02
GRACE risk score	0.99 (0.98–1.01)	0.30
TIMI risk score	1.22 (1.09–1.37)	<0.001
Model 2: baseline characteristics + CMR indexes		
Time to reperfusion, min	1.001 (1.0003–1.001)	<0.001
Anterior infarction	1.38 (0.70–2.70)	0.30
TIMI risk score	1.20 (1.08–1.35)	0.001
LVEF, %	0.96 (0.94–0.98)	<0.001
LV end-systolic volume index, ml/m^2	0.99 (0.97–1.008)	0.30
Edema, % of LV mass	1.01 (0.99–1.04)	0.30
Microvascular obstruction, % of LV mass	1.01 (0.96–1.07)	0.80
Infarct size, % of LV mass	0.99 (0.96–1.02)	0.90
Model 3: baseline characteristics + CMR indexes + Global LS		
Time to reperfusion, min	1.001 (1.0004–1.001)	<0.001
TIMI risk score	1.17 (1.04–1.31)	0.008
LVEF, %	0.99 (0.96–1.02)	0.40
Global LS, %	1.21 (1.11–1.32)	<0.001

Model 1: Baseline characteristics includes the 8 baseline variables showing an association ($p < 0.1$ in Table 1) with the occurrence of MACE. Model 2: Baseline characteristics plus CMR indexes includes variables from Model 1 independently related to the occurrence of MACE plus CMR indexes showing an association with MACE ($p < 0.1$ in Table 2). Model 3: Baseline characteristics plus CMR indexes plus global LS includes variables from Model 2 independently related to the occurrence of MACE plus global longitudinal strain. The hazard ratios with the corresponding 95% CIs are displayed for each model. For the categorical variable Killip class, Killip class = I was considered as the normal reference value. Colinearity of variables tested in Model 3 was as follows: time to reperfusion: tolerance statistic 0.99; variance inflation factor 1.01. TIMI risk score: tolerance statistic 0.88; variance inflation factor 1.13. LVEF: tolerance statistic 0.37; variance inflation factor 2.71; global LS: tolerance statistic 0.35; variance inflation factor 2.83.
Abbreviations as in Tables 1 to 4.

MYOCARDIAL STRAIN BY TT-CMR AND PROGNOSIS AFTER STEMI. Myocardial strain measured by myocardial tissue tagging as assessed by CMR has been considered the gold standard for determining myocardial deformation and function. However, tagging has some limitations, such as the fact that it requires the acquisition of additional sequences and time-consuming post-processing (4).

Strain-encoded imaging was introduced to overcome the limitations of tagging. It permits strain quantification directed orthogonal to the image plane. Its value in predicting cardiac events (18) and late systolic recovery (19), as well as detecting significant coronary disease, was proven (19). However, the use of this technique in routine CMR has so far been limited (20).

TT-CMR holds promise to become the gold standard method for strain quantification. It tracks features of interest along contour lines on routinely acquired cine images, analogous to echocardiographic speckle tracking (4,5). Due to the excellent spatial resolution of CMR, limitations related to image quality are almost nonexistent. TT-CMR predicts late systolic recovery soon after infarction (5), and compared with tagging it, it provides better myocardial tracking, greater interobserver agreement, faster analysis, and stronger correlation with infarct size (4).

Universal cutoff values are far from being established for TT-CMR, and considerable intervendor (21), intercenter, and interobserver variability may exist (20). In the present study, interobserver and intraobserver variability were rigorously assessed, and the cutoff values derived from the study group were prospectively validated in an external cohort.

In univariate analyses, abnormalities in patients with MACE were more severe for all strain indexes. Global LS emerged as the only strain parameter independently related to MACE. LS was suggested to be the most appropriate strain modality by echocardiography

JACC: CARDIOVASCULAR IMAGING, VOL. 11, NO. 10, 2018
OCTOBER 2018:1448–57

in ischemic patients (2,3,17). Based on these observations and on our own results, we only included global LS in subsequent multivariable analyses.

We found that global LS as derived from TT-CMR was associated with the occurrence of MACE. After a comprehensive adjustment for baseline and traditional CMR indexes, only 2 additional robust variables contributed significant information to predict the combined endpoint: time to reperfusion and the TIMI risk score upon presentation. The present study demonstrated the prognostic value of global LS by TT-CMR on highly relevant endpoints in a homogeneous STEMI population. The prospective confirmation in an external validation cohort strengthened our results.

CLINICAL IMPLICATIONS. Although global LS was selected as an independent predictor by the final multivariate models in both the study group and in the external validation cohort, these models did not significantly improve the discrimination accuracy and risk reclassification compared with models that included baseline characteristics and routinely used CMR variables but not global LS. Two factors underlined this observation: 1) the robustness of clinical scores and current technology (in this case, the traditional CMR indexes) for prognostic purposes made it increasingly difficult to achieve substantial improvements in risk prediction by the addition of novel indexes (22); and 2) the presence of colinearity between global LS and LVEF might hamper the additional discriminative power of global LS.

The correlation between the new predictor and the existing variables had a complicated relationship with improvement in discrimination. Testing in new models variables that did not show excessive colinearity with the existing model (tolerance statistic >0.20 and variable inflation factor <5) is warranted (16). This condition was accomplished in the case of global LS and justified the inclusion of global LS in the final multivariate model.

Furthermore, the additional value of a new predictor that was highly and specifically negatively correlated with the existing predictors (as global LS with respect to LVEF, $r = -0.7$) should be explored, because in some settings it could lead to gains in discrimination (23). Global LS was eventually strongly associated with outcomes, but it did not improve discrimination.

The presented data indicated that TT-CMR could be used in routine CMR measurements for prognostic purposes in post-STEMI patients. However, noting the lack of improvement in discrimination, together

FIGURE 3 Kaplan-Meier Curves With 95% CIs Representing Survival Free of MACEs in Patients of the External Validation Cohort With and Without Altered Global LS, CS, and RS

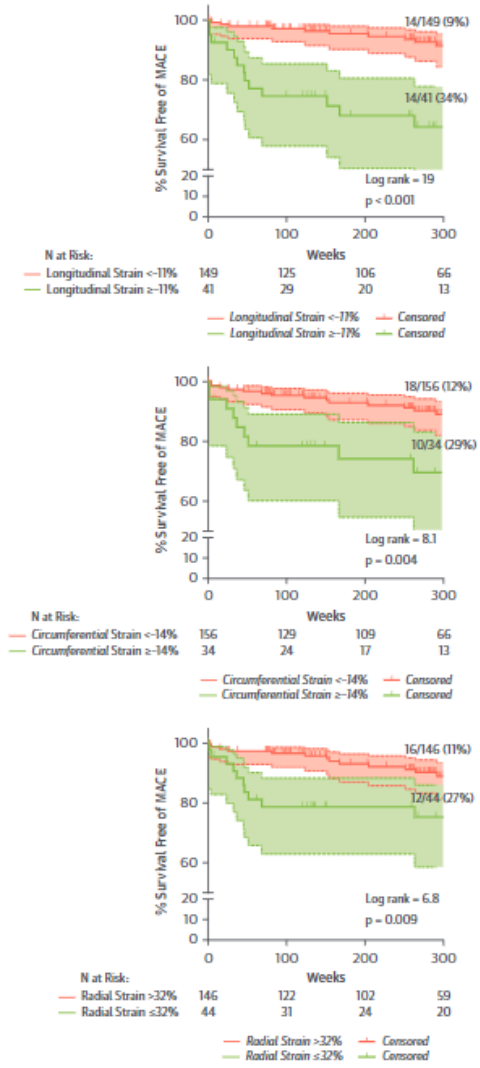

Patients with altered global LS, CS, and RS displayed a significantly higher risk of a first MACE. **Solid lines** represent the survival curves and the **upper and lower lines of the colored areas** correspond to the 95% CIs. Abbreviations as in Figure 2.

TABLE 7 Cross Tabulation of Predicted Risk With and Without Global LS Among Individuals With and Without Events in the Study Group

	Model 3		
MACE	Nonevent	Event	Total
Model 2			
Nonevent			
Nonevent	200	10	210
Event	16	43	59
Total	216	53	269
Event			
Nonevent	19	0	19
Event	2	33	35
Total	21	33	54

Categorical net reclassification improvement index = −0.015 (p = 0.7). Model 2 included baseline characteristics and CMR indexes. Model 3 included baseline characteristics, CMR indexes and global LS. To calculate the categorical net reclassification improvement index, participants were divided into 2 risk categories (<20% and ≥20%).
Abbreviations as in Tables 1 and 3.

with the large body of scientific evidence that supported the prognostic value of LVEF, infarct size, and microvascular obstruction derived from routine CMR after STEMI (7,8), our interpretation was that TT-CMR could supplement, but not substitute, the use of these consolidated indexes. Further studies and larger series of patients will be needed to determine the exact role of myocardial strain by TT-CMR to guide risk stratification and management of STEMI patients.

STUDY LIMITATIONS. Due to the inherent limitations in the use of CMR after STEMI and the retrospective quantification of TT-CMR in the study group, a high dropout rate occurred (219 of 542 patients initially included in the registry). Moreover, changes in the medical and invasive management of STEMI patients applied throughout the long period of inclusion could have exerted a dynamic influence on some of the CMR indexes evaluated and on patient outcomes. Thus, we could not discard that these and other factors exerted residual confounding on our results.

CONCLUSIONS

In STEMI patients studied with CMR, offline assessment of global LS by TT-CMR can be useful in the prediction of cardiac events but does not substantially improve risk stratification compared with routinely used CMR indexes.

ADDRESS FOR CORRESPONDENCE: Dr. Vicente Bodi, Department of Cardiology, Hospital Clínico Universitario-CIBERCV, INCLIVA, University of Valencia, Blasco Ibañez 17, 46010, Valencia, Spain. E-mail: vicente.bodi@uv.es OR Dr. David Garcia-Dorado, Cardiovascular Diseases Research Group, Department of Cardiology, Vall d'Hebron University Hospital and Research Institute, Universitat Autònoma de Barcelona, Pg Vall d'Hebron 119-129, 08035 Barcelona, Spain. E-mail: dgdorado@vhebron.net.

PERSPECTIVES

COMPETENCY IN MEDICAL KNOWLEDGE: The prognostic value of myocardial strain as derived from TT-CMR has not yet been validated. In the present study, we demonstrated the prognostic value of global LS derived from TT-CMR for predicting the clinical course in a large cohort of STEMI patients and in an external validation cohort. However, this index did not substantially improve risk stratification compared with the information provided by baseline characteristics plus traditional CMR variables.

TRANSLATIONAL OUTLOOK: TT-CMR promises to become a new reference technique for assessing global and segmental myocardial strain. In STEMI patients studied with CMR, consideration of offline assessment of global LS by TT-CMR may be warranted for risk stratification. In the setting of STEMI, further studies will be needed to elucidate the exact role of TT-CMR beyond routinely used CMR indexes.

REFERENCES

1. Abate E, Hoogslag GE, Antoni ML, et al. Value of three-dimensional speckle-tracking longitudinal strain for predicting improvement of left ventricular function after acute myocardial infarction. Am J Cardiol 2012;110:961–7.

2. Wang N, Hung CL, Shin SH, et al. Regional cardiac dysfunction and outcome in patients with left ventricular dysfunction, heart failure, or both after myocardial infarction. Eur Heart J 2016;37:466–72.

3. Ersbøll M, Valeur N, Mogensen UM, et al. Prediction of all-cause mortality and heart failure admissions from global left ventricular longitudinal strain in patients with acute myocardial infarction and preserved left ventricular ejection fraction. J Am Coll Cardiol 2013;61:2365–73.

4. Khan JN, Singh A, Nazir SA, Kanagala P, Gershlick AH, McCann GP. Comparison of cardiovascular magnetic resonance feature tracking and tagging for the assessment of left ventricular systolic strain in acute myocardial infarction. Eur J Radiol 2015;84:840–8.

5. Buss SJ, Krautz B, Hofmann N, et al. Prediction of functional recovery by cardiac magnetic

resonance feature tracking imaging in first time ST-elevation myocardial infarction. Comparison to infarct size and transmurality by late gadolinium enhancement. Int J Cardiol 2015;183:162–70.

6. Bodi V, Sanchis J, Lopez-Lereu MP, et al. Usefulness of a comprehensive cardiovascular magnetic resonance imaging assessment for predicting recovery of left ventricular wall motion in the setting of myocardial stunning. J Am Coll Cardiol 2005;46:1747–52.

7. van Kranenburg M, Magro M, Thiele H, et al. Prognostic value of microvascular obstruction and infarct size, as measured by CMR in STEMI patients. J Am Coll Cardiol Img 2014;7:930–9.

8. Bodi V, Sanchis J, Nunez J, et al. Prognostic value of a comprehensive cardiac magnetic resonance assessment soon after a first ST-segment elevation myocardial infarction. J Am Coll Cardiol Img 2009;2:835–42.

9. O'Gara PT, Kushner FG, Ascheim DD, et al. 2013 ACCF/AHA guideline for the management of ST-elevation myocardial infarction. A report of the American College of Cardiology Foundation/American Heart Association Task Force on practice guidelines. J Am Coll Cardiol 2013;61:485–510.

10. Granger CB, Goldberg RJ, Dabbous O, et al. Predictors of hospital mortality in the global registry of acute coronary events. Arch Intern Med 2003;163:2345–53.

11. Morrow DA, Antman EM, Charlesworth A, et al. TIMI risk score for ST-elevation myocardial infarction: a convenient, bedside, clinical score for risk assessment at presentation: an intravenous nPA for treatment of infarcting myocardium early II trial substudy. Circulation 2000;102:2031–7.

12. Henriques JP, Zijlstra F, van't Hof AW, et al. Angiographic assessment of reperfusion in acute myocardial infarction by myocardial blush grade. Circulation 2003;107:2115–9.

13. Cerqueira MD, Weissman NJ, Dilsizian V, et al. Standardized myocardial segmentation and nomenclature for tomographic imaging of the heart. A statement for healthcare professionals from the Cardiac Imaging Committee of the Council on Clinical Cardiology of the American Heart Association. Circulation 2002;105:539–42.

14. Thygesen K, Alpert JS, Jaffe AS, et al. Third universal definition of myocardial infarction. Eur Heart J 2012;33:2551–67.

15. Ponikowski P, Voors AA, Anker SD, et al. 2016 ESC guidelines for the diagnosis and treatment of acute and chronic heart failure. The Task Force for the diagnosis and treatment of acute and chronic heart failure of the European Society of Cardiology (ESC). Eur Heart J 2016;37:2129–200.

16. O'Brien RM. A caution regarding rules of thumb for variance inflation factors. Qual Quantity 2007;41:673–90.

17. Biering-Sørensen T, Jensen JS, Pedersen SH, et al. Regional longitudinal myocardial deformation provides incremental prognostic information in patients with ST-segment elevation myocardial infarction. PLoS One 2016;11:e0158280.

18. Neizel M, Korosoglou G, Lossnitzer D, et al. Impact of systolic and diastolic deformation indexes assessed by strain-encoded imaging to predict persistent severe myocardial dysfunction in patients after acute myocardial infarction at follow-up. J Am Coll Cardiol 2010;56:1056–62.

19. Korosoglou G, Gitsioudis G, Voss A, et al. Strain-encoded cardiac magnetic resonance during high-dose dobutamine stress testing for the estimation of cardiac outcomes. J Am Coll Cardiol 2011;58:1140–9.

20. Pedrizzetti G, Claus P, Kilner PJ, Nagel E. Principles of cardiovascular magnetic resonance feature tracking and echocardiographic speckle tracking for informed clinical use. J Cardiovasc Magn Reson 2016;18:51.

21. Schuster A, Stahnke VC, Unterberg-Buchwald C, et al. Cardiovascular magnetic resonance feature-tracking assessment of myocardial mechanics: intervendor agreement and considerations regarding reproducibility. Clin Radiol 2015;70:989–98.

22. Wang TJ, Gona P, Larson MG, et al. Multiple biomarkers for the prediction of first major cardiovascular events and death. N Engl J Med 2006;355:2631–9.

23. Demler OV, Pencina MJ, D'Agostino RB. Impact of correlation on predictive ability of biomarkers. Stat Med 2013;32:4196–210.

KEY WORDS cardiac magnetic resonance, myocardial infarction, prognosis, strain, tissue tracking

APPENDIX For supplemental tables and figures, please see the online version of this paper.

ONLINE MATERIALS

Cardiovascular magnetic resonance (CMR) acquisition, sequences and quantification

Images were acquired by a phased-array body surface coil during breath-holds and were triggered by electrocardiography. All studies in both study and external validation cohorts were performed using the same CMR scanner characteristics (one in each institution), CMR studies protocol and CMR software. Local cardiologists specialized in CMR with more than 10 years experience from the study group and from the external validation cohorts institutions carried out studies separately in the respective institutions. CMR studies were quantified offline by two different operators (one in each group) with 3 years experience blinded to all patient data using customized software (QMASS MR, 6.1.5, Medis, Leiden, The Netherlands). Traditional CMR data were prospectively recorded and immediately included in the registry database.

Cine images were acquired in two-, three-, and four-chamber views, and in short-axis views using a steady state free precession sequence (repetition time/echo time: 2.8/1.2 ms; flip angle: 58 degrees; matrix: 256 × 300; field of view: 320 × 270 mm; slice thickness: 7 mm).

Late gadolinium enhancement imaging was performed 10 to 15 minutes after administering 0.1 mmol/kg of gadolinium diethylenetriaminepentaacetic acid (Magnograf, Juste S.A.Q.F., Madrid, Spain) in the same locations as in the cine images using a segmented inversion recovery steady state free precession sequence (repetition time/echo time: 750/1.26 ms; flip angle: 45 degrees; matrix: 256 × 184; field of view: 340 × 235 mm; slice thickness: 7 mm). Inversion time was adjusted to nullify normal myocardium.

Black blood, T2-weighted short TI inversion recovery sequences in the same short-axis view as the cine sequences, all in mid-diastole, were carried out. A half-Fourier acquisition single-shot turbo spin echo multisection sequence was used (recovery time: two R-R intervals; echo time: 33 ms; inversion time: 170 ms; slice thickness: 8 mm; interslice interval: 2 mm; flip angle:

160 degrees; matrix: 256 × 151; bandwidth: 781 Hz/pixel). Additionally, a segmented turbo-spin echo sequence was obtained with one slice per breath-hold (recovery time: two R-R intervals; echo time: 100 ms; inversion time: 170 ms; slice thickness: 8 mm; interslice interval: 2 mm; flip angle: 180 degrees; matrix: 256 × 146; bandwidth: 235 Hz/pixel).

Left ventricular (LV) ejection fraction (%), LV end-diastolic volume index (ml/m^2), LV end-systolic volume index (ml/m^2) and LV mass index (g/m^2) were calculated by manual planimetry of endocardial and epicardial borders in short-axis views cine images.

Areas showing late gadolinium enhancement were visually quantified by manual planimetry. Infarct size (% of LV mass) was assessed as the percentage of LV mass showing late gadolinium enhancement. Microvascular obstruction (% of LV mass) was quantified by manual planimetry and defined as the percentage of LV mass showing a lack of contrast uptake in the tissue core showing late gadolinium enhancement.

Myocardial edema was regarded as areas of high T2 signal intensity. All short-axis view slices were separately analyzed and the presence of edema was visually quantified by manual planimetry and expressed as percentage of LV mass. Myocardial salvage index was calculated by subtracting the mass of infarcted myocardium from myocardium showing edema and expressed as percentage of LV mass with myocardial edema.

Tissue tracking (TT)-CMR acquisition

All strain parameters were quantified offline by two different operators (one in each group) with 3 years experience blinded to all patient data using certified software (CMR42, Circle Cardiovascular Imaging Inc., Calgary, Canada).

The first most basal slice to contain 100% of circumferential myocardium in the entire cardiac cycle was identified as the first short axis slice to be analyzed. The end-diastolic endocardial and epicardial LV contours in the short and long axis images of each subject were drawn,

enabling the software to semi-automatically track the myocardium throughout the heart cycle. In long axis images, perpendicular markers to identify the position of the basal and the apical short axis planes were obtained. At least two long axis images are necessary to obtain the longitudinal strain (LS). To calculate the circumferential (CS) and radial strain (RS) the short axis images and at least one long axis images are required.

Variability of measurements

Inter-observer variability in calculating traditional CMR indices was determined by comparing the differences between measurements of each operator from the study and external validation cohort in 30 CMR studies randomly sampled from the study group (Online Table 1A).

Inter-observer variability in the measurement of global LS, CS and RS was obtained in the same manner. For this purpose, the differences between the measurements performed by the two operators in 30 CMR studies (480 segments) randomly sampled from the study group using certified software (CMR42, Circle Cardiovascular Imaging Inc., Calgary, Canada) were determined (Online Table 1A).

Intra-observer variability in calculating traditional CMR indices and in the measurement of global LS, CS and RS was determined by comparing the differences between two repeated measurements carried out by the operator from the study group (with an interval of 1 month from the first to the second measurement) in the 30 CMR studies from the study group used for calculation of inter-observer variability (Online Table 1B).

Inter- and intra-observer variability for the measurements of CMR and TT-CMR indexes (absolute and relative changes, coefficient of variation and intra-class correlation coefficients) is depicted in Online Tables 1A and 1B.

Bland-Altman plots for inter- and intra-observer variability regarding global LS, CS and RS are shown in Online Figure 1.

Online Table 1A. Inter-observer variability for traditional and strain CMR indices.

	Relative change	Absolute change	Coefficient of variation	Intra-class correlation coefficient
LVEF (%)	4±3%	2±1%	0.208	0.989
LV end-diastolic volume index (ml/m²)	7±4%	5±4 ml/m²	0.301	0.981
LV end-systolic volume index (ml/m²)	5±5%	2±2 ml/m²	0.508	0.994
LV mass (g/m²)	8±6%	6±5 g/m²	0.249	0.944
Edema (% of LV mass)	4±6%	1±2% of LV mass	0.688	0.996
Microvascular obstruction (% of LV mass)	3±4%	1±2% of LV mass	1.797	0.981
Infarct size (% of LV mass)	4±5%	1±1% of LV mass	0.813	0.998
Myocardial salvage index (% of LV mass)	3±6%	1±2% of LV mass	0.690	0.996
Global LS (%)	6±7%	0.9±1.3%	0.315	0.954
Global CS (%)	2±3%	0.6±0.4%	0.210	0.990
Global RS (%)	6±4%	2±1%	0.305	0.991

Abbreviations. CMR=Cardiovascular magnetic resonance. CS=Circumferential strain. LS=Longitudinal strain. LV=Left ventricular. LVEF=Left ventricular ejection fraction. RS=Radial strain.

Online Table 1B. Intra-observer variability for traditional and strain CMR indices.

	Relative change	Absolute change	Coefficient of variation	Intra-class correlation coefficient
LVEF (%)	3±2%	1.5±0.7%	0.204	0.994
LV end-diastolic volume index (ml/m²)	5±3%	3±2 ml/m^2	0.293	0.994
LV end-systolic volume index (ml/m²)	4±5%	1±2 ml/m^2	0.504	0.996
LV mass (g/m²)	7±5%	4±4 g/m^2	0.242	0.969
Edema (% of LV mass)	4±5%	1±1% of LV mass	0.685	0.998
Microvascular obstruction (% of LV mass)	2±2%	1±1% of LV mass	1.908	0.993
Infarct size (% of LV mass)	3±4%	0.7±1% of LV mass	0.807	0.998
Myocardial salvage index (% of LV mass)	3±3%	0.6±1% of LV mass	0.682	0.999
Global LS (%)	4±6%	0.8±1%	0.309	0.968
Global CS (%)	2±2%	0.4±0.3%	0.212	0.995
Global RS (%)	3±2%	1.5±0.9%	0.301	0.994

Abbreviations. CMR=Cardiovascular magnetic resonance. CS=Circumferential strain. LS=Longitudinal strain. LV=Left ventricular. LVEF=Left ventricular ejection fraction. RS=Radial strain.

Cut-off values for strain indices

Cut-off values for considering the presence of altered LS, CS and RS were derived from a control group made up of 32 patients submitted to cardiovascular check-up and with no evidence of structural cardiac disease. All these patients underwent TT-CMR.

For segmental LS, CS and RS, the upper 95% percentiles of LS and CS and the lower 95% percentile of RS for each segment in control patients using the 16-segment model were regarded as the cut-off values. Segmental cut-off values are displayed in Online Table 2.

On a per patient basis, cut-off values in the control group were regarded as the upper 95% percentiles of global LS (-11%) and global CS (-14%) and the lower 95% percentile of global RS (32%).

Online Table 2. Cut-off values for considering the presence of altered segmental longitudinal, circumferential and radial strain.

	Longitudinal strain	Circumferential strain	Radial strain
Segments			
1	-10.8	-17.4	27.1
2	-11.1	-17.1	26.5
3	-9.7	-9.8	12.4
4	-8.2	-15.9	23.6
5	-12.8	-18.1	28.6
6	-15.2	-17.4	26.9
7	-20.7	-17	26.4
8	-5.4	-13.9	19.5
9	-2	-11.8	15.9
10	-11.2	-18.4	29.7
11	-12.9	-14.5	21.4
12	-19.6	-18.4	30.3
13	-12.6	-23.6	49.3
14	-6.4	-19.6	40.3
15	-10.8	-17.7	43.6
16	-11.5	-21.8	44.4

Online Table 3. Baseline characteristics of patients with and without MACE in the external validation cohort.

	MACE	No MACE	p
Number of patients	28	162	
Age (years)	63±15	58±13	0.1
Male sex (%)	24 (86)	142 (88)	0.8
Diabetes mellitus (%)	5 (18)	24 (15)	0.7
Hypertension (%)	15 (54)	77 (48)	0.6
Hypercholesterolemia (%)	4 (14)	61 (38)	0.02
Smoker (%)	17 (61)	117 (72)	0.2
Heart rate on admission (beats per min)	77±20	72±16	0.2
Systolic pressure (mm Hg)	130±28	130±28	0.9
Killip class (%)			0.001
I	18 (64)	140 (87)	
II	9 (32)	12 (7)	
III	0 (0)	0 (0)	
IV	1 (4)	10 (6)	
Time to reperfusion (min)	202 [153-270]	190 [150-249]	0.7
Peak creatine kinase MB mass (ng/ml)	369 [271-489]	247 [149-370]	0.001
Anterior infarction (%)	18 (64)	93 (57)	0.5
Multivessel disease (%)	15 (54)	64 (40)	0.03
TIMI flow grade before PCI (%)			0.4

0	27 (96)	146 (90)	
1	1 (4)	11 (7)	
2	0 (0)	2 (1)	
3	0 (0)	3 (2)	
TIMI flow grade after PCI (%)			0.4
0	0 (0)	0 (0)	
1	0 (0)	1 (1)	
2	2 (7)	8 (5)	
3	26 (93)	153 (94)	
GRACE risk score	126±29	113±31	0.04
TIMI risk score	4±2.3	2.6±2	0.001

Abbreviations. GRACE=Global registry of acute coronary events. MACE=Major adverse cardiac events. PCI=Percutaneous coronary intervention. TIMI=Thrombolysis in myocardial infarction.

Categorical variables are expressed as absolute number (percentage). Time to reperfusion is expressed as median [percentile 25-percentile 75]. All other continuous variables are expressed as mean ± SD.

Online Table 4. Cardiovascular magnetic resonance characteristics of patients with and without MACE in the external validation cohort.

	MACE	No MACE	p
Number of patients	28	162	
LVEF (%)	43±12	51±9	0.003
LV end-diastolic volume index (ml/m²)	91±28	78±16	0.02
LV end-systolic volume index (ml/m²)	55±27	38±11	0.004
LV mass (g/m²)	71±17	64±14	0.06
Edema (% of LV mass)	42±16	34±13	0.03
Microvascular obstruction (% of LV mass)	2.6 [1.2-5.8]	0 [0-1.7]	<0.001
Infarct size (% of LV mass)	31±14	21±13	<0.001
Myocardial salvage index (%)	10.3 [4.7-18.5]	12.3 [8.5-17.4]	0.4

Abbreviations. LV=Left ventricular. LVEF=Left ventricular ejection fraction. MACE=Major adverse cardiac events.

Microvascular obstruction and myocardial salvage index are expressed as median [percentile 25-percentile 75]. All other variables are expressed as mean ± SD.

Online Table 5. Correlation matrix in the study group. The analysis includes global LS, CMR indices and independent variables in the final multivariate model.

Variable	Global LS	LVEF	LVEDVI	LVESVI	LV mass	Edema	MVO	Infarct size	Myocardial salvage index	Time to reperfusion	TIMI risk score
Global LS											
Pearson correlation coefficient	…	-0.7	0.3	0.5	0.4	0.5	0.3	0.6	-0.2	0.02	0.3
p	>0.99	<0.001	<0.001	<0.001	<0.001	<0.001	<0.001	<0.001	<0.001	0.7	<0.001
LVEF											

Pearson correlation coefficient	-0.7	…	-0.5	-0.8	-0.3	-0.6	-0.3	-0.7	0.2	-0.06	-0.2
p	<0.001	>0.99	<0.001	<0.001	<0.001	<0.001	<0.001	<0.001	<0.001	0.3	<0.001
LVEDVI											
Pearson correlation coefficient	0.3	-0.5	…	0.8	0.4	0.3	0.2	0.4	-0.1	0.06	0.1
p	<0.001	<0.001	>0.99	<0.001	<0.001	<0.001	<0.001	<0.001	0.002	0.3	0.02
LVESVI											

Pearson correlation coefficient	0.5	-0.8	0.8	…	0.4	0.5	0.3	0.6	-0.2	0.06	0.2
p	<0.001	<0.001	<0.001	>0.99	<0.001	<0.001	<0.001	<0.001	<0.001	0.2	<0.001
LV mass											
Pearson correlation coefficient	0.4	-0.3	0.4	0.4	…	0.3	0.3	0.3	-0.09	0.09	0.1
p	<0.001	<0.001	<0.001	<0.001	>0.99	<0.001	<0.001	<0.001	0.07	0.1	0.008
Edema											

Pearson correlation coefficient	0.5	-0.6	0.3	0.5	0.3	…	0.3	0.7	0.08	0.02	0.2
p	<0.001	<0.001	<0.001	<0.001	<0.001	>0.99	<0.001	<0.001	0.1	0.7	<0.001
MVO											
Pearson correlation coefficient	0.3	-0.3	0.2	0.3	0.3	0.3	…	0.5	-0.2	-0.01	0.1
p	<0.001	<0.001	<0.001	<0.001	<0.001	<0.001	>0.99	<0.001	<0.001	0.8	0.003
Infarct size											

Pearson correlation coefficient	0.6	-0.7	0.4	0.6	0.3	0.7	0.5	…	-0.5	0.02	0.3
p	<0.001	<0.001	<0.001	<0.001	<0.001	<0.001	<0.001	>0.99	<0.001	0.7	<0.001
Myocardial salvage index											
Pearson correlation coefficient	-0.2	0.2	-0.1	-0.2	-0.09	0.08	-0.2	-0.5	…	-0.03	-0.1
p	<0.001	<0.001	0.002	<0.001	0.07	0.1	<0.001	<0.001	>0.99	0.5	<0.001

Time to reperfusion											
Pearson correlation coefficient	0.02	-0.06	0.06	0.06	0.09	0.02	-0.01	0.02	-0.03	…	0.07
p	0.7	0.3	0.3	0.2	0.1	0.7	0.8	0.7	0.5	>0.99	0.2
TIMI risk score											
Pearson correlation coefficient	0.3	-0.2	0.1	0.2	0.1	0.2	0.1	0.3	-0.1	0.07	…

p	<0.001	<0.001	0.02	<0.001	0.008	<0.001	0.003	<0.001	<0.001	0.2	>0.99

Abbreviations. CMR=Cardiovascular magnetic resonance. LS=Longitudinal strain. LV=Left ventricular. LVEDVI=Left ventricular end-diastolic volume index. LVEF=Left ventricular ejection fraction. LVESVI=Left ventricular end-systolic volume index. MVO=Microvascular obstruction. TIMI=Thrombolysis in myocardial infarction.

Online Table 6. Predictors of MACE. Multivariable study of the external validation cohort.

	Hazard Ratio [95% confidence intervals]	**p**
Model 1 – Baseline characteristics		
Hypercholesterolemia	0.33 [0.11-0.95]	0.04
Killip class 1	-	-
Killip class 2 versus 1	2.63 [0.26-26.37]	0.4
Killip class 3 versus 1	3.12 [0.81-1.33]	0.3
Killip class 4 versus 1	7.12 [0.71-72.86]	0.1
Peak creatine kinase MB mass (ng/ml)	1 [0.99-1.003]	0.8
Multivessel disease	1.91 [0.93-3.93]	0.09
GRACE risk score	0.99 [0.97-1.01]	0.3
TIMI risk score	1.3 [1.13-1.5]	<0.001
Model 2 – Baseline characteristics + CMR indices		
Hypercholesterolemia	0.37 [0.1-1.1]	0.06
TIMI risk score	1.39 [1.16-1.67]	<0.001
LVEF (%)	1.1 [0.99-1.21]	0.2
LV end-diastolic volume index (ml/m²)	0.92 [0.85-1.02]	0.3
LV end-systolic volume index (ml/m²)	1.14 [1-1.28]	0.06

LV mass (g/m²)	1.005 [0.97-1.05]	0.8
Edema (% of LV mass)	0.96 [0.89-1.03]	0.2
Microvascular obstruction (% of LV mass)	1.27 [1.16-1.39]	<0.001
Infarct size (% of LV mass)	1.08 [0.99-1.17]	0.06
Model 3 - Baseline characteristics + CMR indices + Global LS		
TIMI risk score	1.36 [1.13-1.64]	0.001
Microvascular obstruction (% of LV mass)	1.21 [1.1-1.33]	<0.001
Global LS (%)	1.18 [1.04-1.33]	0.008

Abbreviations. CMR= Cardiovascular magnetic resonance. GRACE=Global registry of acute coronary events. LS=Longitudinal strain. LV=Left ventricular. LVEF=Left ventricular ejection fraction. MACE=Major adverse cardiac events. TIMI=Thrombolysis in myocardial infarction.

Model 1 – "Baseline characteristics" includes the 6 baseline variables showing an association (p-value<0.1 in Online Table 3) with the occurrence of MACE.

Model 2 – "Baseline Characteristics plus CMR indices" includes variables from Model 1 independently related to the occurrence of MACE plus CMR indices showing an association with MACE (p-value<0.1 in Online Table 4).

Model 3 – "Baseline Characteristics plus CMR indices plus global LS" includes variables from Model 2 independently related to the occurrence of MACE plus global longitudinal strain.

The hazard ratios with the corresponding 95% confidence intervals are displayed for each model.

For the categorical variable Killip class, Killip class=1 was considered as the normal reference value.

Co-linearity of variables tested in Model 3 was as follows:

TIMI risk score: Tolerance statistic 0.95. Variance inflation factor 1.05.

Microvascular obstruction: Tolerance statistic 0.82. Variance inflation factor 1.21.

Global LS: Tolerance statistic 0.79. Variance inflation factor 1.26.

Online Table 7. Cross-tabulation of predicted risk with and without global LS among individuals with and without events in the external validation cohort.

				Model 3		
				Non-event	**Event**	**Total**
MACE	**Non-event**	**Model 2**	**Non-event**	132	9	141
			Event	6	15	21
			Total	138	24	162
	Event		**Non-event**	8	3	11
			Event	3	14	17
			Total	11	17	28

Categorical net reclassification improvement index=-0.019 (p=0.9)

Abbreviations. CMR=Cardiovascular magnetic resonance. LS=Longitudinal strain. MACE=Major adverse cardiac events.

Model 2 included baseline characteristics and CMR indices. Model 3 included baseline characteristics, CMR indices and global LS.

In order to calculate the categorical net reclassification improvement index, participants were divided into 2 risk categories (<20% and ≥20%).

The final multivariate model that included global LS (Model 3 in Online Table 6) did not improve the multivariate model that tested baseline and traditional CMR indices without global LS (Model 2 in Online Table 6) neither in terms of the discrimination accuracy as derived from the c-statistics (Model 2: 0.70 [0.58-0.82], Model 3: 0.70 [0.57-0.82], p=0.8) nor in terms of risk reclassification as derived from the categorical net reclassification improvement index.

Online Figure 1. Bland-Altman plots for inter- and intra-observer variability regarding global LS, CS and RS.

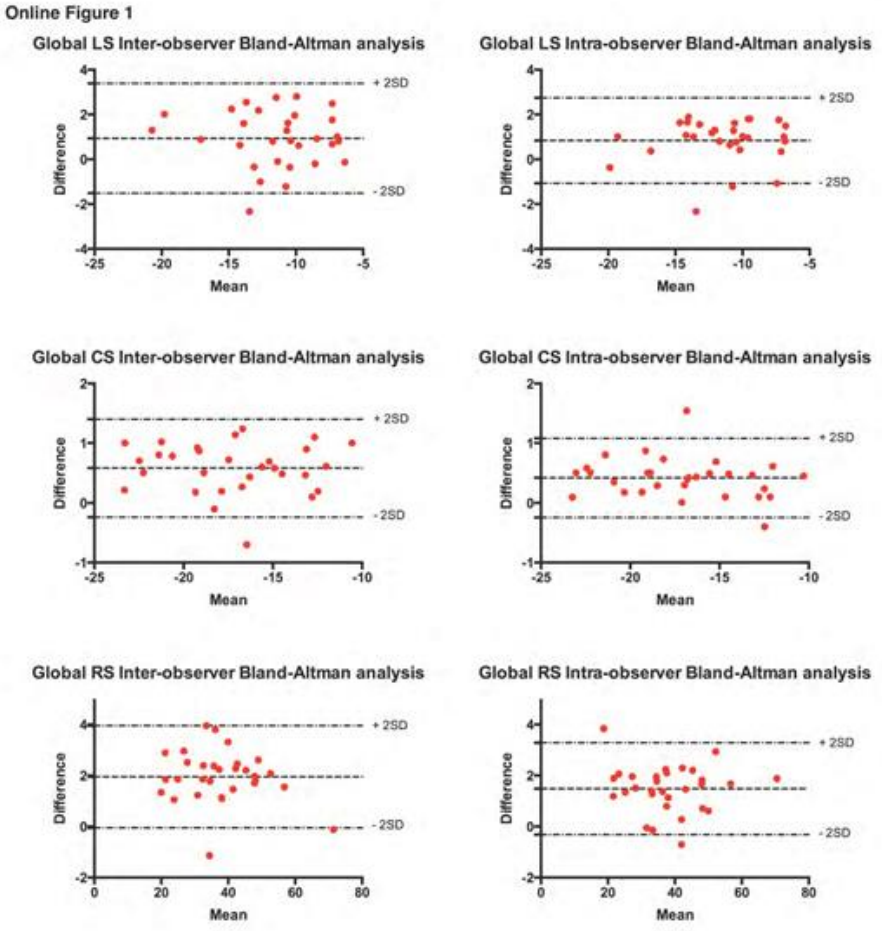

Bland-Altman plots illustrate the low inter- and intra-observer variability in the measurements of LS, CS and RS.
CS=Circumferential strain. LS=Longitudinal strain. RS=Radial strain.

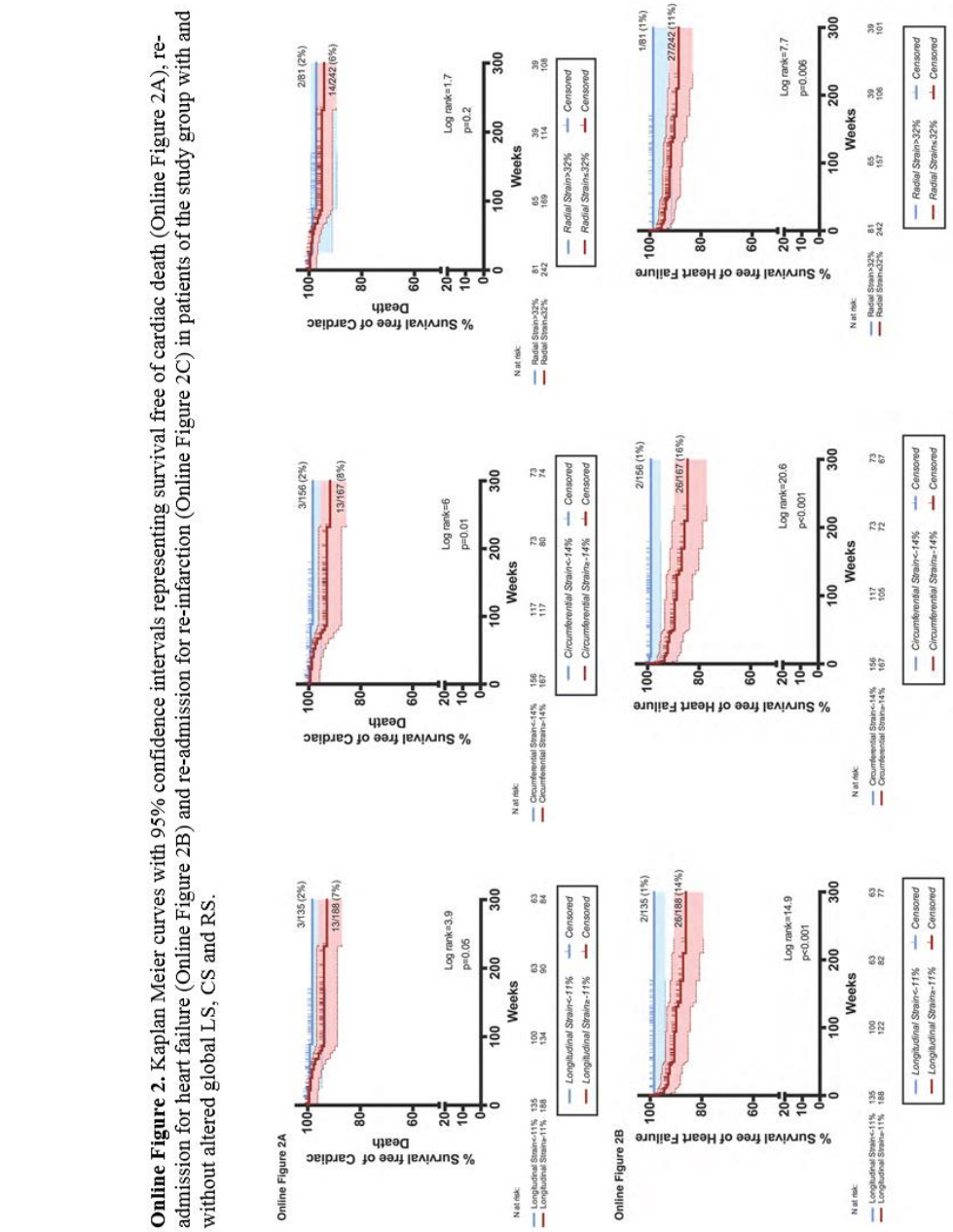

Online Figure 2. Kaplan Meier curves with 95% confidence intervals representing survival free of cardiac death (Online Figure 2A), re-admission for heart failure (Online Figure 2B) and re-admission for re-infarction (Online Figure 2C) in patients of the study group with and without altered global LS, CS and RS.

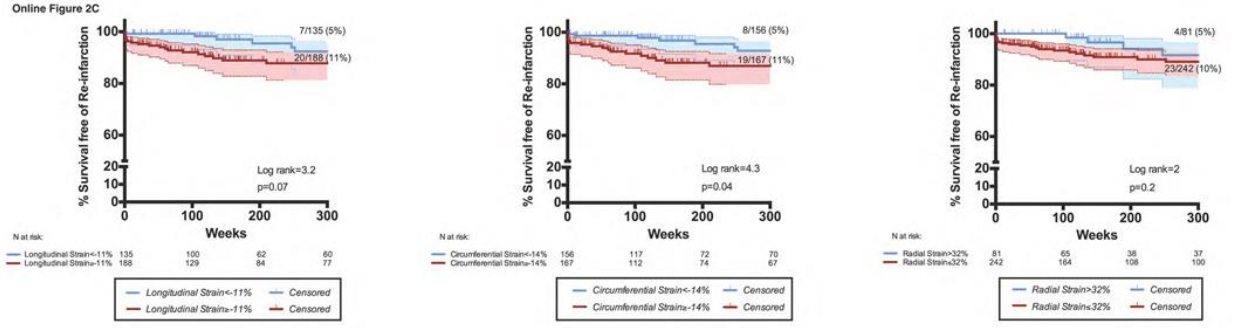

Patients with altered global LS, CS and RS displayed a tendency towards a significantly higher risk of a first major adverse cardiac event. Solid lines represent the survival curves and dashed lines correspond to the 95% confidence intervals.
CS=Circumferential strain. LS=Longitudinal strain. RS=Radial strain.

Online Figure 3. Kaplan Meier curves with 95% confidence intervals representing the survival free of major adverse cardiac events in patients of the study group with TIMI 3 flow after reperfusion with and without altered global LS, CS and RS.

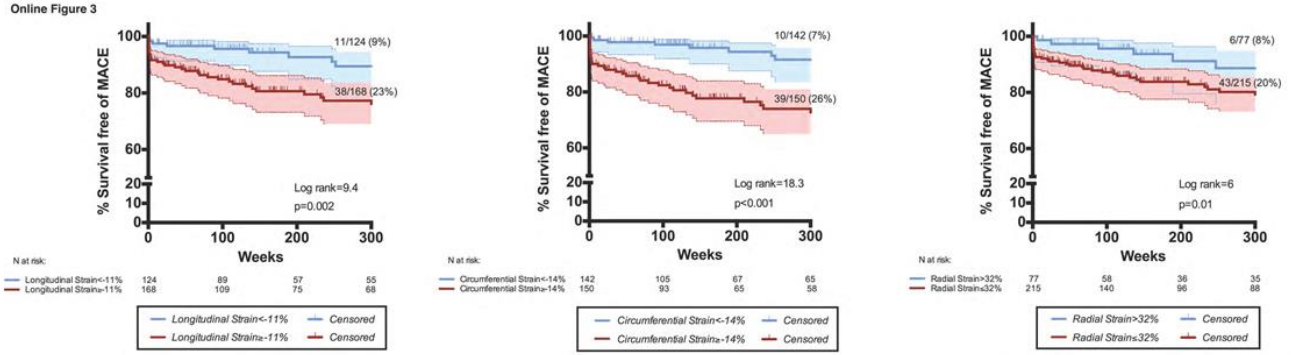

Patients with altered global LS, CS and RS displayed a significantly higher risk of a first major adverse cardiac event. Solid lines represent the survival curves and dashed lines correspond to the 95% confidence intervals.
CS=Circumferential strain. LS=Longitudinal strain. MACE=Major adverse cardiac events. RS=Radial strain. TIMI=Thrombolysis in myocardial infarction.

ANEXO II: Rodríguez-Palomares JF*, Gavara J*, Ferreira-González I, et al. J Am Coll Cardiol 2019;12:2445–56

JACC: CARDIOVASCULAR IMAGING VOL. 12, NO. 12, 2019

ORIGINAL RESEARCH

Prognostic Value of Initial Left Ventricular Remodeling in Patients With Reperfused STEMI

Jose F. Rodriguez-Palomares, MD, PhD,[a,b,*] Jose Gavara, MSc,[c,*] Ignacio Ferreira-González, MD, PhD,[a,d] Filipa Valente, MD,[a,b] César Rios, MSc,[c] Julián Rodríguez-García, MD,[a,b] Clara Bonanad, MD, PhD,[c] Bruno García del Blanco, MD, PhD,[a,b] Gema Miñana, MD, PhD,[c] Maria Mutuberria, MD,[a,b] Julio Nuñez, MD, PhD,[c] José Barrabés, MD, PhD,[a,b] Artur Evangelista, MD, PhD,[a,b] Vicente Bodí, MD, PhD,[c] David García-Dorado, MD, PhD[a,b]

ABSTRACT

OBJECTIVES This study sought to establish the best definition of left ventricular adverse remodeling (LVAR) to predict outcomes and determine whether its assessment adds prognostic information to that obtained by early cardiac magnetic resonance (CMR).

BACKGROUND LVAR, usually defined as an increase in left ventricular end-diastolic volume (LVEDV) is the main cause of heart failure after an ST-segment elevated myocardial infarction; however, the role of assessment of LVAR in predicting cardiovascular events remains controversial.

METHODS Patients with ST-segment elevated myocardial infarction who received percutaneous coronary intervention within 6 h of symptom onset were included (n = 498). CMR was performed during hospitalization (6.2 ± 2.6 days) and after 6 months (6.1 ± 1.8 months). The optimal threshold values of the LVEDV increase and the LV ejection fraction decrease associated with the primary endpoint were ascertained. Primary outcome was a composite of cardiovascular mortality, hospitalization for heart failure, or ventricular arrhythmia.

RESULTS The study was completed by 374 patients. Forty-nine patients presented the primary endpoint during follow-up (72.9 ± 42.8 months). Values that maximized the ability to identify patients with and without outcomes were a relative rise in LVEDV of 15% (hazard ratio [HR]: 2.1; p = 0.007) and a relative fall in LV ejection fraction of 3% (HR: 2.5; p = 0.001). However, the predictive model (using C-statistic analysis) failed to demonstrate that direct observation of LVAR at 6 months adds information to data from early CMR in predicting outcomes (C-statistic: 0.723 vs. 0.795).

CONCLUSIONS The definition of LVAR that best predicts adverse cardiovascular events should consider both the increase in LVEDV and the reduction in LV ejection fraction. However, assessment of LVAR does not improve information provided by the early CMR. (J Am Coll Cardiol Img 2019;12:2445-56) © 2019 The Authors. Published by Elsevier on behalf of the American College of Cardiology Foundation. This is an open access article under the CC BY-NC-ND license (http://creativecommons.org/licenses/by-nc-nd/4.0/).

From the [a]Department of Cardiology, Hospital Universitari Vall d'Hebron, Vall d'Hebron Institut de Recerca, Universitat Autònoma de Barcelona, Barcelona, Spain; [b]Centro de Investigación Biomédica en Red-para enfermedades cardiovasculares, CIBERCV, Madrid, Spain; [c]Department of Cardiology, Hospital Clinico Universitario, CIBERCV, INCLIVA, University of Valencia, Valencia, Spain; and the [d]CIBER de Epidemiología y Salud Pública, CIBERESP, Madrid, Spain. *Drs. Rodriguez-Palomares and Gavara contributed equally to this study. This work was funded by the Instituto de Salud Carlos III and co-funded by the European Regional Development Fund grants EC07/90511, PI17/01836, PIE15/00013, CIBERCV16/11/00486, and CIBERCV16/11/00479. Dr. Ferreira-González served on advisory boards for Bayer, Bristol-Myers Squibb, and Sanofi; and received grants from the Spanish Health Ministry. All other authors have reported that they have no relationships relevant to the contents of this paper to disclose.

Manuscript received October 8, 2018; revised manuscript received January 17, 2019, accepted February 22, 2019.

ISSN 1936-878X https://doi.org/10.1016/j.jcmg.2019.02.025

JACC: CARDIOVASCULAR IMAGING, VOL. 12, NO. 12, 2019
DECEMBER 2019:2445–56

ABBREVIATIONS AND ACRONYMS

AMI = acute myocardial infarction

CI = confidence interval

CMR = cardiac magnetic resonance

HR = hazard ratio

IS = infarct size

LV = left ventricle

LVAR = left ventricular adverse remodeling

LVEDV = left ventricular end-diastolic volume

LVEF = left ventricular ejection fraction

LVESV = left ventricular end-systolic volume

MI = myocardial infarction

MVO = microvascular obstruction

NRI = net reclassification improvement

PCI = percutaneous coronary intervention

STEMI = ST-segment elevation myocardial infarction

Mortality during the acute phase of ST-segment elevation myocardial infarction (STEMI) has steadily decreased over the past 3 decades and appears now to have reached a plateau at lower values than those in the pre-reperfusion era (1). However, the main impact of STEMI is shifting from acute mortality to progressive left ventricular (LV) dysfunction and chronic heart failure (2).

SEE PAGE 2457

The main cause of heart failure after an acute myocardial infarction (AMI) is left ventricular adverse remodeling (LVAR) (3) in response to the increase in wall stress caused by cardiomyocyte loss and distension in the infarct area (4). Post-infarct LVAR is generally defined as a 20% increase in LV end-diastolic volume (LVEDV) (5,6) and has been associated with poorer outcomes (5,7).

The definition of LVAR is controversial. First, the increase in LV volume post-infarction may be associated with a rise or fall in left ventricular ejection fraction (LVEF), which has also been considered a major predictor of outcomes after AMI (8). Changes in LVEDV may reflect changes in LV volume, EF, or both, and its analysis provides less information than the combined analysis of LV volumes and LVEF. Furthermore, LVAR is determined 3 to 6 months after a STEMI (5,9), and, it has been shown that LVEF improves in most patients after 1-month post-STEMI, thereby implying that further delay in clinical decisions may not be warranted (10).

To overcome these limitations, early cardiac magnetic resonance (CMR)-derived parameters such as infarct size (IS), microvascular obstruction (MVO), and LVEF have been considered excellent predictors of adverse cardiovascular events during follow-up (11,12). A recent meta-analysis showed IS measured by CMR or technetium-99m sestamibi single-photon emission computed tomography within 1 month after the primary percutaneous coronary intervention (PCI) to be strongly associated with all-cause mortality and hospitalization for heart failure within 1 year (13). However, although several studies support the prognostic value of baseline CMR data, no studies to date have shown that they are superior to the direct assessment of early LVAR for predicting outcomes.

The present study first tested the hypothesis that changes in both LV volumes and LVEF better define the presence of LVAR because they provide additional prognostic information in patients with STEMI who are undergoing PCI. These changes were correlated with the primary outcome of ventricular arrhythmia, hospitalization for heart failure, or cardiovascular death during follow-up. We also sought to determine whether baseline CMR-derived parameters or LVAR constitutes the best predictor of cardiovascular events during follow-up.

METHODS

STUDY POPULATION. The present study compiled the databases of 2 previous studies (14,15). The first was a large prospective STEMI registry (14) that included consecutive patients admitted for a first STEMI as defined by current definitions (16), treated with PCI, and undergoing CMR pre-discharge. A subsample of 234 patients underwent a second CMR 6 months post-discharge, and they constituted the target population.

The second database stemmed from a double-blind randomized clinical trial in which 201 patients with a STEMI were randomized to receive 4.5 mg of adenosine or saline intracoronary injection immediately before PCI (15). The primary endpoint of this study was the infarct size (%LV) by CMR post-reperfusion.

Per protocol, in both clinical studies, all patients who met the inclusion criteria were scheduled for an early CMR during hospitalization and at 6-month follow-up.

Our target population were patients who survived at least 6 months after a STEMI and in whom LVAR could be assessed with a subsequent CMR after the acute phase and underwent a minimum of 1-year follow-up (**Figure 1**).

Exclusion criteria were death, previously documented MI, severe clinical instability during admission, and any contraindications to CMR, including claustrophobia, existing pacemaker, decision of the patient, and a history of adverse reactions to contrast.

Baseline characteristics were collected prospectively in all cases. The PCI technique was left to the discretion of the interventional cardiologists. Patients were managed both in-hospital and after discharge following specific STEMI guidelines (16).

Both study protocols were approved by the hospital Ethics Committee on Human Research and complied with the 1975 Declaration of Helsinki guidelines.

CMR. All CMR studies were performed with a 1.5-T clinical scanner (Sonata or Avanto scanner, Siemens, Erlangen, Germany). Further details on the technical aspects of CMR acquisition, sequences, and quantification can be found in the Supplemental Appendix. LVEF (%), LVEDV index (ml/m^2), left ventricular end-systolic volume (LVESV) index (ml/m^2), LV mass

JACC: CARDIOVASCULAR IMAGING, VOL. 12, NO. 12, 2019
DECEMBER 2019:2445–56

FIGURE 1 Study Flow Chart

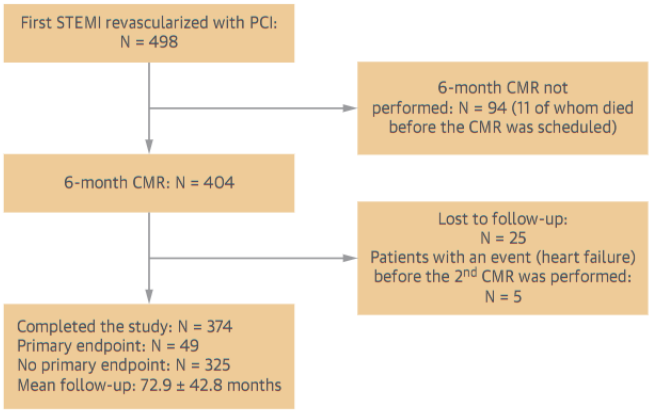

Flow chart of participants through the study. Graph showing selection and attrition of participants through the study. Primary endpoint is cardiovascular mortality, hospitalization for heart failure, or ventricular arrhythmia. CMR = cardiac magnetic resonance; PCI = percutaneous coronary intervention; STEMI = ST-segment elevation myocardial infarction.

index (g/m²), IS (% of LV mass), microvascular obstruction (% of LV mass), myocardial edema (% of LV mass), and myocardial salvage index (% of LV mass) were calculated.

CMR studies were analyzed offline by an experienced observer blinded to all patient data using customized software (QMASS MR 6.15, Medis, Leiden, the Netherlands; or Cvi42, Circle Cardiovascular Imaging Inc., Calgary, Alberta, Canada).

STATISTICAL ANALYSIS. Continuous demographic variables were expressed as mean ± SD. Normality distribution was assessed by the Kolmogorov-Smirnov test. Differences between groups for continuous parameters were assessed by Student's *t*-test if they presented a normal distribution or analysis of variance with Bonferroni correction for multiple comparisons, and Mann-Whitney *U* test if they did not present a normal distribution. For categorical variables, general characteristics of the sample were assessed by percentages (chi-square test or Fisher exact test, accordingly).

Our main hypothesis was that both LVEDV and LVEF provide complementary prognostic information for STEMI after primary PCI and thus both should be considered in the definition of LVAR. The primary endpoint was cardiovascular mortality, hospitalization for heart failure, or ventricular arrhythmia.

The optimal threshold values of the LVEDV increase and the LVEF decrease associated with the primary endpoint were ascertained using a graphic method for biomarker cutoff optimization (17). The hazard ratios (HRs) including 95% confidence intervals (CIs) were plotted regardless of the cutoffs, and vertical lines designated the dichotomization showing the most significant correlation with survival. To avoid absurd estimations, 10% of extreme outliers of LVEDV and LVEF values were excluded as potential candidates to obtain the cutoff points. Finally, the values obtained were rounded up to a superior whole for pragmatic purposes. A scale of 1 percentage unit was used for the decrease in LVEF and a scale of 5 percentage units for LVEDV.

Survival free from the primary endpoint was compared using Kaplan-Meier curves, and log-rank test across the 4 subgroups of patients considered the cutoff points selected: 1) those whose LVEDV and LVEF did not change; 2) those whose LVEDV increased but LVEF did not decrease; 3) those whose LVEDV did not increase but the LVEF decreased; and 4) those whose LVEDV increased and LVEF

JACC: CARDIOVASCULAR IMAGING, VOL. 12, NO. 12, 2019
DECEMBER 2019:2445–56

TABLE 1 Baseline Characteristics of the Entire Study Group and of Patients With or Without Cardiovascular Events

	All Patients (N = 374)		Patients With No Events (n = 325)		Patients With Events (n = 49)		
	N	Mean ± SD or n (%)	n	Mean ± SD or n (%)	n	Mean ± SD or n (%)	p Value
Demographics							
Age, yrs	374	59.2 ± 12	325	58.2 ± 11.8	49	65.5 ± 11.2	<0.001
Female	374	62 (16.6)	325	56 (17.2)	49	6 (12.2)	0.536
Hypertension	374	168 (44.9)	325	144 (44.3)	49	24 (49)	0.542
Hypercholesterolemia	374	144 (38.5)	325	128 (39.4)	49	16 (32.7)	0.432
Diabetes	374	63 (16.8)	325	56 (17.2)	49	7 (14.3)	0.687
Smoking	374	235 (62.8)	325	205 (63.1)	49	30 (61.2)	0.874
Prior coronary heart disease	374	34 (9.1)	325	31 (9.5)	49	3 (6.1)	0.597
Index episode							
AMI location	374		325		49		0.340
Anterior		211 (56.4)		179 (55.1)		32 (65.3)	
Inferior		146 (39)		130 (40)		16 (32.7)	
Lateral		17 (4.5)		16 (4.9)		1 (2)	
Heart rate	374	77.6 ± 18.8	325	76.3 ± 17.8	49	86.3 ± 22.4	0.003
Systolic blood pressure	374	129.1 ± 28.8	325	128.7 ± 28.8	49	131.8 ± 29	0.541
Killip class >I	374	51 (13.6)	325	43 (13.2)	49	8 (16.3)	0.510
PCI <12 h	368	247 (67.1)	319	215 (67.4)	49	32 (65.3)	0.747
Coronary artery	371		323		48		0.149
LAD		210 (56.6)		178 (55.1)		32 (66.7)	
LCX		130 (35)		115 (35.6)		15 (31.3)	
RCA		31 (8.4)		30 (9.3)		1 (2.1)	
Multivessel disease	366	116 (31.7)	317	103 (32.5)	49	13 (26.5)	0.510
Initial TIMI	369		321		48		0.052
Occlusion		236 (64)		210 (65.4)		26 (54.2)	
Low		24 (6.5)		22 (6.9)		2 (4.2)	
Intermediate		27 (7.3)		23 (7.2)		4 (8.3)	
Normal		82 (22.2)		66 (20.6)		16 (33.3)	
Final TIMI	374		325		49		0.850
Occlusion		6 (1.6)		6 (1.8)		0 (0)	
Low		2 (0.5)		2 (0.6)		0 (0)	
Intermediate		27 (7.2)		20 (6.2)		7 (14.3)	
Normal		339 (90.6)		297 (91.4)		42 (85.7)	
Drug-eluting stent	241	0.4 ± 0.5	219	0.4 ± 0.5	22	0.1 ± 0.4	0.009
Stents, total number	229	1.2 ± 0.6	208	1.2 ± 0.6	21	1.3 ± 0.9	0.544
CK-MB mass	319	267.4 ± 382.2	270	258.8 ± 404.1	49	314.9 ± 223.6	0.022

Continued on the next page

decreased. The association between LVEDV and LVEF changes were estimated in multivariable crude and adjusted Cox models. All baseline variables were analyzed for their association with the primary outcome (Supplemental Table 1). Specifically, the baseline variables of age, sex, heart rate, LVEF, IS, and MVO were selected for statistical adjustment.

The estimated best model to identify patients with the primary outcome during follow-up was based on the C-statistic. The objective of this analysis was to compare the predictive ability of 4 different models: 1) models including information exclusively from the early CMR; 2) models including information exclusively from the 6-month CMR; 3) models that included information related to the change between the early and 6-month CMR; and 4) models that included information from the early CMR and the change in LVEDV and LVEF. All models were adjusted for age and sex.

Finally, the discrimination ability of each model to classify patients at a higher risk for the primary outcome was additionally assessed by the net reclassification improvement (NRI). Considering a baseline model including only the variables age and sex, the NRI was estimated for each new model. NRI was estimated at the median follow-up (297 weeks) and considered a threshold of 20% to define a high-risk patient.

JACC: CARDIOVASCULAR IMAGING, VOL. 12, NO. 12, 2019
DECEMBER 2019:2445–56

TABLE 1 Continued

	All Patients (N = 374)		Patients With No Events (n = 325)		Patients With Events (n = 49)		
	N	Mean ± SD or n (%)	n	Mean ± SD or n (%)	n	Mean ± SD or n (%)	p Value
CMR baseline data							
LVEF, %	374	51.6 ± 12	325	52.5 ± 11.5	49	45.8 ± 13.3	0.001
LVEDV, ml	374	79.7 ± 21.9	325	79.1 ± 20.8	49	83.9 ± 28.2	0.422
LVESV, ml	374	39.6 ± 18.8	325	38.4 ± 17.6	49	47.6 ± 23.9	0.018
Edema, % of LV mass	360	31.3 ± 16	312	30.6 ± 15.8	48	36 ± 16.5	0.038
Myocardial salvage index, %	359	22 ± 22.9	311	23.2 ± 23.8	48	14.5 ± 14.4	0.039
IS, % of LV mass	373	21.9 ± 14.3	324	20.8 ± 13.8	49	28.7 ± 15.6	0.001
MVO, % of LV mass	373	1.8 ± 3.8	324	1.6 ± 3.6	49	2.9 ± 4.3	0.004
Global CS, %	229	−16.5 ± 4	198	−16.8 ± 3.8	31	−14.3 ± 4.2	0.001
Global LS, %	229	−10.4 ± 3.1	198	−10.7 ± 3.1	31	−8.5 ± 2.5	<0.001
Global RS, %	229	38.5 ± 11.7	198	39 ± 11.6	31	34.8 ± 11.9	0.066
Medication at follow-up							
Antiplatelet agent	374	374 (100)	325	325 (100)	49	49 (100)	NA
Anticoagulation	374	43 (11.5)	325	41 (12.6)	49	2 (4.1)	0.094
Beta-blockers	373	306 (82)	324	271 (83.6)	49	35 (71.4)	0.046
ACE Inhibitors	374	251 (67.1)	325	220 (67.7)	49	31 (63.3)	0.625
Angiotensin II receptor antagonist	374	42 (11.2)	325	38 (11.7)	49	4 (8.2)	0.629
Statin	374	354 (94.7)	325	307 (94.5)	49	47 (95.9)	1.000

Values are n, mean ± SD, or n (%).

ACE = angiotensin-converting enzyme inhibitor; AMI = acute myocardial infarction; CK-MB = creatine kinase-myocardial band; CMR = cardiac magnetic resonance; CS = circumferential strain; IS = infarct size; LAD = left anterior descending coronary artery; LCX = left circumflex coronary artery; LS = longitudinal strain; LV = left ventricle; LVEDV = left ventricular end-diastolic volume; LVEF = left ventricular ejection fraction; LVESV= left ventricular end-systolic volume; MVO = microvascular obstruction; NA = not applicable; PCI = percutaneous coronary intervention; RCA = right coronary artery; RS = radial strain; TIMI = Thrombolysis in Myocardial Infarction flow grade.

All analyses were made with SPSS statistical package (SPSS Statistics 23.0, IBM, Armonk, New York) and R (version 3.4.3, R Foundation for Statistical Computing, Vienna, Austria).

RESULTS

BASELINE CHARACTERISTICS. Ninety-four of the 498 patients with a first STEMI revascularized with PCI were excluded because a second CMR was not performed at 6 months. Twenty-five patients (6.2%) were lost to follow-up, and 5 (1.2%) had an event (heart failure) before the second CMR was scheduled; thus, 374 patients were finally included in the study. The mean time between the PCI and early CMR was 6.2 ± 2.6 days. Baseline data of the study population are shown in Table 1. Most patients had an anterior STEMI (n = 211; 56.4%). The culprit artery was the left anterior descending coronary artery (n = 210; 56.6%), which in most cases was completely occluded (n = 236; 64%). Multivessel coronary artery disease was present in 116 patients (31.7%). PCI was performed in the first 12 h after initial chest pain in the majority of patients (n = 247; 67.1%), in most of whom (n = 339; 90.6%) it achieved normal coronary flow. Early CMR showed a baseline EF of 51.6 ± 12% and mean IS (%LV) was 21.9 ±14.3%. No differences

TABLE 2 Differences Between Baseline and 6-Month LVEDV, LVESV, LVEF, and IS (%LV Mass) in Patients With and Without the Cardiovascular Event

	Global (n = 374)	Event (n = 49)	No Event (n = 325)	p Value
LVEDV				
Baseline	80 ± 22	84 ± 28	79 ± 21	0.422
6-month	82 ± 26	90 ± 37	80 ± 24	0.278
Difference	2 ± 17.8	6 ± 23.1	1.4 ± 16.8	0.255
Relative difference, %	4 ± 23.2	8.3 ± 26.6	3.4 ± 22.7	0.224
p Value	0.031	0.076	0.136	
LVESV				
Baseline	40 ± 19	48 ± 24	38 ± 18	0.018
6-month	39 ± 23	52 ± 32	37 ± 20	0.005
Difference	−0.3 ± 12.8	4.4 ± 18.4	−1 ± 11.6	0.052
Relative difference, %	1.6 ± 34.5	12.1 ± 41.8	0.1 ± 33	0.032
p Value	0.662	0.099	0.122	
LVEF				
Baseline	52 ± 12	46 ± 13	53 ± 12	0.001
6-month	55 ± 12	46 ± 14	56 ± 11	<0.001
Difference	3 ± 8.4	0.6 ± 10	3.4 ± 8.1	0.018
Relative difference, %	7.6 ± 20	3.4 ± 27.2	8.3 ± 18.6	0.017
p Value	<0.001	0.689	<0.001	
IS (% of LV mass)				
Baseline	25.4 ± 13	31.7 ± 14.4	24.2 ± 12.4	<0.001
6-month	22.9 ± 13.7	28.7 ± 15.8	21.7 ± 13.1	0.001
Difference	−2.5 ± 6	−3.1 ± 7.9	−2.4 ± 5.6	0.499
Relative difference, %	−10.9 ± 19.9	−10.9 ± 21	−10.9 ± 18.7	0.985
p Value	<0.001	0.009	<0.001	

Values are mean ± SD unless otherwise indicated. Event is considered a cardiovascular mortality, hospitalization for heart failure, or ventricular arrhythmia.

Abbreviations as in Table 1.

FIGURE 2 HR Curves

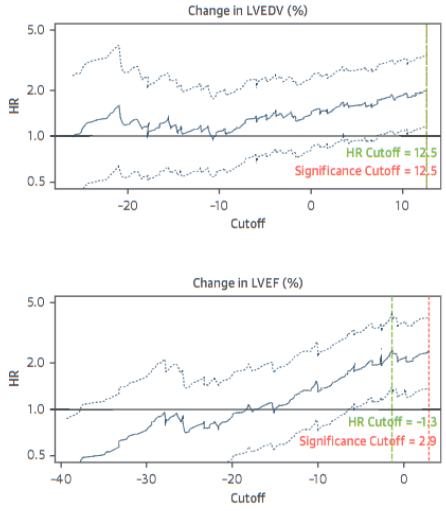

Hazard ratio (HR) curves to ascertain the best cutoff point in left ventricular end-diastolic volume (LVEDV) and left ventricular ejection fraction (LVEF) to predict the event. Values that maximized the ability to distinguish between patients with and without a subsequent event were a relative increase of 12.5% in LVEDV and a relative decrease in LVEF of 2.9%.

existed in medical treatment at discharge between groups.

FOLLOW-UP AND CMR CHANGES. After discharge, a second CMR was performed at a mean time of 6.1 ± 1.8 months, and patients were followed up for a mean of 72.9 ± 42.8 months. Forty-nine patients (13.1%) presented with the primary outcome: 3 ventricular arrhythmias (0.8%); 28 hospitalization for heart failure (7.5%); and 26 cardiovascular death (7%). In 325 patients (86.9%), none of the primary outcomes occurred. All-cause mortality also occurred in 26 patients (7%). Differences between patients with and without the primary outcome are presented in Table 1. Patients with cardiovascular events were older; had a higher heart rate at admission; lower LVEF and myocardial salvage index at the baseline CMR; and higher LVESV, area at risk, IS, and MVO ($p < 0.005$ in all cases).

After 6 months, LVEDV presented a relative increase of 4 ± 23.2% (Table 2). This increase tended to be greater in patients who had the primary outcome during follow-up (6 ± 23.1 ml; 8.3 ± 26.6%; $p = 0.076$) than in those without an event (1.4 ± 16.8 ml; 3.4 ± 22.7%; $p = 0.136$), although these differences were not statistically significant ($p = 0.224$). Also, LVEF presented a relative increase of 7.6 ± 20% ($p < 0.001$). This increase was greater ($p = 0.017$) in patients without the primary outcome during follow-up (relative increase 8.3 ± 18.6%; $p < 0.001$) than in those with events (relative 3.4 ± 27.2%; $p = 0.689$). A decrease in infarct size of 10.9 ± 19.9% was observed in the overall population with no differences between patients with or without major cardiovascular events ($p = 0.985$).

These results show that patients with and without events during follow-up can present similar changes in LVEDV and IS during the first 6 months after STEMI; however, they do present differences in the change in LVEF during this period.

CLINICAL EVENTS AND LV REMODELING. In the univariate analysis, age, heart rate, Killip class >I, infarction in the left anterior descending artery, basal LVEF (%), LVESV (ml), myocardial edema (% of LV mass), myocardial salvage index (%), MVO, and infarct size (% of LV mass) constituted the main predictors of cardiovascular events during follow-up (Supplemental Table 1). After analysis of the association with the primary outcome, the following baseline variables were selected for adjustment: age, sex, heart rate, IS, MVO, and LVEF.

HR for the primary outcome across the whole range of values of relative change in LVEDV and relative change in LVEF at 6 months after the index episode are shown in Figure 2. Values that maximized the ability to distinguish between patients with and without a subsequent event were a relative increase of 12.5% in LVEDV (HR: 1.98; 95% CI: 1.16 to 3.4; $p = 0.013$) and a relative decrease in LVEF of 2.9% (HR: 2.38; 95% CI: 1.39 to 4.06; $p = 0.001$). Rounding up to the superior whole corresponded to a relative increase in LVEDV of 15% (HR: 2.10; 95% CI: 1.22 to 3.61; $p = 0.007$) and a relative decrease in LVEF of 3% (HR: 2.50; 95% CI: 1.47 to 4.27; $p = 0.001$).

Classification of the population according to the relative changes in LVEDV and LVEF resulted in 4 groups with different prognoses (Figure 3). Thus, the survival rate of patients with neither an increase in LVEDV (<15%) nor a decrease in LVEF (<3%) was the highest, whereas the presence of both an increase in LVEDV >15% and a decrease in LVEF >3% identified a subgroup of patients with the poorest prognosis.

The association between the changes in LVEDV and LVEF at 6 months and the primary outcome

JACC: CARDIOVASCULAR IMAGING, VOL. 12, NO. 12, 2019
DECEMBER 2019:2445–56

was also present on crude Cox regression analyses (Table 3), which showed HR for the primary outcome of 2.8 (95% CI: 1.2 to 6.4; p = 0.015) in patients with no decrease in LVEF (<3%) but an increase in LVEDV >15%, an HR of 3.5 (95% CI: 1.7 to 7.2; p = 0.001) in those with a decrease in LVEF >3% without an increase in LVEF (<15%), and an HR of 3.9 (95% CI: 1.7 to 8.8; p = 0.001) in those with both conditions, an increase in LVEDV, and a decrease in LVEF.

In the Cox-adjusted regression analysis, the poorest prognosis was observed in patients with both conditions (HR: 6.4; 95% CI: 2.6 to 15.4; p < 0.001). Patients in this group were predominantly men (p = 0.022), who at admission presented lower initial TIMI (Thrombolysis In Myocardial Infarction) flow grade (p = 0.026), a higher area at risk (p = 0.023), larger IS (p = 0.039), and a higher MVO (p = 0.044) (Table 4).

CMR PREDICTORS OF CLINICAL EVENTS. The ability of different models, assessed by the C-statistic, to detect patients with a higher risk for the primary outcome is shown in Table 5. We observed that the combination of a decrease in LVEF associated with an increase in LVEDV exceeded the predictive ability of the individual change for these parameters. However, this predictive ability was lower than that of the model including exclusively the baseline CMR-derived parameters LVEDV, LVEF, and IS: C-statistic: 0.714 (95% CI: 0.661 to 0.766) versus 0.770 (95% CI: 0.707 to 0.823). In addition, complementing the information from the baseline CMR-derived parameters with the occurrence of LVAR did not significantly increase the prediction capacity for cardiovascular events: C-statistic: 0.775 (95% CI: 0.707 to 0.823) versus 0.798 (95% CI: 0.741 to 0.848). These results suggest that the information provided by a second CMR at 6 months does not increase the prognostic implications of the baseline CMR. The same data were obtained using the NRI that showed a higher improvement in the reclassification based on the

FIGURE 3 Kaplan-Meier Cumulative Event Curves

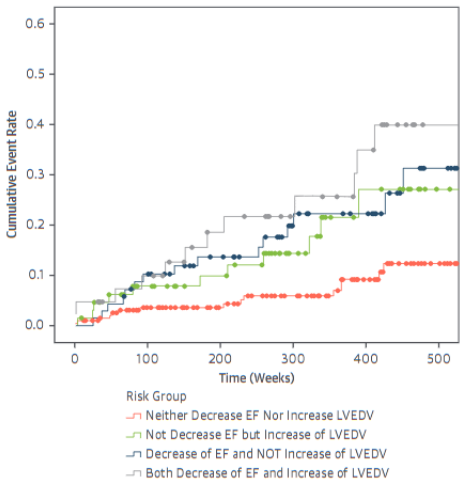

Kaplan-Meier cumulative event curves for the presence of the primary endpoint (cardiovascular death, hospitalization for heart failure, and ventricular arrhythmias) in the 4 different groups based on the variations in LVEF and LVEDV during follow-up (n = 379). Abbreviations as in Figure 2.

TABLE 3 Association Between LV Remodeling and the Primary Outcome

	Crude Model			Adjusted Model		
	HR	(95% CI)	p Value	HR	(95% CI)	p Value
Risk group (reference no decrease LVEF nor increase LVEDV)	1.00		0.002	1.00		0.000
No decrease LVEF and increase LVEDV >15%	2.80	(1.22–6.4)	0.015	1.89	(0.80–4.50)	0.149
Decrease LVEF >3% and not increase LVEDV	3.48	(1.67–7.24)	0.001	4.02	(1.88–8.62)	0.000
Decrease LVEF >3% and increase of LVEDV >15%	3.86	(1.69–8.8)	0.001	6.38	(2.64–15.42)	0.000
Age				1.07	(1.05–1.10)	0.000
Female				0.65	(0.26–1.60)	0.348
Heart rate, beats/min				1.01	(1.00–1.03)	0.079
Baseline IS, % of LV mass				1.00	(0.99–1.02)	0.605
Baseline LVEF, %				0.95	(0.92–0.97)	<0.000
MVO, % of LV mass				0.99	(0.93–1.06)	0.832

Association between LV remodeling defined by LVEDV and LVEF changes and the primary outcome when adjusted for sex (female), heart rate (beats/min), baseline IS (% of LV mass), baseline LVEF (%), and MVO (% of LV mass).
CI = confidence interval; HR = hazard ratio; other abbreviations as in Table 1.

TABLE 4 Baseline Characteristics of the 4 Different Groups of Patients

	No Changes LVEF (n = 265)					Decrease LVEF >3% (n = 109)					
	No Changes LVEDV		Increase LVEDV >15%			No Changes LVEDV		Increase LVEDV >15%			
	n	Mean ± SD or n (%)	N	Mean ± SD or n (%)	p Value	n	Mean ± SD or n (%)	n	Mean ± SD or n (%)	p Value	p Value
Age, yrs	200	59.2 ± 11.7	65	59.4 ± 12	0.992	69	60.3 ±12.7	40	56.5 ± 12	0.121	0.436
Female	200	43 (21.5)	65	6 (9.2)	0.028	69	9 (13)	40	4 (10)	0.765	0.022
Hypertension	200	82 (41)	65	31 (47.7)	0.387	69	34 (49.3)	40	21 (52.5)	0.843	0.098
Hypercholesterolemia	200	82 (41)	65	24 (36.9)	0.662	69	21 (30.4)	40	17 (42.5)	0.218	0.462
Diabetes	200	32 (16)	65	11 (16.9)	0.848	69	12 (17.4)	40	8 (20)	0.800	0.551
Smoking	200	125 (62.5)	65	41 (63.1)	1.000	69	43 (62.3)	40	26 (65)	0.839	0.837
Prior coronary heart disease	200	22 (11)	65	3 (4.6)	0.149	69	6 (8.7)	40	3 (7.5)	1.000	0.364
Index episode											
AMI location	200		65		0.830	69		40		0.649	0.964
Anterior		112 (56)		35 (53.8)			39 (56.5)		25 (62.5)		
Inferior		81 (40.5)		28 (43.1)			25 (36.2)		12 (30)		
Lateral		7 (3.5)		2 (3.1)			5 (7.2)		3 (7.5)		
Heart rate	200	76.8 ± 17.1	65	78.6 ± 23	0.942	69	79.3 ± 17	40	77 ± 22.3	0.558	0.759
Systolic blood pressure	200	130.5 ± 29.1	65	121.1 ± 19.5	0.019	69	134.1 ± 34.7	40	127 ± 27.2	0.444	0.086
Killip class >I	200	25 (12.5)	65	9 (13.8)	0.831	69	11 (15.9)	40	6 (15)	1.000	0.483
PCI <12 h	197	126 (64)	63	48 (76.2)	0.090	68	42 (61.8)	40	31 (77.5)	0.136	0.258
Coronary artery	198		65		0.930	68		40		0.940	0.947
LAD		111 (56.1)		35 (53.8)			40 (58.8)		24 (60)		
RCA		72 (36.4)		26 (40)			21 (30.9)		11 (27.5)		
LCX		15 (7.6)		4 (6.2)			7 (10.3)		5 (12.5)		
Multivessel disease	194	63 (32.5)	65	15 (23.1)	0.164	68	24 (35.3)	39	14 (35.9)	1.000	0.656
Initial TIMI	196	0.9 (1.3)	65	0.6 (1.1)	0.045	68	1.1 (1.4)	40	0.6 (1.1)	0.026	0.026
Final TIMI	200	2.9 (0.5)	65	2.9 (0.2)	0.443	69	2.9 (0.3)	40	2.8 (0.6)	0.154	0.252
Drug-eluting stent	128	0.4 ± 0.5	47	0.4 ± 0.5	0.519	42	0.3 ± 0.5	24	0.3 ± 0.5	1.000	0.568
Stents, total number	121	1.2 ± 0.6	45	1.2 ± 0.5	0.948	40	1.3 ± 0.7	23	1.2 ± 0.5	0.949	0.995
CMR data											
LVEF, %	200	51.8 ± 10.9	65	46.1 ± 12.4	0.001	69	55.3 ± 12.1	40	53.7 ± 13.2	0.571	<0.001
LVEDV	200	82 ± 19.8	65	67.7 ± 19.8	<0.001	69	84.5 ± 22.5	40	79.7 ± 27.6	0.162	<0.001
LVESV	200	40.6 ± 17.5	65	37.2 ± 17	0.204	69	39.2 ± 20.1	40	39.7 ± 24.6	0.602	0.302
Edema, % of LV mass	190	29.8 ± 15.6	63	36.6 ± 16	0.003	68	29.9 ± 15.8	39	33 ± 16.6	0.485	0.023
Myocardial salvage index, %	190	23.4 ± 22.9	63	19.3 ± 17.4	0.521	68	19.2 ± 24.1	38	24.9 ± 28.4	0.323	0.339
IS, % of LV mass	200	19.9 ± 12.3	65	25.7 ± 13.3	0.003	69	22.7 ± 17.3	39	23.7 ± 17.8	0.778	0.039
MVO, % of LV mass	200	1.1 ± 2.1	65	2.4 ± 3.5	0.005	69	1.7 ± 3	39	4.1 ± 8.5	0.335	0.044

Values are n, mean ± SD, or n (%). Baseline characteristics in the 4 different groups based on the variations in LVEF and LVEDV during follow-up.
Abbreviations as in Table 1.

baseline CMR variables (12.9%) compared with the presence of LVAR (4.7%) (Table 5).

DISCUSSION

During the weeks following a STEMI, the LV may undergo changes in volume, geometry, and function associated with the development of heart failure and worse prognosis, a process known as adverse post-infarction remodeling (5,18,19). Although there is no universally accepted definition of adverse post-infarction remodeling, a 15% to 20% increase in LVEDV is the most widely used criterion (5,20). The incidence and extent of LVAR after an AMI have declined in the era of PCI and the almost systematic use of "antiremodeling" medications (such as angiotensin-converting enzyme inhibitors and beta-blockers). However, these improvements in AMI management have not abolished LVAR, which remains a relatively frequent event after an anterior MI (21,22).

The present study shows that the incidence of major cardiovascular events during a mean follow-up of 72.9 months in patients treated with PCI after a STEMI is not trivial (13.1%). Our data also show that the definition of LVAR should necessarily consider not only changes in LVEDV but also changes in LVEF to increase its prognostic significance. Moreover, after adjustment for baseline LVEF and other variables, the isolated increase in LVEDV was not statistically associated with an adverse outcome. However, the

JACC: CARDIOVASCULAR IMAGING, VOL. 12, NO. 12, 2019
DECEMBER 2019:2445–56

increase in LVEDV in the presence of a decrease in LVEF implied worse prognosis. The cutoff analysis identified an increase in LVEDV of 15% or more and an absolute reduction of 3% or more in LVEF during the 6 months following a STEMI as the criteria that best identify patients according to their risk of cardiovascular death, readmission for heart failure, or ventricular arrhythmias in subsequent years. Patients not fulfilling either of the 2 criteria had the best prognosis, and those fulfilling both criteria had the worst. However, analysis of changes in LVEDV and LVEF over the first 6 months after STEMI did not increase the prognostic value of the principal CMR-derived variables obtained during hospitalization. These results underline the importance of considering both LVEDV and LVEF to define LVAR but do not favor the routine analysis of early LVAR with CMR to identify patients at high risk of cardiovascular events, because this strategy provides delayed prognostic information and does not improve that provided by CMR-derived variables determined in the early setting.

TABLE 5 C-Statistic and NRI for Evaluation of Added Benefit of Different CMR Variables Alone and in Combined Models in Predicting the Primary Endpoint

	C-Statistic* (95% CI)	NRI† (95% CI) (%)
Decrease LVEF >3% and increase of LVEDV >15% at 6 months	0.714 (0.661 to 0.766)	4.7 (−19.8 to 14.5)
Change in LVEF at 6 months, %	0.694 (0.625 to 0.757)	3.3 (−12.5 to 23.4)
Change in LVEDV at 6 months, ml	0.708 (0.658 to 0.762)	−9.6 (−22.4 to 12.0)
Baseline IS, % of LV mass	0.701 (0.637 to 0.759)	−2.0 (−13.6 to 13.9)
Baseline LVEF, %	0.768 (0.707 to 0.820)	10.2 (−10.9 to 33.1)
Baseline LVEDV, ml	0.705 (0.645 to 0.762)	2.1 (−11.7 to 22.3)
6-month IS, % of LV mass	0.700 (0.636 to 0.762)	−0.3 (−14.7 to 19.1)
6-month LVEF, %	0.792 (0.732 to 0.846)	10.8 (−9.9 to 32.9)
6-month LVEDV, ml	0.746 (0.694 to 0.796)	1.3 (−21.2 to 28.7)
Model 1: Baseline LVEF (%) + IS (%) + LVEDV (ml)	0.770 (0.707 to 0.823)	12.9 (−8.4 to 33.7)
Model 2: Model 1 + decrease LVEF >3% and increase of LVEDV >15% at 6 months	0.798 (0.741 to 0.848)	8.0 (4.1 to 12.1)
Model 3: 6-month LVEF (%) + IS (%) + LVEDV (ml)	0.795 (0.737 to 0.848)	8.7 (−7.7 to 39.9)

The primary endpoint is cardiovascular death, heart failure, or ventricular arrhythmias. *Adjusted for sex and age. †NRI assessed at median follow-up. Every value represents the NRI of patients with a higher risk (>20%) for the primary outcome, of each model over a baseline model including the variables sex and age.
NRI = net reclassification improvement; other abbreviations as in Tables 1 and 3.

LVEF AND LVEDV IN POST-INFARCTION REMODELING. LVEF is a key prognostic factor in coronary heart disease and should be assessed in all patients after a STEMI (23). Patients with reduced LVEF have a greater likelihood of developing progressive LVEDV and LVESV dilation during follow-up. However, a subgroup of patients with normal baseline LVEF can also increase the ventricular volumes over time (24). Wu et al. (24) showed that 15% of patients with a smaller infarct size (<18.5% of LV mass) developed LVAR (defined as an increase in LVEDV >10 ml/m^2) and 60% of patients with larger IS (≥18.5% of LV mass) did not present LVAR. Thus, IS and LV function in the acute phase do not permit accurate prediction of LVAR occurrence. This could be explained in part by subtle abnormalities of segmental LV function that are not amenable to quantification with a global endpoint such as LVEF. Thus, LVAR has been proposed as a surrogate marker in clinical trials (21,25) and as a parameter to predict outcomes (26,27). Variables measuring LVAR are expected to be more closely correlated with clinical outcomes because they integrate different aspects of post-infarction pathophysiology. Some are global (e.g., LV volumes) and some regional (e.g., LVEF or strain).

After a STEMI, the loss of contractile activity in the infarct segments and its expansion may increase wall tension in distant LV wall segments. In the infarcted segments, early neutrophil infiltration and proinflammatory cytokine liberation recruit other inflammatory cells that are involved in removing necrotic cardiomyocytes and in the differentiation of fibroblasts into myofibroblasts that play an essential role in the healing process (28). The reparative phase is associated with reductions in proinflammatory cells and an increase in anti-inflammatory Ly6C^{low}, mononuclear cell, and M2 macrophages. Increased wall stress in the healthy distant myocardium may lead to progressive eccentric hypertrophy, LV dilation, heart failure, and LVAR (29). It is important to note that salvaged and distant myocardia are also infiltrated by inflammatory cells that modulate hypertrophy and fibrosis (30,31).

Our results showed that patients with major cardiovascular events presented a trend toward a higher increase in LVEDV at 6 months when compared with those without events; however, these differences did not reach statistical significance ($p = 0.224$). Furthermore, the predictive model (using C-statistic analysis and the NRI) of the combination of increase in LVEDV and reduction in LVEF was superior (C-statistic: 0.714; 95% CI: 0.661 to 0.766) to that estimated by the LVEDV individually. Although a 3% reduction in LVEF may be subtle, these variations can be identified (32) because of the accuracy and reproducibility of CMR. A recent study showed that treatment with intravenous beta-blockers in STEMI patients can induce changes in LVEF of the same magnitude (an improvement in LVEF of 3.49%) (33). Our results, however, failed to demonstrate that direct observation of LVAR at 6 months is superior to data from CMR in the acute phase for predicting outcomes.

CENTRAL ILLUSTRATION **Best Definition of LV Adverse Remodeling and its Prognostic Implications**

379 patients with STEMI receiving PCI
CMR at baseline and at 6 months follow-up
Mean follow-up: 72.9 ± 42.8 months

Primary endpoint:
- Cardiovascular death
- Hospitalization for heart failure
- Ventricular arrhythmias

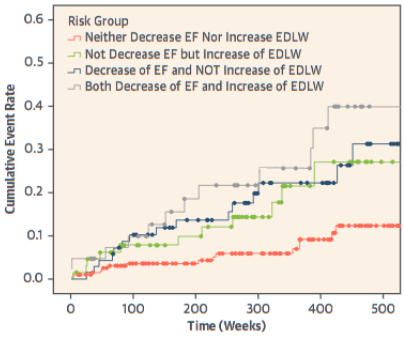

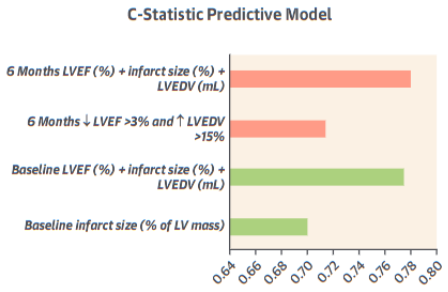

LV remodeling definition with best prognostic implications : ↓LVEF >3% and ↑LVEDV >15% at 6 months

LV adverse remodeling does not add prognostic information over basal CMR

Rodriguez-Palomares, J.F. et al. J Am Coll Cardiol Img. 2019;12(12):2445-56.

LV adverse remodeling definition with best prognostic implications includes an increase in LVEDV >15% and a concomitant reduction of LVEF >3%. However, the occurrence of LV adverse remodeling during the first 6 months of evolution post-STEMI does not add prognostic information over that provided by basal CMR. CMR = cardiac magnetic resonance; LVEDV = left ventricular end-diastolic volume; LVEF = left ventricular ejection fraction; PCI = percutaneous coronary intervention; STEMI = ST-segment elevation myocardial infarction.

IS AND LV CHANGES IN THE ACUTE PHASE OF STEMI. CMR has been considered the gold standard technique in the assessment of both acute and chronic MI (34). Several studies in STEMI patients have shown IS and LV dysfunction severity to be closely related (5,24). Hence, the main objective of myocardial reperfusion is to reduce of IS (35), and PCI, when performed early, may limit adverse post-infarction remodeling (9). However, different studies have shown that PCI results in little myocardial salvage in most patients when performed beyond 4 h after symptom onset and, in a substantial number of patients, myocardial salvage is slight after shorter ischemic times (13,23,35,36). However, there is solid evidence that reperfusion within 12 h of symptom onset improves the prognosis of patients with STEMI, and that this effect is mediated somehow in part through the beneficial effect on infarct healing and scar formation (35,37). Our results show that a model based on the information provided by early CMR (LVEDV, IS, and LVEF) is superior to a model based on the presence of LVAR (C-statistic: 0.770 [95% CI: 0.707 to 0.823] vs. 0.714 [95% CI: 0.661 to 0.766]) and as good as a model based on the information provided by CMR at 6 months (**Central Illustration**). These results are consistent with previous studies showing the prognostic significance of acute IS to predict outcomes after a STEMI (11,13). In a recent multicenter study, Eitel et al. (11) demonstrated that after an AMI, an LVEF ≤47%, IS ≥19% LV, and the presence of MVO

predicted the occurrence of major adverse cardiac events.

A recent meta-analysis showed IS measured by CMR or single-photon emission computed tomography 1 month after PCI to be strongly associated with 1-year hospitalization for heart failure and all-cause mortality (13). Furthermore, both microvascular obstruction and intramyocardial hemorrhage are associated with larger IS, adverse LV remodeling, and worse clinical outcomes. Given the prognostic significance of the information obtained from the early CMR, it is not surprising that the information obtained from the follow-up CMR does not increase its prognostic value. Also, the reduction in the IS at follow-up usually occurs in the first 4 months after a STEMI with few subsequent changes, and thus it is not justified to delay the evaluation of the patient 6 or more months (38). Finally, in our study, the early CMR was performed at a mean of 6.2 days after the STEMI when most of the dynamic changes in the infarcted area (e.g., edema, microvascular obstruction) had occurred and the necrosis was more stable (39). This could also potentially influence the absence of an increase in the prognostic value of the follow-up CMR.

Overall, these results are consistent with the notion that early changes in the LV in the acute phase of STEMI, as evaluated by CMR, summarize both effects of reperfusion and are important in determining LVAR and outcomes.

STUDY LIMITATIONS. CMR at 6 months could not be performed in 94 of 498 patients, which could imply a risk of selection bias. However, baseline data of these patients were like those who had the second CMR performed (Supplemental Table 2). Additionally, 25 patients were lost to follow-up; however, their baseline characteristics did not differ from those of patients followed up and with 2 CMR studies (Supplemental Table 3).

CONCLUSIONS

The definition of LV remodeling that best predicts adverse cardiovascular events should consider both the increase in LVEDV and the reduction in LVEF. In this regard, an increase in LVEDV (>15%) in the presence of a decrease in LVEF (>3%) implies worse prognosis. However, assessment of LVAR does not increase the prognostic value of the principal CMR-derived variables provided by the early CMR.

ACKNOWLEDGMENT The authors would like to thank Christine O'Hara for English revisions.

ADDRESS FOR CORRESPONDENCE: Dr. David García-Dorado, Department of Cardiology, Hospital Universitari Vall d'Hebron, Vall d'Hebron Institut de Recerca (VHIR) Paseo Vall d'Hebron 119-129, 08035 Barcelona, Spain. E-mail: dgdorado@vhebron.net. OR Dr. Vicente Bodi, Department of Cardiology, Hospital Clinico Universitario, INCLIVA, University of Valencia, Blasco Ibañez 17, 46010 Valencia, Spain. E-mail: vicente.bodi@uv.es.

PERSPECTIVES

COMPETENCY IN MEDICAL KNOWLEDGE: Our results show that the criteria for defining LVAR should include not only changes in LVEDV but also in LVEF to provide better prognostic information and yield optimal cutoff values for LVEDV and LVEF in the case of CMR. The present study also helps to establish which patients may benefit most from this technique and at what time after PCI it should be performed to give the most useful clinical information. Our data show that CMR during the acute phase of STEMI may identify patients at higher risk of developing adverse outcomes during the following months and years, whereas a routine second examination at 6 months does not add significant prognostic information and has the major limitation of not permitting prediction of events during the first 6 months of follow-up.

TRANSLATIONAL OUTLOOK: LV remodeling after STEMI is a long-term process; however, most studies evaluate LVAR between the third and sixth months post-AMI. Further studies should determine the best time to evaluate its presence for prognostic purposes. Furthermore, LVAR defined considering changes in LVEF in addition to LVEDV better predicts adverse events and has more potential value as a surrogate endpoint in clinical studies in patients with STEMI receiving PCI.

REFERENCES

1. Mehta RH, Harjai KJ, Cox D, et al., for the PAMI Investigators. Clinical and angiographic correlates and outcomes of suboptimal coronary flow in patients with acute myocardial infarction undergoing primary percutaneous coronary intervention. J Am Coll Cardiol 2003;42:1739–46.

2. Roger VL, Go AS, Lloyd-Jones DM, et al. Heart disease and stroke statistics—2011 update: a report from the American Heart Association. Circulation 2011;123:e18–209.

3. Carrick D, Haig C, Rauhalammi S, et al. Pathophysiology of LV remodeling in survivors of STEMI inflammation, remote myocardium, and prognosis. J Am Coll Cardiol Img 2015;8:779–89.

4. Pfeffer MA, Braunwald E. Ventricular remodeling after myocardial infarction: experimental observations and clinical implications. Circulation 1990;81:1161–72.

5. Bolognese L, Neskovic AN, Parodi G, et al. Left ventricular remodeling after primary coronary angioplasty: patterns of left ventricular dilation and long-term prognostic implications. Circulation 2002;106:2351–7.

6. Bulluck H, Go YY, Crimi G, et al. Defining left ventricular remodeling following acute ST-segment elevation myocardial infarction using cardiovascular magnetic resonance. J Cardiovasc Magn Reson 2017;19:26.

7. St. John Sutton M, Pfeffer MA, Moye L, et al. Cardiovascular death and left ventricular remodeling two years after myocardial infarction: baseline predictors and impact of long-term use of captopril: information from the Survival and Ventricular Enlargement (SAVE) trial. Circulation 1997;96:3294–9.

8. Brooks GC, Lee BK, Rao R, et al. Predicting persistent left ventricular dysfunction following myocardial infarction. J Am Coll Cardiol 2016;67:1186–96.

9. Sheiban I, Fragasso G, Rosano GMC, et al. Time course and determinants of left ventricular function recovery after primary angioplasty in patients with acute myocardial infarction. J Am Coll Cardiol 2001;38:464–71.

10. Sjöblom J, Muhrbeck J, Witt N, Alam M, Frykman-Kull V. Evolution of left ventricular ejection fraction after acute myocardial infarction implications for implantable cardioverter-defibrillator eligibility. Circulation 2014;130:743–8.

11. Eitel I, de Waha S, Wöhrle J, et al. Comprehensive prognosis assessment by CMR imaging after ST-segment elevation myocardial infarction. J Am Coll Cardiol 2014;64:1217–26.

12. Izquierdo M, Ruiz-Granell R, Bonanad C, et al. Value of early cardiovascular magnetic resonance for the prediction of adverse arrhythmic cardiac events after a first noncomplicated ST-segment-elevation myocardial infarction. Circ Cardiovasc Imaging 2013;6:755–61.

13. Stone GW, Selker HP, Thiele H, et al. Relationship between infarct size and outcomes following primary PCI: patient-level analysis from 10 randomized trials. J Am Coll Cardiol 2016;67:1674–83.

14. Bodí V, Sanchis J, López-Lereu MP, et al. Usefulness of a comprehensive cardiovascular magnetic resonance imaging assessment for predicting recovery of left ventricular wall motion in the setting of myocardial stunning. J Am Coll Cardiol 2005;46:1747–52.

15. García-Dorado D, García-del-Blanco B, Otaegui I, et al. Intracoronary injection of adenosine before reperfusion in patients with ST-segment elevation myocardial infarction: a randomized controlled clinical trial. Int J Cardiol 2014;177:935–41.

16. Ibanez B, James S, Agewall S, et al., for the ESC Scientific Document Group. 2017 ESC guidelines for the management of acute myocardial infarction in patients presenting with ST-segment elevation: the Task Force for the management of acute myocardial infarction in patients presenting with ST-segment elevation of the European Society of Cardiology (ESC). Eur Heart J 2018;39:119–77.

17. Budczies J, Klauschen F, Sinn BV, et al. Cutoff finder: a comprehensive and straightforward Web application enabling rapid biomarker cutoff optimization. PLoS One 2012;7:e51862.

18. Gheorghiade M, Bonow RO. Chronic heart failure in the United States: a manifestation of coronary artery disease. Circulation 1998;97:282–9.

19. Goldberg RJ, Konstam MA. Assessing the population burden from heart failure: need for sentinel population-based surveillance systems. Arch Intern Med 1999;159:15–7.

20. Gaudron P, Eilles C, Kugler I, Ertl G. Progressive left ventricular dysfunction and remodeling after myocardial infarction: potential mechanisms and early predictors. Circulation 1993;87:755–63.

21. Cung TT, Morel O, Cayla G, et al. Cyclosporine before PCI in patients with acute myocardial infarction. N Engl J Med 2015;373:1021–31.

22. Savoye C, Equine O, Tricot O, et al. Left ventricular remodeling after anterior wall acute myocardial infarction in modern clinical practice (from the REmodelage VEntriculaire [REVE] study group). Am J Cardiol 2006;98:1144–9.

23. Ndrepepa G, Mehilli J, Martinoff S, Schwaiger M, Schömig A, Kastrati A. Evolution of left ventricular ejection fraction and its relationship to infarct size after acute myocardial infarction. J Am Coll Cardiol 2007;50:149–56.

24. Wu E, Ortiz JT, Tejedor P, et al. Infarct size by contrast enhanced cardiac magnetic resonance is a stronger predictor of outcomes than left ventricular ejection fraction or end-systolic volume index: prospective cohort study. Heart 2008;94:730–6.

25. Perin EC, Willerson JT, Pepine CJ, et al., for the CCTRN Investigators. Effect of transendocardial delivery of autologous bone marrow mononuclear cells on functional capacity, left ventricular function, and perfusion in chronic heart failure: the FOCUS-CCTRN trial. JAMA 2012;307:1717–26.

26. Torabi A, Cleland JGF, Khan NK, et al. The timing of development and subsequent clinical course of heart failure after a myocardial infarction. Eur Heart J 2008;29:859–70.

27. Kramer DG, Trikalinos TA, Kent DM, Antonopoulos GV, Konstam MA, Udelson JE. Quantitative evaluation of drug or device effects on ventricular remodeling as predictors of therapeutic effects on mortality in patients with heart failure and reduced ejection fraction. J Am Coll Cardiol 2010;56:392–406.

28. Frangogiannis NG. The inflammatory response in myocardial injury, repair, and remodelling. Nat Rev Cardiol 2014;11:255–65.

29. Shah AM, Solomon SD. A unified view of ventricular remodelling. Eur J Heart Fail 2010;12:779–81.

30. Inserte J, Hernando V, Garcia-Dorado D. Contribution of calpains to myocardial ischaemia/reperfusion injury. Cardiovasc Res 2012;96:23–31.

31. Frangogiannis NG. Regulation of the inflammatory response in cardiac repair. Circ Res 2012;110:159–73.

32. Grothues F, Smith GC, Moon JC, et al. Comparison of interstudy reproducibility of cardiovascular magnetic resonance with two-dimensional echocardiography in normal subjects and in patients with heart failure or left ventricular hypertrophy. Am J Cardiol 2002;90:29–34.

33. Pizarro G, Fernández-Friera L, Fuster V, et al. Long-term benefit of early pre-reperfusion metoprolol administration in patients with acute myocardial infarction: results from the METOCARD-CNIC trial (Effect of Metoprolol in Cardioprotection During an Acute Myocardial Infarction). J Am Coll Cardiol 2014;63:2356–62.

34. Kim RJ, Fieno DS, Parrish TB, et al. Relationship of MRI delayed contrast enhancement to irreversible injury, infarct age, and contractile function. Circulation 1999;100:1992–2002.

35. Keeley EC, Boura JA, Grines CL. Primary angioplasty versus intravenous thrombolytic therapy for acute myocardial infarction: a quantitative review of 23 randomised trials. Lancet 2003;361:13–20.

36. Fieno DS, Hillenbrand HB, Rehwald WG, et al. Infarct resorption, compensatory hypertrophy, and differing patterns of ventricular remodeling following myocardial infarctions of varying size. J Am Coll Cardiol 2004;43:2124–31.

37. Chan W, Duffy SJ, White DA, et al. Acute left ventricular remodeling following myocardial infarction: coupling of regional healing with remote extracellular matrix expansion. J Am Coll Cardiol Img 2012;5:884–93.

38. Pokorney SD, Rodriguez JF, Ortiz JT, Lee DC, Bonow RO, Wu E. Infarct healing is a dynamic process following acute myocardial infarction. J Cardiovasc Magn Reson 2012;14:62.

39. Bulluck H, Hammond-Haley M, Weinmann S, Martinez-Macias R, Hausenloy DJ. Myocardial infarct size by CMR in clinical cardioprotection studies: insights from randomized controlled trials. J Am Coll Cardiol Img 2017;10:230–40.

KEY WORDS cardiac magnetic resonance, infarct size, left ventricular ejection fraction, left ventricular end-diastolic volume, left ventricular end-systolic volume, left ventricular remodeling, microvascular obstruction, prognosis, ST-segment elevation myocardial infarction

APPENDIX For a supplemental appendix including tables, please see the online version of this paper.

CMR PROTOCOL

All CMR studies were performed with a 1.5 T clinical scanner (Sonata or Avanto scanner Siemens, Erlangen, Germany) using a phased-array cardiac receiver coil. Electrocardiogram-gated breath-hold short-axis cine views were performed to quantify volumes and ejection fraction (SSFP sequences; slice thickness: 6 mm; space between slices 67%; matrix: 256 × 256: field of view: 300 to 370 mm; temporal resolution <50 ms). Additional 2-chamber, 3-chamber, and 4-chamber views were also obtained. LGE images were acquired at identical slice positions to the cine images after the administration of 0.2 mmol/kg of body weight Gadolinium-DTPA (Gd-DTPA) (Berlex, Montville, NJ, USA).

STIR sequences were used in the same view as the cine sequences, all in mid-diastole to evaluate the edema, (slice thickness: 8 mm; space between slices 20%; matrix: 256 × 256: FOV: 300 to 370 mm; temporal resolution <50 ms; repetition time: 2 R-R intervals; echo time: 100 ms; inversion time: 170 ms; flip angle: 160°; bandwidth, 781 Hz/pixel).

A segmented inversion-recovery (seg-IR) gradient-echo sequence was acquired starting at 10 to 15 min after contrast administration (Matrix 256 × 197, voxel size 2.0 × 1.6 × 6 mm, TE 4.91 ms, TR 700 ms, flip angle 30°; and the bandwidth 140 Hz/pixel).

Image analysis

Quantitative analyses of left ventricular (LV) mass, end-diastolic volume (EDV), end-systolic volume (ESV), and ejection fraction (EF) were performed by manually tracing the epicardial and endocardial borders as previously described. Volume indices were calculated by dividing the EDV or ESV by body surface area. Contractility was analyzed and the wall motion score index estimated (WMSI).

The myocardial edema was quantified in STIR sequences delineating the areas of intensity, plus 2 standard deviations above average, obtained from the remote healthy myocardium, and normalized by the left ventricular mass. Myocardial salvage index (MSI) was calculated as the difference in myocardial edema minus the size of the necrosis obtained through late enhancement sequences divided by the myocardial edema.

Quantification of the infarcted myocardium was assessed by delineating the regions of LGE with ≥ 5 standard deviations (SD) over remote signal intensity on each of the contrast-enhanced CMR tomograms and summed, as previously described. MVO was considered if there was presence of dark areas of absent contrast surrounded by hyperenhanced tissue on LGE images. Areas of MVO were included in the total LGE area. The summed area was multiplied by the specific gravity of myocardium to obtain the LGE volume.

Relative volumes were the percentage of total LV mass (% of LV mass) that presented LGE.

Tissue Tracking CMR

All strain parameters were quantified offline by an experienced observer blinded to patient data. These analyses were carried out retrospectively using currently available certified software (CMR42, Circle Cardiovascular Imaging Inc., Calgary, Alberta, Canada). Data were expressed on a per-patient basis. The global peak longitudinal strain (LS), circumferential strain (CS), and radial strain (RS) were calculated as the mean of the respective peak values in the 16 segments.

Supplemental Table 1: Hazard ratio (HR) of the association between baseline variables with the primary outcome: cardiovascular mortality, hospitalization for heart failure or ventricular arrhythmia. Abbreviations as in table 1.

Values are mean (standard deviation) or n (%).

		HR	95% CI	p
Demographics				
Age	*mean (SD)*	1,05	(1,03 - 1,08)	0,000
Sex (women)	*n (%)*	0,64	(0,27 - 1,51)	0,311
Hypertension	*n (%)*	1,22	(0,7 - 2,14)	0,485
Hypercholesterolemia	*n (%)*	0,86	(0,47 - 1,57)	0,631
Diabetes	*n (%)*	0,84	(0,38 - 1,88)	0,677
Smoking	*n (%)*	0,97	(0,54 - 1,72)	0,905
Prior Coronary Heart Disease	*n (%)*	0,82	(0,26 - 2,65)	0,744
Index episode				
AMI location	*n (%)*			
Anterior		1,00		0,143
Inferior		0,61	(0,33 - 1,11)	0,104
Lateral		0,27	(0,04 - 2,01)	0,203
Heart rate	*mean (SD)*	1,02	(1 - 1,03)	0,005
Systolic blood pressure	*mean (SD)*	1,01	(1 - 1,02)	0,210
killip class > I	*n (%)*	1,66	(0,78 - 3,55)	0,191
PCI < 12 hours	*n (%)*	1,70	(0,91 - 3,17)	0,093
Coronary Artery	*n (%)*			
ADA		1,00		0,099
ACD		0,61	(0,33 - 1,13)	0,117
ACX		0,19	(0,03 - 1,41)	0,105
Multi-vessel disease	*n (%)*	0,97	(0,51 - 1,83)	0,916
Initial TIMI	*n (%)*			
Occlusion		1,00		0,957
Low		0,73	(0,17 - 3,07)	0,667
Intermediate		0,93	(0,32 - 2,68)	0,887
Normal		1,08	(0,57 - 2,05)	0,813
Initial TIMI	*mean (SD)*	1,02	(0,83 - 1,27)	0,834
Final TIMI	*mean (SD)*	0,83	(0,47 - 1,46)	0,522
Drug-eluting Stent	*mean (SD)*	0,38	(0,11 - 1,3)	0,122
Total Number of stents	*mean (SD)*	1,26	(0,68 - 2,32)	0,457
MRI baseline data				
LVEF	*mean (SD)*	0,95	(0,93 - 0,98)	<0,000
LV end-diastolic volume	*mean (SD)*	1,01	(1 - 1,02)	0,12

LV end-systolic volume	*mean (SD)*	1,02	(1,01 - 1,03)	<0,000
Edema (% of LV mass)	*mean (SD)*	1,03	(1,01 - 1,05)	0,002
Myocardial salvage index (%)	*mean (SD)*	0,98	(0,96 - 1)	0,022
Infarct Size (% of LV mass)	*mean (SD)*	1,03	(1,02 - 1,05)	<0,000
MVO (% of LV mass)	*mean (SD)*	1,04	(1 - 1,08)	0,042

Supplemental Table 2: Baseline characteristics of the entire study group and of patients whether the CMR at 6 months was or not performed. Abbreviations as in Table 1.

Values are mean (standard deviation) or n (%).

		All patients (n = 498)		CMR at 6 months (No, n = 94)		CMR at 6 months (Yes, n = 404)		p value
		N	n (%)	N	n (%)	N	n (%)	
Demographics								
Age (years)	*mean (SD)*	488	59.7 (11.9)	94	61.1 (12.1)	394	59.4 (11.9)	0.167
Gender (female)	*n (%)*	490	81 (16.5%)	94	14 (14.9%)	396	67 (16.9%)	0.758
Hypertension	*n (%)*	480	234 (48.8%)	94	59 (62.8%)	386	175 (45.3%)	0.003
Hypercholesterolemia	*n (%)*	480	200 (41.7%)	94	53 (56.4%)	386	147 (38.1%)	0.002
Diabetes	*n (%)*	480	93 (19.4%)	94	28 (29.8%)	386	65 (16.8%)	0.008
Smoking	*n (%)*	480	292 (60.8%)	94	49 (52.1%)	386	243 (63%)	0.060
Prior coronary heart disease	*n (%)*	480	46 (9.6%)	94	11 (11.7%)	386	35 (9.1%)	0.437
Index episode								
AMI location	*n (%)*	491		93		398		0.009
Anterior			273 (55.6%)		40 (43%)		233 (58.5%)	
Inferior			192 (39.1%)		44 (47.3%)		148 (37.2%)	
Lateral			26 (5.3%)		9 (9.7%)		17 (4.3%)	
Heart rate	*mean (SD)*	479	77.3 (19.7)	93	75.5 (22.1)	386	77.8 (19.1)	0.277
Systolic blood pressure	*mean (SD)*	480	128.4 (29)	94	126.1 (30)	386	128.9 (28.8)	0.423
Killip class > I	*n (%)*	484	81 (16.7%)	94	22 (23.4%)	390	59 (15.1%)	0.064
PCI < 12 h	*n (%)*	468	319 (68.2%)	88	61 (69.3%)	380	258 (67.9%)	0.899
Coronary artery	*n (%)*	468		91		377		0.002
LAD			253 (54.1%)		38 (41.8%)		215 (57%)	
RCA			165 (35.3%)		35 (38.5%)		130 (34.5%)	
LCX			49 (10.5%)		17 (18.7%)		32 (8.5%)	
Multivessel disease	*n (%)*	465	147 (31.6%)	89	28 (31.5%)	376	119 (31.6%)	1.000
Initial TIMI	*n (%)*	468		89		379		0.584
Occlusion			303 (64.7%)		57 (64%)		246 (64.9%)	
Low			33 (7.1%)		9 (10.1%)		24 (6.3%)	
Intermediate			36 (7.7%)		9 (10.1%)		27 (7.1%)	
Normal			96 (20.5%)		14 (15.7%)		82 (21.6%)	
Final TIMI	*n (%)*	480		94		386		0.078
Occlusion			13 (2.7%)		5 (5.3%)		8 (2.1%)	
Low			2 (0.4%)		0 (0%)		2 (0.5%)	
Intermediate			36 (7.5%)		9 (9.6%)		27 (7%)	
Normal			429 (89.4%)		80 (85.1%)		349 (90.4%)	
Drug-eluting stent	*mean (SD)*	317	0.5 (0.5)	68	0.7 (0.5)	249	0.4 (0.5)	0.000
Stents total number	*mean (SD)*	300	1.2 (0.6)	68	1.1 (0.6)	232	1.2 (0.6)	0.098
CMR baseline data								
LVEF (%)	*mean (SD)*	498	51.6 (12.1)	94	52.9 (12.8)	404	51.3 (11.9)	0.092
LV end-diastolic volume (mL)	*mean (SD)*	498	79.7 (21.9)	94	79 (22.6)	404	79.8 (21.8)	0.511

		All patients (n = 498)		CMR at 6 months (No, n = 94)		CMR at 6 months (Yes, n = 404)		
		N	n (%)	N	n (%)	N	n (%)	p value
LV end-systolic volume (mL)	*mean (SD)*	497	39.9 (19.1)	93	38.8 (20.3)	404	40.1 (18.9)	0.180
Edema (% of LV mass)	*mean (SD)*	461	31.4 (16.4)	94	30.2 (17.1)	367	31.7 (16.2)	0.334
Myocardial salvage index (%)	*mean (SD)*	460	24 (24.9)	94	31.4 (30.7)	366	22.1 (22.9)	0.128
Infarct size (% of LV mass)	*mean (SD)*	475	22.1 (14.6)	94	21.7 (15.5)	381	22.2 (14.4)	0.537
MVO (% of LV mass)	*mean (SD)*	474	1.9 (4)	94	2.4 (4.8)	380	1.8 (3.8)	0.983

Supplemental Table 3: Baseline characteristics of the entire study group and of patients who completed the study and the ones who were lost of follow-up. Abbreviations as in Table 1.

		All patients (n = 404)		Lost to follow-up (Yes, n = 25)		Not lost to follow-up (No, n = 379)		p value
		N	n (%)	N	n (%)	N	n (%)	
Demographics								
Age (years)	*mean (SD)*	394	59.4 (11.9)	15	61.3 (8.5)	379	59.3 (12)	0.478
Gender (female)	*n (%)*	396	67 (16.9%)	17	3 (17.6%)	379	64 (16.9%)	1.000
Hypertension	*n (%)*	386	175 (45.3%)	7	4 (57.1%)	379	171 (45.1%)	0.706
Hypercholesterolemia	*n (%)*	386	147 (38.1%)	7	2 (28.6%)	379	145 (38.3%)	0.713
Diabetes	*n (%)*	386	65 (16.8%)	7	2 (28.6%)	379	63 (16.6%)	0.335
Smoking	*n (%)*	386	243 (63%)	7	6 (85.7%)	379	237 (62.5%)	0.267
Prior coronary heart disease	*n (%)*	386	35 (9.1%)	7	0 (0%)	379	35 (9.2%)	1.000
Index episode								
AMI location	*n (%)*	398		19		379		0.019
Anterior			233 (58.5%)		17 (89.5%)		216 (57%)	
Inferior			148 (37.2%)		2 (10.5%)		146 (38.5%)	
Lateral			17 (4.3%)		0 (0%)		17 (4.5%)	
Heart rate	*mean (SD)*	386	77.8 (19.1)	7	70 (14.5)	379	77.9 (19.1)	0.301
Systolic blood pressure	*mean (SD)*	386	128.9 (28.8)	7	132.6 (31.9)	379	128.9 (28.8)	0.649
Killip class > I	*n (%)*	390	59 (15.1%)	11	5 (45.5%)	379	54 (14.2%)	0.015
PCI < 12 h	*n (%)*	380	258 (67.9%)	7	7 (100%)	373	251 (67.3%)	0.102
Coronary artery	*n (%)*	377		1		376		0.004
LAD			215 (57%)		0 (0%)		215 (57.2%)	
RCA			130 (34.5%)		0 (0%)		130 (34.6%)	
LCX			32 (8.5%)		1 (100%)		31 (8.2%)	
Multivessel disease	*n (%)*	376	119 (31.6%)	5	2 (40%)	371	117 (31.5%)	0.653
Initial TIMI	*n (%)*	379		5		374		0.124
Occlusion			246 (64.9%)		5 (100%)		241 (64.4%)	
Low			24 (6.3%)		0 (0%)		24 (6.4%)	
Intermediate			27 (7.1%)		0 (0%)		27 (7.2%)	
Normal			82 (21.6%)		0 (0%)		82 (21.9%)	
Final TIMI	*n (%)*	386		7		379		0.000
Occlusion			8 (2.1%)		2 (28.6%)		6 (1.6%)	
Low			2 (0.5%)		0 (0%)		2 (0.5%)	
Intermediate			27 (7%)		0 (0%)		27 (7.1%)	
Normal			349 (90.4%)		5 (71.4%)		344 (90.8%)	
Drug-eluting stent	*mean (SD)*	249	0.4 (0.5)	5	1.8 (0.4)	244	0.4 (0.5)	0.000
Stents total number	*mean (SD)*	232	1.2 (0.6)	0	n.a.	232	1.2 (0.6)	n.a.
CMR baseline data								
LVEF (%)	*mean (SD)*	404	51.3 (11.9)	25	48.7 (10)	379	51.4 (12)	0.265
LV end-diastolic volume (mL)	*mean (SD)*	404	79.8 (21.8)	25	78.8 (18)	379	79.9 (22)	0.988
LV end-systolic volume (mL)	*mean (SD)*	404	40.1 (18.9)	25	43 (17.4)	379	39.9 (19)	0.330
Edema (% of LV mass)	*mean (SD)*	367	31.7 (16.2)	2	55.3 (1)	365	31.6 (16.1)	0.040

Myocardial salvage index (%)	*mean (SD)*	366	22.1 (22.9)	2	41 (24)	364	21.9 (22.9)	0.154
Infarct size (% of LV mass)	*mean (SD)*	381	22.2 (14.4)	3	31.6 (9.2)	378	22.1 (14.4)	0.151
MVO (% of LV mass)	*mean (SD)*	380	1.8 (3.8)	2	0.6 (0.8)	378	1.8 (3.8)	0.872

ANEXO III: Gavara J*, Rodriguez-Palomares JF*, Ríos-Navarro C, et al. Int J Cardiovasc Imaging 2020. Doi: 10.1007/s10554-020-01890-w

The International Journal of Cardiovascular Imaging
https://doi.org/10.1007/s10554-020-01890-w

ORIGINAL PAPER

Longitudinal strain in remote non-infarcted myocardium by tissue tracking CMR: characterization, dynamics, structural and prognostic implications

Jose Gavara[1,2] · Jose F. Rodriguez-Palomares[3] · Cesar Rios-Navarro[1] · Filipa Valente[3] · Jose V. Monmeneu[4] · Maria P. Lopez-Lereu[4] · Ignacio Ferreira-Gonzalez[3,5] · Bruno Garcia del Blanco[3] · Imanol Otaegui[3] · Joaquim Canoves[1] · Elena de Dios[1,6] · Nerea Perez[1] · Paolo Racugno[1] · Clara Bonanad[1] · Gema Minana[1] · Victor Marcos[1] · Jose A. Barrabes[3] · Arturo Evangelista[3] · David Moratal[2] · Antoni Bayes-Genis[6,7,8] · Julio Nunez[1] · Francisco J. Chorro[1,6] · Vicente Bodi[1,6]

Received: 21 October 2019 / Accepted: 15 May 2020

Abstract

Purpose In ST-segment elevation myocardial infarction (STEMI) patients, longitudinal strain (LS) in remote non-infarcted myocardium (RNM) has not yet been characterized by tissue tracking (TT) cardiovascular magnetic resonance (CMR). In STEMI patients, we aimed to characterize RNM-LS by TT-CMR and to assess both its dynamics and its structural and prognostic implications.

Methods We recruited 271 patients with a first STEMI studied with TT-CMR 1 week after infarction. Of these patients, 145 underwent 1-week and 6-month TT-CMR and were used to characterize both the dynamics and the short-term and long-term structural implications of RNM-LS. Based on previously validated data, RNM areas were defined depending on the culprit coronary artery.

Results Reduced RNM-LS at 1 week (n = 70, 48%) was associated with larger infarct size and more depressed left ventricular ejection fraction (LVEF) at both the 1-week and 6-month TT-CMR (p value < 0.001). Late normalization of RNM-LS was frequent (28/70, 40%) and independently related to late recovery of LVEF (p value = 0.002). Patients with reduced RNM-LS at 1-week TT-CMR had more major adverse cardiac events (death, heart failure or re-infarction) in both the 271 patients included in the study group (26% vs. 11%, p value = 0.002) and in an external validation cohort made up of 177 STEMI patients (57% vs. 13%, p value < 0.001).

Conclusion After STEMI, reduced RNM-LS by TT-CMR is common and is associated with more severe short- and long-term structural damage. There is a beneficial tendency towards recovery of RNM-LS that parallels late recovery of LVEF. More events occur in patients with reduced RNM-LS.

Keywords Cardiovascular magnetic resonance · Myocardial infarction · Prognosis · Strain · Tissue tracking

Abbreviations

CMR	Cardiovascular magnetic resonance
EF	Ejection fraction
LAD	Left anterior descending
LCX	Left circumflex
LS	Longitudinal strain
LV	Left ventricular
MACE	Major adverse cardiac events
RCA	Right coronary artery
RNM	Remote non-infarcted myocardium
STEMI	ST-segment elevation myocardial infarction
TT	Tissue tracking

Jose Gavara and Jose F. Rodriguez-Palomares contributed equally to this work

Electronic supplementary material The online version of this article (https://doi.org/10.1007/s10554-020-01890-w) contains supplementary material, which is available to authorized users.

✉ Cesar Rios-Navarro
cesar_rios1@hotmail.com

✉ Vicente Bodi
vicente.bodi@uv.es

Extended author information available on the last page of the article

Published online: 02 June 2020

Introduction

Based on echocardiography, strain has emerged as a novel concept for evaluating systolic function [1, 2]. This knowledge has rapidly moved into the field of cardiovascular magnetic resonance (CMR) using tissue tracking (TT). Longitudinal strain (LS) measured by TT-CMR promises to become the gold standard for an accurate quantification of systolic function in different scenarios [3, 4].

TT-CMR can provide valuable information to characterize motion in remote non-infarcted myocardium (RNM) and to monitor its dynamics and structural implications after infarction [5]. Nevertheless, so far no specific study addressing this issue has been undertaken. Moreover, the prognostic significance of systolic function in RNM remains undetermined.

In the setting of ST-segment elevation myocardial infarction (STEMI) and using LS measured by TT-CMR we addressed the following objectives: 1) Characterize the dynamics of RNM-LS within the first six months after infarction. 2) Analyze the short- and long-term structural implications of RNM-LS status soon after infarction. 3) Evaluate the impact of the dynamics of RNM-LS on the recovery of left ventricular (LV) ejection fraction (EF). As a secondary objective we explored the potential prognostic implications resulting from the presence of reduced RNM-LS soon after infarction.

Methods

Study group

This study originates from a large STEMI registry compiled in a tertiary university hospital since 2002 and recently used by our group to address the prognostic value of global LS [6]. TT-CMR data were collected retrospectively. All patients gave written informed consent to be included in the database. The study protocol was approved by the local ethics committee on human research and complies with the 1975 Declaration of Helsinki guidelines.

All baseline and CMR data (with the exception of TT-CMR indices) were prospectively collected and immediately registered into the database. The occurrence of clinical events was updated on a yearly basis [7].

Due to the fact that the software for TT-CMR measurements was not available until 2016, quantification of RNM-LS had to be performed retrospectively. The vast majority of studies acquired between 2002 and 2010 were not technically valid since the required Cine imaging protocol for TT analysis was not routinely adopted in our institution until 2011. Thus, the study group comprised patients included in the registry from 2011 to 2014.

Inclusion criteria were patients admitted for a first STEMI on the basis of current definitions [8], treated with percutaneous coronary intervention and undergoing pre-discharge CMR. We enrolled 340 patients between 2011 and 2014.

Exclusion criteria were death (n = 13), re-infarction (n = 9), severe clinical instability (n = 10) during admission, and any contraindications to CMR: claustrophobia (n = 2), previous pacemaker (n = 3), patient's decision (n = 2), and previous history of adverse reactions to gadolinium contrast (n = 2). Finally, patients with significant multivessel disease (stenosis greater than 90% in the non-culprit artery or 50–90% plus evidence of ischemia in pre-discharge vasodilator stress CMR, n = 18), and those with insufficient image acquisition for an accurate assessment of TT-CMR indices (n = 10) were also excluded. Thus the final study group comprised 271 patients.

From 2011 to 2012, CMR was repeated (per protocol) at 6 months post-STEMI in 145 patients (2320 segments).

Thrombolysis in myocardial infarction flow grade in the culprit artery was recorded before and after percutaneous coronary intervention [9]. Patients were managed both in-hospital and after discharge by a STEMI unit, and the European Society of Cardiology recommendations were strictly followed [8].

CMR

All patients included in the study group were examined with a 1.5 T System (Sonata Magnetom, Siemens, Erlangen, Germany) 7 ± 2 days after STEMI in accordance with our previously validated study protocol [10, 11]. The subgroup of 145 patients re-evaluated at 6 months underwent the second CMR study 182 ± 39 days after STEMI.

CMR acquisition and sequences

Cine images were acquired in two-, three-, and four-chamber views, and in short-axis views using a steady-state free precession sequence (repetition time/echo time: 2.8/1.2 ms; flip angle: 58°; matrix: 256 × 300; field of view: 320 × 270 mm; slice thickness: 7 mm).

Late gadolinium enhancement imaging was performed 10 min after administering the gadolinium-based contrast agent in the same locations as in the cine images using a segmented inversion recovery steady-state free precession sequence (repetition time/echo time: 2.5 ms/1.26 ms; flip angle: 45°; matrix: 256 × 184; field of view: 340 × 235 mm; slice thickness: 7 mm; interslice interval: 3 mm). Inversion time was adjusted to nullify normal myocardium [10, 11].

Black blood, T2-weighted short TI inversion recovery sequences in the same short-axis view as the cine sequences,

all in mid-diastole, were carried out. A half-Fourier acquisition single-shot turbo spin echo multisection sequence was used (recovery time: two R-R intervals; echo time: 33 ms; inversion time: 170 ms; slice thickness: 8 mm; interslice interval: 2 mm; flip angle: 160°; matrix: 256×151; bandwidth: 781 Hz/pixel). Additionally, a segmented turbo-spin echo sequence was obtained with one slice per breath-hold (recovery time: two R-R intervals; echo time: 100 ms; inversion time: 170 ms; slice thickness: 8 mm; interslice interval: 2 mm; flip angle: 180°; matrix: 256×146; bandwidth: 235 Hz/pixel) [10, 11].

CMR indices quantification

Traditional CMR indices were quantified offline, by 2 operators with > 10-year experience blinded to all patient data, using customized software (QMASS MR, 6.1.5, Medis, Leiden, The Netherlands). Indices were prospectively recorded and immediately included in the registry database.

LVEF (%), LV end-diastolic volume index (ml/m^2), LV end-systolic volume index (ml/m^2) and LV mass index (g/m^2) were calculated by manual planimetry of endocardial and epicardial borders in short-axis view cine images.

Infarct size (% of LV mass) was pre-defined as the percentage of LV mass showing an intensity > 5 standard deviations in comparison with the remote non-infarcted territory; all cases were visually revised and quantified by manual planimetry. Microvascular obstruction (% of LV mass) was quantified by manual planimetry and defined as the percentage of LV mass showing a lack of contrast uptake in the tissue core showing late gadolinium enhancement [10, 11].

Myocardial edema (% of LV mass) was regarded as areas of high T2 signal intensity. All short-axis view slices were separately analyzed, and the presence of edema was visually quantified by manual planimetry and expressed as the percentage of LV mass showing edema. LV mass was measured in T2 sequences for normalization. Myocardial salvage index (% of LV mass with myocardial edema not showing late enhancement) was calculated as the percentage of myocardium at risk not showing late gadolinium enhancement, considering that the myocardium at risk was the myocardium showing edema [10, 11].

Definition of RNM in CMR images

Based on previously validated data [12], RNM areas were defined for each patient on the basis of the respective culprit coronary artery: left anterior descending (LAD), left circumflex (LCX), and right coronary artery (RCA). Figure 1 displays within the 16-segment model [13] which segments were categorized as infarct or RNM depending on the culprit coronary artery.

TT-CMR

An experienced observer retrospectively quantified strain parameters (RNM-LS and infarct-LS) using certified software (CMR42, Circle Cardiovascular Imaging Inc., Calgary, Canada).

In order to avoid data overload and based on recent literature showing that LS provides the highest prognostic information after STEMI, we focused strain analyses on LS and not on circumferential or radial strain [6].

The 16-segment model was used for calculation of the peak LS (%) in each segment [13]. Negative values were transformed into absolute numbers. Segments were considered to show normal or reduced LS based on previously validated cut-off values (Supplemental Table 1) [6].

RNM-LS (%) and infarct-LS (%) were calculated individually for each patient as the mean of the peak values of segments included in RNM or infarct area depending on the culprit coronary artery (Fig. 1).

Regarding the cut-off values to define reduced LS in infarct and RNM areas, six different cut-off values were calculated in relation to the area (infarct or RNM) and the culprit coronary artery (LAD, LCX, or RCA). To calculate

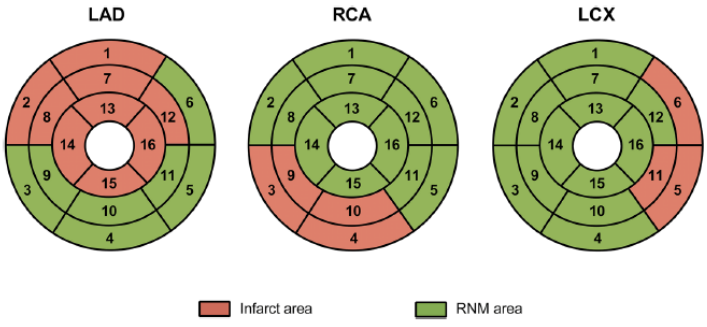

Fig. 1 Classification of each segment as RNM or infarct according to the infarct-related coronary artery (adapted from [12]). Based on [12], RNM (green) and infarct (orange) areas were defined within the 16-segment model depending on the culprit coronary artery: LAD (left), RCA (central), or LCX (right). *LAD* Left anterior descending, *LCX* Left circumflex, *RCA* Right coronary artery, *RNM* Remote non-infarcted myocardium

these values, we used the control group of 32 patients employed in the same STEMI registry for addressing the prognostic implications of global LS [6] to obtain LS in the 16 segments of the LV. Subsequently, according to the three main infarct-related coronary arteries, the cut-off values used to define reduced infarct-LS or RNM-LS were calculated as the lower 95% percentile of the mean LS value from those segments categorized as infarct or RNM in Fig. 1. Consequently, depending on the culprit coronary artery, the following cut-off values to define reduced LS (in both RNM and infarct areas) were obtained: LAD (RNM-LS ≤ 11.2%, and infarct-LS ≤ 11.1%); LCX (RNM-LS ≤ 10.8%, and infarct-LS ≤ 12.9%), and RCA (RNM-LS ≤ 12.1%, and infarct-LS ≤ 8.9%) (Supplemental Table 2).

Inter- and intra-observer variability for all TT-CMR and traditional CMR indices used in the present study are shown in Supplemental Tables 3a and 3b and in Supplemental Fig. 1a and b.

End-points

We addressed the following primary end-points:

1) Characterization of the dynamics of RNM-LS.

2) Short- and long-term structural implications of reduced 1 week RNM-LS on the status of traditional indices at 1-week and 6-month CMR.

3) Relationship between the relative percentage change of RNM-LS (ΔRNM-LS, %) from 1 week to 6 months and late systolic recovery of LVEF (ΔLVEF, %).

As a secondary end-point we explored the potential prognostic implications of the presence of reduced 1 week RNM-LS. For this purpose, we determined time to first major adverse cardiac event (MACE) defined as a combined end-point that included death, re-admission for heart failure or re-admission for re-infarction, whichever occurred first. Current European Society of Cardiology definitions were applied [8, 14]. All events were prospectively reviewed using both the local and the regional electronic registries and consensus between 3 cardiologists was required to finally assign a cardiac event.

In order to prospectively confirm the potential prognostic implications of RNM-LS obtained in the study group we followed-up an entirely prospective (including TT-CMR data collection) external validation cohort made up of 177 patients admitted for STEMI in a different tertiary hospital. Further details on the study group and the external validation cohort can be consulted in the Supplementary Material as well as in Supplemental Tables 4, 5, 6, and 7.

Statistical methods

Data were tested for normal distribution using the Kolmogorov–Smirnov test. Continuous normally distributed data were expressed as the mean ± the standard deviation of the mean and compared using the paired and unpaired Student's t-tests. Non-parametric data were expressed as the median with the interquartile range and compared using the Mann–Whitney U-test. Group percentages were compared using the Chi-square test or Fisher's exact test where appropriate.

We analyzed the relationship between ΔRNM-LS (%) and ΔLVEF (%) using multivariable linear regression models (enter or stepwise modalities where appropriate) in the entire study group and separately in patients with preserved and with depressed LVEF at 1-week CMR based on individualized and currently accepted cut-off values of LVEF by CMR [15]. Additional analyses were carried out using cut-off values previously validated by our group for prognostic purposes: > 30% of LV mass considered as presence of extensive infarct area [16] and > 15% of relative increase in LV end-diastolic volume index from 1-week to 6-month CMR (ΔLV end-diastolic volume index, %) considered as presence of significant adverse remodeling [17].

The associations of variables with time to first MACE were assessed using Cox proportional hazard regression analyses (enter or stepwise modalities where appropriate). The respective hazard ratios with the corresponding 95% confidence intervals were computed. The association between reduced RNM-LS and infarct-LS at 1-week CMR with time to first MACE was also assessed using Kaplan–Meier curves and the log-rank test.

Further details on the strategy applied to obtain the final multivariable model as well as on co-linearity of variables are depicted in Supplemental Tables 8 and 9.

Statistical significance was considered for a two-tailed p value < 0.05. The SPSS statistical package (version 15.0, SPSS Inc., Chicago, Illinois) and STATA (Version 9.0, StataCorp, College Station, Texas) were used throughout.

Results

Dynamics and structural implications of RNM-LS

Dynamics and structural implications of RNM-LS were examined in the group of 145 patients (2320 segments) in whom TT-CMR was carried at 1 week and at 6 months post-STEMI. Baseline characteristics are shown in Table 1.

Patients with reduced RNM-LS at 1 week (n = 70, 48%) (Fig. 2a) exhibited more severe structural abnormalities at both the 1-week and 6-month CMR studies (Table 2) including more depressed LVEF and larger infarct size (p value < 0.001 for all comparisons). Similarly, patients categorized with depressed LVEF or larger infarct size at 6 months displayed significantly lower RNM-LS and

Table 1 Baseline characteristics of patients restudied at 6 months. Comparison between patients with reduced and not reduced RNM-LS at 1-week TT-CMR

	All patients	Non-reduced RNM-LS	Reduced RNM-LS	p value
Number of patients	145	75	70	
Age (years)	58 ± 12	58 ± 12	58 ± 11	0.9
Male sex (%)	120 (83)	55 (73)	65 (93)	0.002
Diabetes mellitus (%)	23 (16)	11 (15)	12 (17)	0.7
Hypertension (%)	56 (39)	31 (41)	25 (36)	0.5
Hypercholesterolemia (%)	55 (38)	24 (32)	31 (44)	0.1
Smoker (%)	86 (59)	36 (48)	50 (71)	0.004
Heart rate on admission (beats per min)	82 ± 22	76 ± 19	88 ± 23	0.001
Systolic pressure (mmHg)	125 ± 24	125 ± 25	125 ± 24	0.9
Killip class 1 versus >1 (%)				0.09
1	134 (92)	72 (96)	62 (89)	
>1	11 (8)	3 (4)	8 (11)	
Time to reperfusion (min)	180 [124–331]	180 [119–323]	182 [135–370]	0.4
Peak creatine kinase MB mass (ng/ml)	187 [74–300]	101 [48–253]	265 [122–392]	<0.001
Anterior infarction (%)	80 (55)	38 (51)	42 (60)	0.3
TIMI flow grade before PCI (%)				0.9
0	58 (40)	30 (40)	28 (40)	
1	13 (9)	7 (9)	6 (9)	
2	17 (12)	10 (13)	7 (10)	
3	57 (39)	28 (38)	29 (41)	
TIMI flow grade after PCI (%)				0.4
0	2 (1)	2 (3)	0 (0)	
1	0 (0)	0 (0)	0 (0)	
2	10 (7)	5 (7)	5 (7)	
3	133 (92)	68 (90)	65 (93)	
GRACE risk score	139 ± 29	135 ± 30	143 ± 27	0.1
TIMI risk score	2 [1–4]	2 [1–3]	3 [1–4]	0.3

Patients restudied at 6 months were dichotomized as with or without reduced RNM-LS at 1 week according to cut-off values displayed in Supplementary Table 2

CMR Cardiovascular magnetic resonance, *GRACE* Global registry of acute coronary events, *LS* Longitudinal strain, *PCI* Percutaneous coronary intervention, *RNM* Remote non-infarcted myocardium, *TIMI* Thrombolysis in myocardial infarction, *TT* Tissue tracking

infarct-LS values at both 1-week and 6-month CMR (Table 3) (p value < 0.01 for all comparisons).

Almost half the patients with reduced RNM-LS at 1 week (28/70, 40%) improved to normal values of RNM-LS at 6 months (Fig. 2b). These patients exhibited more preserved LVEF in chronic phase (p value < 0.01, Table 4).

A significant improvement from 1 week to 6 months RNM-LS was found in the whole study group (11.2 ± 3.5% vs. 12.5 ± 3.4%, p value < 0.001) due to changes in patients with reduced RNM-LS at 1 week (8.4 ± 2.2% vs. 10.9 ± 2.7%, p value < 0.001) but not in those with preserved RNM-LS at 1 week (13.9 ± 2.1% vs. 14.1 ± 3.2%, p value = 0.6) (Fig. 2c).

On a segmental basis, a total of 2320 segments were sequentially studied. Of 1348 segments located in the RNM area, 500 (37%) displayed abnormal LS (Fig. 2a) at 1-week TT-CMR. Around half these segments (234/500, 47%) improved until reaching normal LS values at 6-month TT-CMR (Fig. 2b).

Characterization and dynamics of infarct-LS on a per-patient and on a segmental basis are summarized in Supplemental Fig. 2.

Dynamic changes in RNM-LS and improvement of LVEF

Once adjusted for the status of all 1-week CMR and TT-CMR indices, ΔRNM-LS (Table 5) demonstrated a positive, independent, and linear correlation with ΔLVEF (Fig. 3a).

As shown in Fig. 3b, the positive correlation between ΔRNM-LS and ΔLVEF existed only in patients with depressed LVEF at 1-week CMR (n = 95) but not in those with preserved LVEF at 1-week CMR (n = 50). Thus, in patients with depressed LVEF at 1-week CMR (but not

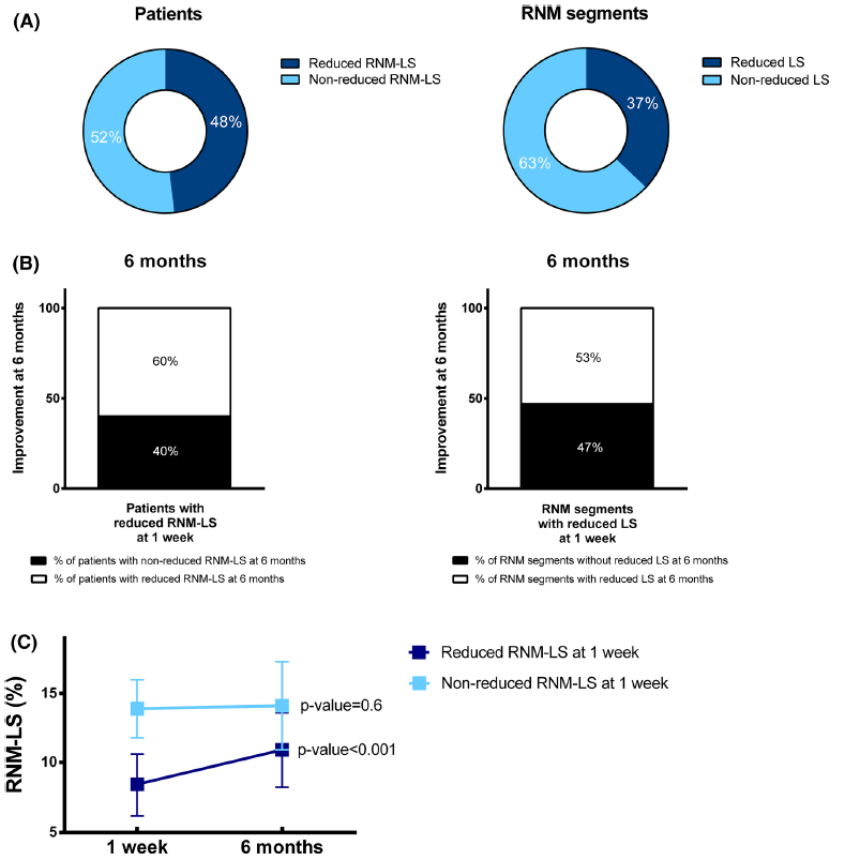

Fig. 2 Characterization and dynamics of RNM-LS on a per patient and on a segmental basis. **a** Percentage of patients and of segments located in RNM with and without reduced RNM-LS at 1 week. **b** Percentage of patients and of segments located in RNM with reduced RNM-LS at 1 week and normal RNM-LS at 6 months. **c** Dynamics of RNM-LS (from 1 week to 6 months) in patients with and without reduced RNM-LS at 1 week. *LS* Longitudinal strain, *RNM* Remote non-infarcted myocardium

in those with preserved LVEF), the higher the increase in RNM-LS from 1 week to 6 months the higher the later improvement in LVEF.

Regarding LV remodeling, patients with reduced RNM-LS at 1 week displayed more dilated LV end-diastolic volume at 6 months (Table 2). Patients with adverse remodeling (ΔLV end-diastolic volume index > 15%, n = 34) showed lower RNM-LS values at 1 week compared to those without adverse remodeling (ΔLV end-diastolic volume index < 15%, n = 111): 9.9 ± 3.7 vs. 11.6 ± 3.4 (p value = 0.01). Indeed, a significant inverse correlation existed between RNM-LS at 1 week and ΔLV end-diastolic volume index (r = -0.2, p value = 0.03).

RNM-LS at 1 week and MACE in the study group and in the validation cohort

Baseline characteristics in the whole study group of 271 patients and in those with and without MACE are displayed in Supplemental Table 4. During a median follow-up of 1302 days [range 504 to 3017 days], 52 first MACE were

Table 2 Traditional CMR and TT-CMR characteristics at 1 week and at 6 months of patients with and without reduced RNM-LS at 1-week TT-CMR

	All patients	Non-reduced RNM-LS	Reduced RNM-LS	p value
Number of patients	145	75	70	
LVEF (%)				
1 week	52 ± 13	59 ± 10	45 ± 12	< 0.001
6 months	57 ± 13	62 ± 11	51 ± 12	< 0.001
p value	< 0.001	0.001	< 0.001	
LV end-diastolic volume index (ml/m^2)				
1 week	78 ± 23	76 ± 17	80 ± 28	0.3
6 months	78 ± 27	74 ± 18	83 ± 34	0.05
p value	0.7	0.2	0.3	
LV end-systolic volume index (ml/m^2)				
1 week	38 ± 20	32 ± 13	45 ± 24	< 0.001
6 months	36 ± 24	29 ± 14	44 ± 29	< 0.001
p value	0.1	0.02	0.7	
LV mass (g/m^2)				
1 week	75 ± 20	68 ± 13	83 ± 23	< 0.001
6 months	68 ± 17	62 ± 13	73 ± 19	< 0.001
p value	< 0.001	< 0.001	< 0.001	
Edema (% of LV mass)				
1 week	30 ± 17	26 ± 16	35 ± 16	< 0.001
Microvascular obstruction (% of LV mass)				
1 week	0 [0–2]	0 [0–1]	0.3 [0–4.4]	0.003
6 months	0 [0–0]	0 [0–0]	0 [0–0]	0.4
p value	< 0.001	< 0.001	< 0.001	
Infarct size (% of LV mass)				
1 week	23 ± 15	16 ± 12	30 ± 15	< 0.001
6 months	18 ± 12	14 ± 10	23 ± 12	< 0.001
p value	< 0.001	0.002	< 0.001	
Myocardial salvage index (%)				
1 week	23.3 [3.5–46.2]	35.8 [5.3–57.1]	10.9 [1.8–34.6]	0.001
RNM-LS (%)				
1 week	11.2 ± 3.5	13.9 ± 2.1	8.4 ± 2.2	< 0.001
6 months	12.5 ± 3.4	14.1 ± 3.2	10.9 ± 2.7	< 0.001
p value	< 0.001	0.6	< 0.001	
Infarct-LS (%)				
1 week	8.1 ± 3.9	9.9 ± 3.9	6.2 ± 3.1	< 0.001
6 months	9.8 ± 3.9	11.2 ± 4	8.3 ± 3.1	< 0.001
p value	< 0.001	< 0.001	< 0.001	

Group of patients restudied at 6 months

Patients restudied at 6 months were dichotomized as with or without reduced RNM-LS at 1 week according to cut-off values displayed in Supplementary Table 2 and the main CMR and TT-CMR indices were compared

CMR Cardiovascular magnetic resonance, *LS* Longitudinal strain, *LV* Left ventricular, *LVEF* Left ventricular ejection fraction, *RNM* Remote non-infarcted myocardium, *TT* Tissue tracking

documented (18 deaths, 16 re-admissions for heart failure and 18 re-admissions for re-infarction).

Patients with MACE had more altered traditional CMR and TT-CMR than those without clinical events (Supplemental Table 5). Patients with reduced RNM-LS at 1-week TT-CMR had a significantly higher risk of MACE during follow-up in univariate analyses (26% vs. 11%, p value = 0.002) (Fig. 4a, left). When events were considered separately, patients with reduced RNM-LS at 1-week TT-CMR exhibited a higher risk of death and of re-admission for heart failure but not of re-infarction (Supplemental Fig. 3).

Time to reperfusion, global registry of acute coronary events risk score and RNM-LS were found to be independent

Table 3 TT-CMR indices at 1 week and at 6 months of patients with and without depressed LVEF and/or extensive infarct size at 6-month CMR

	RNM-LS (%)			Infarct-LS (%)		
	1 week	6 months	p value	1 week	6 months	p value
Depressed LVEF at 6 months (n = 68)	9.5 ± 3.1	10.7 ± 3.1	0.002	6.2 ± 3.2	7.6 ± 3.5	< 0.001
Non-depressed LVEF at 6 months (n = 77)	12.7 ± 3.2	14.2 ± 2.8	< 0.001	9.8 ± 3.7	11.8 ± 3.1	< 0.001
p value	< 0.001	< 0.001		< 0.001	< 0.001	
Extensive infarct size at 6 months (n = 23)	8.5 ± 2.9	10.9 ± 3.6	0.002	4.6 ± 2.0	5.4 ± 2.2	0.05
Non-extensive infarct size at 6 months (n = 122)	11.7 ± 3.4	12.9 ± 3.3	< 0.001	8.8 ± 3.8	10.6 ± 3.5	< 0.001
p value	< 0.001	0.01		< 0.001	< 0.001	

Based on previously validated cut-off values [15, 16], patients were dichotomized as preserved or depressed LVEF at 6 months and extensive or non-extensive infarct size at 6 months. The association between RNM-LS and infarct-LS (both at 1-week and 6-month CMR) were compared depending on LVEF (preserved or depressed) and infarct size (extensive and non-extensive) at 6-month CMR

CMR Cardiovascular magnetic resonance, *LS* Longitudinal strain, *LVEF* Left ventricular ejection fraction, *RNM* Remote non-infarcted myocardium, *TT* Tissue tracking

Table 4 Traditional CMR and TT-CMR characteristics at 6 months of patients with and without improvement in RNM-LS at 6-month TT-CMR

CMR and TT-CMR indices at 6 months	With improvement in RNM-LS	Without improvement in RNM-LS	p value
Number of patients	28	42	
LVEF (%)	56 ± 10	47 ± 12	0.002
LV end-diastolic volume index (ml/m^2)	81 ± 22	84 ± 40	0.6
LV end-systolic volume index (ml/m^2)	37 ± 17	48 ± 35	0.08
LV mass (g/m^2)	70 ± 14	75 ± 21	0.3
Microvascular obstruction (% of LV mass)	0 [0–0]	0 [0–0]	0.7
Infarct size (% of LV mass)	21 ± 11	24 ± 13	0.4
RNM-LS (%)	13.5 ± 1.6	9.1 ± 1.8	< 0.001
Infarct-LS (%)	9.0 ± 2.4	7.9 ± 3.4	0.1

Subgroup of patients with reduced RNM-LS at 1-week TT-CMR

In this analysis, patients with reduced RNM-LS at 1 week (n = 70) were included and categorized as: with improvement in RNM-LS, including patients with reduced RNM-LS at 1 week and non-reduced RNM-LS at 6 months (n = 28) or without improvement in RNM-LS, defined as those with reduced RNM-LS at 1 week and 6 months (n = 42)

CMR Cardiovascular magnetic resonance, *LS* Longitudinal strain, *LV* Left ventricular, *LVEF* Left ventricular ejection fraction, *RNM* Remote non-infarcted myocardium, *TT* Tissue tracking

predictors of the occurrence of MACE (Supplemental Table 8). After adjustment, RNM-LS displayed a significant association with MACE (p value < 0.001) (Fig. 4b, Supplemental Table 8).

Characteristics of all patients and of those with (n = 29) and without (n = 148) MACE in the entire validation cohort can be consulted in Supplemental Tables 6 and 7. Similar to the study group, patients with reduced RNM-LS at 1-week TT-CMR displayed a significantly higher risk of MACE during follow-up than those with non-reduced RNM-LS (57% vs. 13%, p value < 0.001), (Fig. 4a, right).

Lastly, in both the study group and the validation cohort, patients with reduced infarct-LS at 1 week displayed a significantly higher risk of MACE during follow-up (p value < 0.05), (Supplemental Fig. 4).

Discussion

The main findings of the present study are that after STEMI, abnormalities in RNM-LS by TT-CMR are common and are associated with the extent of the structural damage in the LV. RNM-LS tends to recover within the months following STEMI and this parallels late recovery of LVEF. More events occur in patients with abnormal RNM-LS.

Table 5 Multivariable stepwise linear regression analysis for predicting ΔLVEF

CMR and TT-CMR indices	β	95% CI	p value
LVEF (%)	− 0.83	[− 2.02 to − 1.26]	<0.001
LV end-diastolic volume index (ml/m^2)	− 0.59	[− 1.12 to 0.21]	0.1
LV end-systolic volume index (ml/m^2)	0.69	[− 0.15 to 1.63]	0.5
LV mass (g/m^2)	0.07	[− 0.11 to 0.28]	0.6
Edema (% of LV mass)	0.16	[− 0.09 to 0.59]	0.3
Microvascular obstruction (% of LV mass)	− 0.20	[− 2.65 to − 0.34]	0.01
Infarct size (% of LV mass)	− 0.42	[− 1.09 to − 0.36]	<0.001
Myocardial salvage index (%)	− 0.17	[− 0.31 to − 0.02]	0.02
RNM-LS (%)	0.34	[1.02 to 3.99]	0.001
Infarct-LS (%)	0.12	[− 0.37 to 1.94]	0.5
ΔRNM-LS (%)	0.48	[0.19 to 0.36]	<0.001

ΔLVEF means relative change (%) in LVEF from 1-week to 6-month CMR

ΔRNM-LS means relative change (%) in RNM-LS from 1-week to 6-month TT-CMR

CMR and TT-CMR characteristics at 1 week as well as ΔRNM-LS were included in the multivariable analysis. The β coefficients with the corresponding 95% confidence intervals of variables not selected as independent (p value < 0.05) were obtained applying the enter modality to the linear regression analysis of the model

CI Confidence interval, *CMR* Cardiovascular magnetic resonance, *LS* Longitudinal strain, *LV* Left ventricular, *LVEF* Left ventricular ejection fraction, *RNM* Remote non-infarcted myocardium, *TT* Tissue tracking

TT-CMR has become an excellent technique for quantifying myocardial strain in post-infarction patients [3, 5]. The pathophysiological and diagnostic implications of this method have already been reported; its prognostic value and utility in guiding novel therapies in STEMI patients has recently been confirmed [18, 19].

Dynamics and structural implications of RNM-LS

Traditionally, a certain controversy has existed regarding contractility in the RNM area: whereas some studies have suggested the presence of compensatory enhanced motion [20], others have reported systolic function deterioration and structural abnormalities [21, 22].

The CMR-derived dynamics and structural implications of RNM-LS measured by either speckle-tracking echocardiography or by TT-CMR have not been addressed so far.

Nearly half (48%) of patients and 37% of segments located in RNM displayed reduced RNM-LS (Video S1). The presence of reduced RNM-LS at 1-week TT-CMR associated with severe abnormalities in traditional CMR parameters (such as LVEF or infarct size) not only at 1-week but also at 6-month CMR.

The pathophysiological mechanisms underlying these associations are not completely understood. Though a certain degree of remote fibrosis or cell loss cannot be discarded in chronic phase in patients with very large infarctions, our current and previous data seem to suggest that abnormalities in wall motion of the non-infarcted area in these patients (especially those detected soon after infarction) are mainly due to hemodynamic overload. In fact, it could be speculated that the efficacy of different recommended therapies in this setting (i.e. beta-blockers, inhibition of the renin–angiotensin–aldosterone system or sacubitril-valsartan) could be partially driven by reducing overload on RNM [8, 14].

A spontaneous tendency towards recovery of RNM-LS was observed. This tendency mirrors the well-known trajectory of the infarcted area in the context of myocardial stunning [10]. Improvement mostly occurred in patients with reduced RNM-LS at 1 week, in such a way that differences with respect to patients with preserved RNM-LS significantly shortened in chronic phase after infarction.

Changes in RNM-LS were not without their significance. In fact, late improvement in RNM-LS was associated with more preserved LVEF at 6 months. ΔRNM-LS was independently related to late LVEF recovery, benefitting mainly those patients who needed it most, namely patients with depressed LVEF soon after infarction.

LVEF still represents the most consolidated variable in risk stratification after STEMI [6, 8]. The dynamics of RNM-LS improvement (as a proxy of the remote myocardium that remains alive after infarction) seems to reflect the spontaneous tendency towards progressive recovery of systolic function (and LVEF) observed in reperfused patients with large infarctions and depressed LVEF.

Prognostic implications of RNM-LS

A consistent univariate association between the presence of more reduced RNM-LS, both as a continuous and as a categorical variable, and the MACE rate was detected. As far as we know this is the first study demonstrating

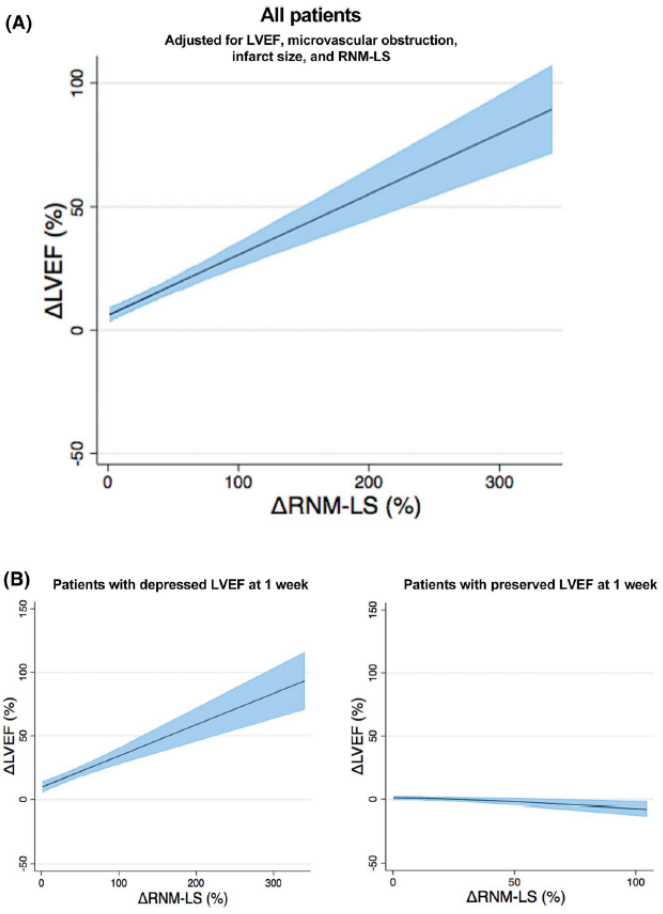

Fig. 3 Association of the relative change, from 1 week to 6 months, of RNM-LS with the relative change of LVEF. **a** In the study group, after adjustment, ΔRNM-LS showed a positive linear relationship with ΔLVEF. **b** The association of ΔRNM-LS with ΔLVEF occurred in patients with depressed LVEF at 1 week (left panel) but not in those with preserved LVEF at 1 week (right panel). *LS* Longitudinal strain, *LVEF* Left ventricular ejection fraction, *RNM* Remote non-infarcted myocardium, *ΔLVEF* Relative percentage change (%) in LVEF from 1 week to 6 months. *ΔRNM-LS* Relative percentage change (%) in RNM-LS from 1 week to 6 months

a relationship between reduced systolic motion in RNM after STEMI and patients outcome. In the multivariable analyses, RNM-LS showed an independent association with the occurrence of MACE. Similar data were recently obtained when we addressed the prognostic value of global LS in this same registry of patients [6].

Demonstrating the independent prognostic value of RNM-LS or suggesting its routine use for risk stratification beyond the wide spectrum of well-established clinical scores, biomarkers and potent structural parameters that now permit an accurate risk stratification of STEMI patients [8] was completely outside the scope of the present study. Nevertheless, our data might be helpful to illustrate the potential deleterious clinical impact of reduced wall motion in RNM, and so the need to pay more attention to RNM after STEMI.

The fact that the infarcted area comprises dysfunctional and already necrotic myocardium probably motivated the finding that its dynamic changes were less striking than those observed in viable RNM-LS. Moreover, in general CMR-derived RNM represents a much larger part of the LV than the infarcted area. This probably explains why the influence of RNM-LS on the late recovery of LVEF and on the occurrence of MACE was stronger than that observed in the case of infarct-LS.

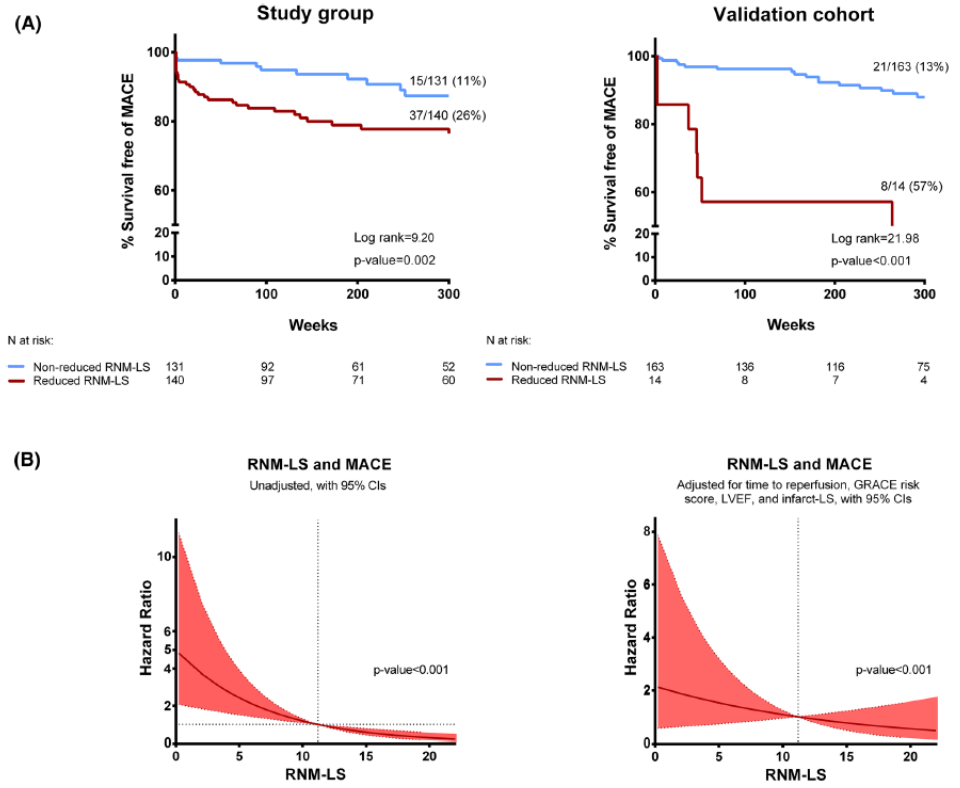

Fig. 4 Hazard of occurrence of a first MACE based on the status of RNM-LS at 1 week. **a** The Kaplan–Meier curve of patients of the study group with reduced RNM-LS displayed a significantly higher risk of a first MACE than those with preserved RNM-LS (left). Similar results were detected in the validation cohort (right). **b** In the study group, the univariate (left) and adjusted (right) hazards of a first MACE increases in parallel with the magnitude of dysfunction of RNM-LS. *GRACE* Global registry of acute coronary events, *LS* Longitudinal strain, *LVEF* Left ventricular ejection fraction, *MACE* Major adverse cardiac events. *RNM* Remote non-infarcted myocardium

Limitations

We admit that results obtained on the prognostic value of RNM-LS are merely exploratory and should be taken with caution for 2 reasons. Firstly, TT-CMR data in the study group were collected retrospectively. Secondly, TT-CMR is an evolving method and, consequently, derived results and especially cut-off values need further confirmation in validation cohorts larger than that used in the present study. However, even though retrospective quantification of TT-CMR in the study group could have introduced some confusion, the results obtained were confirmed in an external validation cohort.

T1 mapping data [23] and sequential determinations of natriuretic peptides were not acquired. These parameters could have improved our understanding of the pathological and pathophysiological factors underlying the dynamics and the structural and clinical implications of RNM.

Although RNM-LS could in future be incorporated into our daily armamentarium to improve early risk stratification of STEMI patients, this was not the objective of our study. Further research and validation beyond the wide spectrum of robust current scores and recommendations will be needed to achieve this goal.

Conclusions

Our data suggest that LS by TT-CMR represents an excellent tool for analyzing the status of wall motion in RNM myocardium and its implications. In STEMI patients, reduced RNM-LS as measured by TT-CMR occurs in nearly half of cases soon after infarction and is associated with more severe short- and long-term structural consequences on the LV and with a higher risk of clinical events. A tendency towards spontaneous improvement of RNM-LS in the months following infarction takes place and contributes to late LVEF recovery. From a clinical perspective these observations highlight the need to pay more attention to the non-infarcted area. Further research in this field is of utmost importance if we are to better understand the pathophysiology of STEMI as well as the action mechanism of therapies already in use or under investigation.

Acknowledgements This work was supported by the Instituto de Salud Carlos III and co-funded by Fondo Europeo de Desarrollo Regional (FEDER) [Grant Numbers PI17/01836, PIE15/00013, CIBERCV16/11/00486, CIBERCV16/11/00479 and a postgraduate contract FI18/00320 to C. R.-N.] and by the Generalitat Valenciana [Grant Number GV/2018/116]. JG and DM acknowledge financial support from the Agència Valenciana de la Innovació, Generalitat Valenciana (Grant INNCAD00/18/026).

Compliance with ethical standards

Conflict of interest The authors declare that they have no conflict of interest.

Informed consent Informed consent was obtained from all individual participants included in the study.

References

1. Abate E, Hoogslag GE, Antoni ML et al (2012) Value of three-dimensional speckle-tracking longitudinal strain for predicting improvement of left ventricular function after acute myocardial infarction. Am J Cardiol 110:961–967
2. Gorcsan J 3rd, Tanaka H (2011) Echocardiographic assessment of myocardial strain. J Am Coll Cardiol 58:1401–1413
3. Khan JN, Singh A, Nazir SA et al (2015) Comparison of cardiovascular magnetic resonance feature tracking and tagging for the assessment of left ventricular systolic strain in acute myocardial infarction. Eur J Radiol 84:840–848
4. Riffel JH, Keller MG, Aurich M et al (2015) Assessment of global longitudinal strain using standardized myocardial deformation imaging: a modality independent software approach. Clin Res Cardiol 104:591–602
5. Buss SJ, Krautz B, Hofmann N et al (2015) Prediction of functional recovery by cardiac magnetic resonance feature tracking imaging in first time ST-elevation myocardial infarction. Comparison to infarct size and transmurality by late gadolinium enhancement. Int J Cardiol 183:162–170
6. Gavara J, Rodriguez-Palomares JF, Valente F et al (2018) Prognostic value of strain by tissue tracking cardiovascular magnetic resonance after ST-segment elevation myocardial infarction. J Am Coll Cardiol Img 11:1448–1457
7. Granger CB, Goldberg RJ, Dabbous O et al (2003) Predictors of hospital mortality in the global registry of acute coronary events. Arch Intern Med 163:2345–2353
8. Ibanez B, James S, Agewall S et al (2018) 2017 ESC Guidelines for the management of acute myocardial infarction in patients presenting with ST-segment elevation: the Task Force for the management of acute myocardial infarction in patients presenting with ST-segment elevation of the European Society of Cardiology (ESC). Eur Heart J 39:119–177
9. Henriques JP, Zijlstra F, van't Hof AW et al (2003) Angiographic assessment of reperfusion in acute myocardial infarction by myocardial blush grade. Circulation 107:2115–2119
10. Bodi V, Sanchis J, Lopez-Lereu MP et al (2005) Usefulness of a comprehensive cardiovascular magnetic resonance imaging assessment for predicting recovery of left ventricular wall motion in the setting of myocardial stunning. J Am Coll Cardiol 46:1747–1752
11. Bodi V, Sanchis J, Nunez J et al (2009) Prognostic value of a comprehensive cardiac magnetic resonance assessment soon after a first ST-segment elevation myocardial infarction. J Am Coll Cardiol Img 2:835–842
12. Ortiz-Perez JT, Rodríguez J, Meyers SN, Lee DC, Davidson C, Wu E (2008) Correspondence between the 17-segment model and coronary arterial anatomy using contrast-enhanced cardiac magnetic resonance imaging. J Am Coll Cardiol Img 1:282–293
13. Cerqueira MD, Weissman NJ, Dilsizian V et al (2002) Standardized myocardial segmentation and nomenclature for tomographic imaging of the heart. A statement for healthcare professionals from the Cardiac Imaging Committee of the Council on Clinical Cardiology of the American Heart Association. Circulation 105:539–542
14. Ponikowski P, Voors AA, Anker SD et al (2016) 2016 ESC guidelines for the diagnosis and treatment of acute and chronic heart failure: the Task Force for the diagnosis and treatment of acute and chronic heart failure of the European Society of Cardiology (ESC). Eur Heart J 37:2129–2200
15. Kawel-Boehm N, Maceira A, Valsangiacomo-Buechel ER et al (2015) Normal values for cardiovascular magnetic resonance in adults and children. J Cardiovasc Magn Reson 17:29
16. Bonanad C, Monmeneu JV, Lopez-Lereu MP et al (2016) Prediction of long-term major events soon after a first ST-segment elevation myocardial infarction by cardiovascular magnetic resonance. Eur J Radiol 85:585–592
17. Rodriguez-Palomares JF, Gavara J, Ferreira-Gonzalez I et al (2019) Prognostic value of initial left ventricular remodeling in patients with reperfused STEMI. J Am Coll Cardiol Img 12:2445–2456
18. Bodi V (2018) Strain by feature tracking: a short summary of the journey of CMR in STEMI. J Am Coll Cardiol Img 27:1199–1201
19. Podlesnikar T, Pizarro G, Fernández-Jiménez R et al (2018) Effect of early metoprolol during ST-segment elevation myocardial infarction on left ventricular strain: feature-tracking cardiovascular magnetic resonance substudy from the METOCARD-CNIC trial. J Am Coll Cardiol Img 12:1188–1198
20. Ito S, Suzuki T, Hosokawa H et al (1999) Increased hyperkinesis in noninfarcted areas during short-term follow-up in patients with first anterior acute myocardial infarction treated by direct percutaneous transluminal coronary angioplasty. Jpn Heart J 40:549–560
21. Bodi V, Sanchis J, Berenguer A et al (1999) Wall motion of noninfarcted myocardium. Relationship to regional and global systolic function and to early and late left ventricular dilation. Int J Cardiol 71:157–165

22. Husser O, Chaustre F, Sanchis J et al (2012) Function of remote non-infarcted myocardium after STEMI: analysis with cardiovascular magnetic resonance. Int J Cardiol Img 28:2057–2064
23. Reinstadler SJ, Stiermaier T, Liebetrau J et al (2018) Prognostic significance of remote myocardium alterations assessed by quantitative noncontrast T1 mapping in ST-segment elevation myocardial infarction. J Am Coll Cardiol Img 11:411–419

Affiliations

Jose Gavara[1,2] · Jose F. Rodriguez-Palomares[3] · Cesar Rios-Navarro[1] · Filipa Valente[3] · Jose V. Monmeneu[4] · Maria P. Lopez-Lereu[4] · Ignacio Ferreira-Gonzalez[3,5] · Bruno Garcia del Blanco[3] · Imanol Otaegui[3] · Joaquim Canoves[1] · Elena de Dios[1,6] · Nerea Perez[1] · Paolo Racugno[1] · Clara Bonanad[1] · Gema Minana[1] · Victor Marcos[1] · Jose A. Barrabes[3] · Arturo Evangelista[3] · David Moratal[2] · Antoni Bayes-Genis[6,7,8] · Julio Nunez[1] · Francisco J. Chorro[1,6] · Vicente Bodi[1,6]

1 Hospital Clínico Universitario de Valencia, Department of Cardiology, Instituto de Investigación Sanitaria del Hospital Clínico Universitario de Valencia (INCLIVA), University of Valencia, Blasco Ibanez 17, 46010 Valencia, Spain

2 Center for Biomaterials and Tissue Engineering, Universitat Politècnica de València, Valencia, Spain

3 Hospital Universitari Vall d'Hebron, Department of Cardiology, Vall d'Hebron Institut de Recerca (VHIR), Universitat Autònoma de Barcelona, Barcelona, Spain

4 Cardiovascular Magnetic Resonance Unit, Exploraciones Radiológicas Especiales (ERESA), Valencia, Spain

5 Centro de Investigación Biomédica en Red de Epidemiología y Salud Pública (CIBER-ESP), Madrid, Spain

6 Centro de Investigación Biomédica en Red de Enfermedades Cardiovasculares (CIBER-CV), Madrid, Spain

7 Cardiology Department and Heart Failure Unit, Hospital Universitari Germans Trias i Pujol, Badalona, Spain

8 Department of Medicine, Universitat Autònoma de Barcelona, Barcelona, Spain

SUPPLEMENTARY MATERIAL

Cardiovascular magnetic resonance (CMR) acquisition and quantification

Images were acquired by a phased-array body surface coil during breath-holds and were triggered by electrocardiography. CMR studies were carried out by 2 operators with >10-year experience.

All strain parameters were obtained retrospectively at 2016, when certified software was available (CMR42, Circle Cardiovascular Imaging Inc., Calgary, Canada). Measurements were carried out offline by an experienced observer with >3-year experience blinded to all patient data. In previously acquired cine images, the first most basal slice to contain 100% of circumferential myocardium in the entire cardiac cycle was identified as the first short axis slice to be analyzed. The end-diastolic endocardial and epicardial LV contours in the short- and long-axis images of each subject were drawn, enabling the software to semi-automatically track the myocardium throughout the heart cycle. In long-axis images, perpendicular markers identifying the position of the basal and the apical short axis planes were obtained. At least two high-quality long-axis views were required to properly quantify longitudinal strain (LS).

Cut-off values of LS for segments

Cut-off values for considering the presence of reduced LS were derived from a control group made up of 32 patients submitted to cardiovascular check-up and with no evidence of structural cardiac disease. All these patients underwent tissue tracking (TT) CMR.

For segmental LS, the lower 95% percentile for each segment in control patients using the 16-segment model was regarded as the cut-off value. Segmental cut-off values are displayed in Supplemental Table 1.

Variability of measurements

Inter-observer variability in calculating traditional CMR indices and strain parameters was determined by comparing the differences between 2 measurements of the same case study performed separately by one of the operators from the study group and the operator from the external validation cohort; 30 CMR studies randomly sampled from the study group were used for this purpose (Supplemental Table 3a).

Intra-observer variability in calculating traditional CMR indices and strain parameters was determined by comparing the differences between 2 repeated measurements carried out by one of the operators from the study group (with an interval of 1 month from the first to the second measurement) in the 30 CMR studies from the study group used for calculation of inter-observer variability (Supplemental Table 3b).

Inter- and intra-observer variability for the measurements of CMR and TT-CMR indexes (absolute and relative changes, coefficient of variation and intra-class correlation coefficients) are depicted in Supplemental Tables 3a and 3b.

Bland-Altman plots for inter- and intra-observer variability regarding LS in the remote non-infarcted myocardium and in the infarcted areas are shown in Supplemental Figure 1a and 1b.

External validation cohort

The inclusion and exclusion criteria, patient management strategies, CMR scanner characteristics, study protocol and CMR software used in the validation cohort were the same as those described for the study group. Further details on the external validation cohort can be consulted in Supplemental Tables 6 and 7.

Supplemental Table 1. Cut-off values for considering the presence of reduced segmental longitudinal strain.

	Longitudinal strain (%)
Segments	
1	10.8
2	11.1
3	9.7
4	8.2
5	12.8
6	15.2
7	20.7
8	5.4
9	2
10	11.2
11	12.9
12	19.6
13	12.6
14	6.4

15	10.8
16	11.5

Supplemental Table 2. Cut-off values used to define reduced infarct-LS or RNM-LS according to infarct-related coronary arteries.

Infarct-related artery	Cut-off value in infarct area (Infarct-LS) (%)	Cut-off value in RNM area (RNM-LS) (%)
Left anterior descending	11.1	11.2
Left circumflex	8.9	12.1
Right coronary artery	12.9	10.8

Abbreviations. LS=Longitudinal strain. RNM=Remote non-infarcted myocardium.

Supplemental Table 3A. Inter-observer variability for traditional and strain CMR indices.

	Relative change	Absolute change	Coefficient of variation	Intra-class correlation coefficient
LVEF (%)	4±3%	2±1%	0.208	0.989
LV end-diastolic volume index (ml/m²)	7±4%	5±4 ml/m²	0.301	0.981
LV end-systolic volume index (ml/m²)	5±5%	2±2 ml/m²	0.508	0.994
LV mass (g/m²)	8±6%	6±5 g/m²	0.249	0.944
Edema (% of LV mass)	4±6%	1±2% of LV mass	0.688	0.996
Microvascular obstruction (% of LV mass)	3±4%	1±2% of LV mass	1.797	0.981
Infarct size (% of LV mass)	4±5%	1±1% of LV mass	0.813	0.998
Myocardial salvage index (% of LV mass)	3±6%	1±2% of LV mass	0.690	0.996

RNM-LS (%)	6±7%	0.9±1.3%	0.315	0.954
Infarct-LS (%)	5±3%	0.5±1.2%	0.505	0.956

Abbreviations. CMR=Cardiovascular magnetic resonance. LS=Longitudinal strain. LV=Left ventricular. LVEF=Left ventricular ejection fraction. RNM=Remote non-infarcted myocardium.

Supplemental Table 3B. Intra-observer variability for traditional and strain CMR indices.

	Relative change	Absolute change	Coefficient of variation	Intra-class correlation coefficient
LVEF (%)	3±2%	1.5±0.7%	0.204	0.994
LV end-diastolic volume index (ml/m²)	5±3%	3±2 ml/m²	0.293	0.994
LV end-systolic volume index (ml/m²)	4±5%	1±2 ml/m²	0.504	0.996
LV mass (g/m²)	7±5%	4±4 g/m²	0.242	0.969
Edema (% of LV mass)	4±5%	1±1% of LV mass	0.685	0.998
Microvascular obstruction (% of LV mass)	2±2%	1±1% of LV mass	1.908	0.993
Infarct size (% of LV mass)	3±4%	0.7±1% of LV mass	0.807	0.998
Myocardial salvage index (% of LV mass)	3±3%	0.6±1% of LV mass	0.682	0.999

RNM-LS (%)	4±6%	0.8±1%	0.309	0.968
Infarct-LS (%)	9±7%	0.5±1.2%	0.509	0.954

Abbreviations. CMR=Cardiovascular magnetic resonance. LS=Longitudinal strain. LV=Left ventricular. LVEF=Left ventricular ejection fraction. RNM=Remote non-infarcted myocardium.

Supplemental Table 4. Baseline characteristics of the whole study group and of patients with and without MACE.

	All Patients	MACE	No MACE	Hazard Ratio [95% confidence intervals]	p-value
Number of patients	271	52	219		
Age (years)	60±12	62±13	59±11	1.02 [0.99-1.05]	0.09
Male sex (%)	228 (84)	42 (81)	186 (85)	0.81 [0.4-1.61]	0.5
Diabetes mellitus (%)	54 (20)	9 (17)	45 (21)	0.97 [0.47-1.99]	0.9
Hypertension (%)	125 (46)	27 (52)	98 (45)	1.35 [0.78-2.32]	0.3
Hypercholesterolemia (%)	118 (44)	24 (46)	94 (43)	1.35 [0.78-2.34]	0.3
Smoker (%)	152 (56)	32 (62)	120 (55)	1.21 [0.69-2.12]	0.5
Heart rate on admission (beats per min)	79±20	87±26	77±19	1.02 [1.007-1.03]	0.002

Systolic pressure (mmHg)	127±30	125±32	128±29	0.99 [0.99-1.007]	0.6
Killip class 1 versus >1 (%)				1.62 [0.8-3.27]	0.2
1	224 (83)	42 (81)	182 (83)		
>1	47 (17)	10 (19)	37 (17)		
Time to reperfusion (min)	180 [120-300]	260 [150-456]	175 [120-280]	1.001 [1-1.001]	<0.001
Peak creatine kinase MB mass (ng/ml)	201 [83-300]	241 [68-300]	192 [85-300]	1 [0.99-1.001]	0.5
Anterior infarction (%)	136 (50)	32 (62)	104 (47)	1.83 [1.04-3.23]	0.04
TIMI flow grade before PCI (%)				0.94 [0.77-1.16]	0.6
0	145 (53)	24 (45)	121 (55)		
1	21 (8)	5 (10)	16 (7)		

2	30 (11)	5 (10)	25 (12)		
3	75 (28)	18 (35)	57 (26)		
TIMI flow grade after PCI (%)				1.04 [0.54-2.02]	0.9
0	3 (1)	0 (0)	3 (1)		
1	1 (1)	0 (0)	1 (1)		
2	21 (7)	5 (10)	16 (7)		
3	246 (91)	47 (90)	199 (91)		
GRACE risk score	136±31	150±31	134±30	1.02 [1.004-1.03]	0.005
TIMI risk score	2.5 [1-4]	3 [1-5.8]	2 [1-4]	1.21 [1.08-1.35]	0.001

Abbreviations. GRACE=Global registry of acute coronary events. MACE=Major adverse cardiac events. PCI=Percutaneous coronary intervention. TIMI=Thrombolysis in myocardial infarction.

Supplemental Table 5. Traditional CMR and TT-CMR characteristics at 1 week of the whole study group and of patients with and without MACE.

	All Patients	MACE	No MACE	Hazard Ratio [95% confidence intervals]	p-value
Number of patients	271	52	219		
LVEF (%)	52±13	47±14	54±12	0.96 [0.94-0.98]	<0.001
LV end-diastolic volume index (ml/m²)	80±24	83±25	79±23	1.006 [0.99-1.02]	0.2
LV end-systolic volume index (ml/m²)	39±20	46±24	38±20	1.02 [1.005-1.03]	0.004
LV mass (g/m²)	78±21	81±24	77±20	1.01 [1.001-1.02]	0.04
Edema (% of LV mass)	30±17	33±18	29±17	1.02 [1-1.03]	0.04
Microvascular obstruction (% of LV mass)	0 [0-2.8]	0.6 [0-6]	0 [0-2.6]	1.08 [1.03-1.14]	0.003

Infarct size (% of LV mass)	23±15	28±18	21±14	1.03 [1.01-1.05]	0.001
Myocardial salvage index (%)	22 [2.7-43.3]	12.5 [1.6-37.3]	23.8 [3.1-45.4]	0.99 [0.98-1.006]	0.3
RNM-LS (%)	11.2±3.4	9.6±3.4	11.5±3.3	0.87 [0.80-0.94]	<0.001
Infarct-LS (%)	8.3±4.0	6.6±2.8	8.7±4.2	0.86 [0.79-0.93]	<0.001

Abbreviations. CMR=Cardiovascular magnetic resonance. LS=Longitudinal strain. LV=Left ventricular. LVEF=Left ventricular ejection fraction. MACE=Major adverse cardiac events. RNM=Remote non-infarcted myocardium. TT=Tissue tracking.

Supplemental Table 6. Baseline characteristics of patients with and without MACE in the external validation cohort.

	All Patients	MACE	No MACE	Hazard Ratio [95% confidence intervals]	p-value
Number of patients	177	29	148		
Age (years)	59±13	63±15	58±13	1.03 [1-1.06]	0.05
Male sex (%)	156 (88)	25 (86)	131 (89)	0.85 [0.30-2.45]	0.8
Diabetes mellitus (%)	25 (14)	4 (14)	21 (14)	0.95 [0.33-2.73]	0.9
Hypertension (%)	82 (46)	15 (52)	67 (45)	1.27 [0.61-2.64]	0.5
Hypercholesterolemia (%)	57 (32)	4 (14)	53 (36)	0.33 [0.11-0.94]	0.04
Smoker (%)	124 (70)	18 (62)	106 (72)	0.67 [0.32-1.42]	0.3
Heart rate on admission (beats per min)	73±16	75±17	72±16	1.01 [0.98-1.03]	0.4

Systolic pressure (mmHg)	130±28	127±27	130±28	0.99 [0.99-1.01]	0.9
Killip class 1 versus >1 (%)				2.91 [1.32-6.39]	0.008
1	149 (84)	20 (69)	129 (87)		
>1	28 (16)	9 (31)	19 (13		
Time to reperfusion (min)	191 [150-256]	230 [157-269]	188 [150-246]	1.001 [0.99-1.004]	0.5
Peak creatine kinase MB mass (ng/ml)	258 [158-397]	341 [249-488]	247 [148-371]	1.003 [1.001-1.004]	<0.001
Anterior infarction (%)	105 (59)	17 (59)	88 (59)	1.39 [0.66-2.94]	0.4
TIMI flow grade before PCI (%)				0.1 [0-33.35]	0.4
0	165 (93)	29 (100)	136 (92)		
1	9 (5)	0 (0)	9 (6)		

2	2 (1)	0 (0)	2 (1)		
3	1 (1)	0 (0)	1 (1)		
TIMI flow grade after PCI (%)				0.76 [0.26-2.20]	0.6
0	0 (0)	0 (0)	0 (0)		
1	1 (1)	0 (0)	1 (1)		
2	10 (6)	3 (10)	7 (5)		
3	166 (93)	26 (90)	140 (94)		
GRACE risk score	114±29	125±30	112±29	1.01 [1.001-1.03]	0.03
TIMI risk score	3 [1-4]	3 [2-5.5]	2 [1-4]	1.28 [1.09-1.49]	0.002

Abbreviations. GRACE=Global registry of acute coronary events. MACE=Major adverse cardiac events. PCI=Percutaneous coronary intervention. TIMI=Thrombolysis in myocardial infarction.

Supplemental Table 7. Traditional CMR and TT-CMR characteristics of patients with and without MACE in the external validation cohort.

	All Patients	MACE	No MACE	Hazard Ratio [95% confidence intervals]	p-value
Number of patients	177	29	148		
LVEF (%)	50±10	44±13	51±9	0.94 [0.91-0.97]	0.001
LV end-diastolic volume index (ml/m²)	80±19	87±29	79±16	1.02 [1.003-1.04]	0.02
LV end-systolic volume index (ml/m²)	41±16	52±28	39±11	1.04 [1.02-1.05]	<0.001
LV mass (g/m²)	66±15	71±18	64±14	1.02 [0.99-1.05]	0.09
Edema (% of LV mass)	35±13	42±18	34±12	1.05 [1.02-1.08]	0.001
Microvascular obstruction (% of LV mass)	0.06 [0-2.4]	2.6 [1.2-6]	0 [0-1.6]	1.28 [1.18-1.39]	<0.001
Infarct size (% of LV mass)	23±13	31±16	21±12	1.04 [1.02-1.06]	<0.001

Myocardial salvage index (%)	12.3 [8.2-17.8]	10.5 [4.1-18.1]	12.4 [8.5-17.7]	0.98 [0.92-1.04]	0.5
RNM-LS (%)	15.7±3.2	14.0±4.1	16.0±2.8	0.86 [0.78-0.95]	0.002
Infarct-LS (%)	10.8±4.2	7.9±3.9	11.4±4.1	0.81 [0.73-0.90]	<0.001

Abbreviations. CMR=Cardiovascular magnetic resonance. LS=Longitudinal strain. LV=Left ventricular. LVEF=Left ventricular ejection fraction. MACE=Major adverse cardiac events. RNM=Remote non-infarcted myocardium. TT=Tissue tracking.

Supplemental Table 8. Predictors of MACE. Multivariable study.

	Hazard Ratio [95% confidence intervals]	**p-value**
Model 1 – Baseline characteristics		
Age (years)	1.008 [0.97-1.04]	0.8
Heart rate on admission (beats per min)	1.01 [1.002-1.03]	0.03
Time to reperfusion (min)	1.001 [1-1.001]	<0.001
Anterior infarction	1.63 [0.85-3.15]	0.1
GRACE risk score	1.02 [1.005-1.03]	0.004
TIMI risk score	0.99 [0.82-1.19]	0.7
Model 2 – Baseline characteristics + traditional CMR indices		
Heart rate on admission (beats per min)	1.007 [0.99-1.02]	0.3
Time to reperfusion (min)	1.001 [1-1.001]	0.001
GRACE risk score	1.02 [1.006-1.03]	0.002
LVEF (%)	0.96 [0.94-0.98]	<0.001

LV end-systolic volume index (ml/m²)	0.98 [0.96-1.005]	0.2
LV mass (g/m²)	1.006 [0.99-1.02]	0.7
Edema (% of LV mass)	1.002 [0.98-1.02]	0.6
Microvascular obstruction (% of LV mass)	1.06 [0.98-1.15]	0.2
Infarct size (% of LV mass)	0.99 [0.95-1.02]	0.7

Model 3 - Baseline characteristics + traditional CMR indices + TT-CMR indices

Time to reperfusion (min)	1.001 [1-1.001]	<0.001
GRACE risk score	1.02 [1.004-1.03]	0.006
LVEF (%)	0.99 [0.96-1.03]	0.2
RNM-LS (%)	0.86 [0.79-0.93]	<0.001
Infarct-LS (%)	0.90 [0.79-1.03]	0.06

Abbreviations. CMR=Cardiovascular magnetic resonance. GRACE=Global registry of acute coronary events. LS=Longitudinal strain. LV=Left ventricular. LVEF=Left ventricular ejection fraction. MACE=Major adverse cardiac events. RNM=Remote non-infarcted myocardium. TIMI=Thrombolysis in myocardial infarction. TT=Tissue tracking.

In order to avoid variable overfitting of the final multivariable model, we carried out the following steps using sequential stepwise Cox proportional hazard regression analyses:

1) "Model 1 - Baseline characteristics" tested baseline variables showing an association with the occurrence of MACE (p-value<0.1 in Supplemental Table 4: age, heart rate on admission, time to reperfusion, anterior infarction, GRACE risk score and TIMI risk score).

2) "Model 2 - Baseline characteristics plus traditional CMR indices" tested variables from Model 1 independently related to the occurrence of MACE (p-value<0.05 in Model 1: heart rate on admission, time to reperfusion and GRACE risk score) plus traditional CMR indices showing an association with the occurrence of MACE (p-value<0.1 in Supplemental Table 5: LVEF, LV end-systolic volume index, LV mass, edema, microvascular obstruction and infarct size).

3) The final multivariable model ("Model 3 - Baseline characteristics plus traditional CMR indices plus TT-CMR indices") tested variables from Model 2 independently related to the occurrence of MACE (p-value<0.05 in model 2: time to reperfusion, GRACE risk score and LVEF) plus strain parameters showing an association with the occurrence of MACE (p-value<0.1 in Supplemental Table 5: RNM-LS and infarct-LS).

The hazard ratios with the corresponding 95% confidence intervals of variables selected as independent (p-value<0.05) are displayed for each model.

The hazard ratios with the corresponding 95% confidence intervals of variables not selected as independent (p-value<0.05) were obtained applying the enter modality to the Cox proportional hazard regression analyses of each model.

Co-linearity of variables tested in the final multivariate Model 3 was assessed using the tolerance statistic (excessive if <0.20) and the variance inflation factor (excessive if >5) and was as follows:

Time to reperfusion: tolerance statistic 0.98; variance inflation factor 1.02.

GRACE risk score: tolerance statistic 0.95; variance inflation factor 1.05.

LVEF: tolerance statistic 0.40; variance inflation factor 2.5.

RNM-LS: tolerance statistic 0.50; variance inflation factor 1.99.

Infarct-LS: tolerance statistic 0.55; variance inflation factor 1.81.

Thus, none of the tested variables exhibited an excessive tolerance statistic or variance inflation factor. The correlation matrix is provided in Supplemental Table 9.

In the final multivariate model, time to reperfusion, GRACE risk score and RNM-LS were the independent predictors of the occurrence of MACE and the area under the curve of this model was 0.75 [0.67-0.84], p-value<0.001. In the external validation cohort, the area under the curve of this same model was 0.74 [0.64-0.85], p-value<0.001. The inclusion of RNM-LS into the multivariable model did not improve the area under the curve neither in the study group nor in the validation cohort.

Supplemental Table 9. Correlation matrix in the study group. The analysis includes TT-CMR, traditional CMR indices and independent variables in the final multivariate model.

Variable	RNM-LS	Infarct-LS	LVEF	LVEDVI	LVESVI	LV mass	Edema	MVO	Infarct size	Myocardial salvage index	Time to reperfusion	GRACE risk score
RNM-LS												
Pearson correlation coefficient	…	0.6	0.7	-0.2	-0.5	-0.4	-0.4	-0.4	-0.5	0.3	-0.05	-0.2
p-value	>0.99	<0.001	<0.001	0.001	<0.001	<0.001	<0.001	<0.001	<0.001	<0.001	0.5	<0.001
Infarct-LS												

Pearson correlation coefficient	0.6	…	0.7	-0.2	-0.5	-0.3	-0.4	-0.3	-0.6	0.2	-0.02	-0.2
p-value	<0.001	>0.99	<0.001	<0.001	<0.001	<0.001	<0.001	<0.001	<0.001	<0.001	0.8	0.002
LVEF												
Pearson correlation coefficient	0.7	0.7	…	-0.5	-0.8	-0.4	-0.5	-0.4	-0.7	0.3	-0.1	-0.1
p-value	<0.001	<0.001	>0.99	<0.001	<0.001	<0.001	<0.001	<0.001	<0.001	<0.001	0.1	0.02
LVEDVI												

Pearson correlation coefficient	-0.2	-0.2	-0.5	…	0.9	0.5	0.3	0.3	0.3	-0.1	0.08	-0.01
p-value	0.001	<0.001	<0.001	>0.99	<0.001	<0.001	<0.001	<0.001	<0.001	0.03	0.2	0.9
LVESVI												
Pearson correlation coefficient	-0.5	-0.5	-0.8	0.9	…	0.5	0.4	0.4	0.6	-0.2	0.1	0.1
p-value	<0.001	<0.001	<0.001	<0.001	>0.99	<0.001	<0.001	<0.001	<0.001	<0.001	0.1	0.1
LV mass												

Pearson correlation coefficient	-0.4	-0.3	-0.4	0.5	0.5	…	0.3	0.4	0.4	-0.1	0.07	-0.02
p-value	<0.001	<0.001	<0.001	<0.001	<0.001	>0.99	<0.001	<0.001	<0.001	0.06	0.3	0.8
Edema												
Pearson correlation coefficient	-0.4	-0.4	-0.5	0.3	0.4	0.3	…	0.3	0.7	0.1	-0.005	-0.05
p-value	<0.001	<0.001	<0.001	<0.001	<0.001	<0.001	>0.99	<0.001	<0.001	0.06	0.9	0.4
MVO												

Pearson correlation coefficient	-0.4	-0.3	-0.4	0.3	0.4	0.4	0.4	…	0.6	-0.3	-0.02	0.06
p-value	<0.001	<0.001	<0.001	<0.001	<0.001	<0.001	<0.001	>0.99	<0.001	<0.001	0.8	0.3
Infarct size												
Pearson correlation coefficient	-0.5	-0.6	-0.7	0.3	0.6	0.4	0.7	0.6	…	-0.5	0.02	0.2
p-value	<0.001	<0.001	<0.001	<0.001	<0.001	<0.001	<0.001	<0.001	>0.99	<0.001	0.8	0.006
Myocardial												

salvage index												
Pearson correlation coefficient	0.3	0.2	0.3	-0.1	-0.2	-0.1	0.1	-0.3	-0.5	…	-0.07	-0.2
p-value	<0.001	<0.001	<0.001	0.03	<0.001	0.06	0.06	<0.001	<0.001	>0.99	0.3	<0.001
Time to reperfusion												
Pearson correlation coefficient	-0.05	-0.02	-0.1	0.08	0.1	0.07	-0.005	-0.02	0.02	-0.07	…	0.05

p-value	0.5	0.8	0.1	0.2	0.1	0.3	0.9	0.8	0.8	0.3	>0.99	0.5
GRACE risk score												
Pearson correlation coefficient	-0.2	-0.2	-0.1	-0.01	0.1	-0.02	-0.05	0.06	0.2	-0.2	0.05	…
p-value	<0.001	0.002	0.02	0.9	0.1	0.8	0.4	0.3	0.006	<0.001	0.5	>0.99

Abbreviations. CMR=Cardiovascular magnetic resonance. GRACE=Global registry of acute coronary events. LS=Longitudinal strain. LV=Left ventricular. LVEDVI=Left ventricular end-diastolic volume index. LVEF=Left ventricular ejection fraction. LVESVI=Left ventricular end-systolic volume index. MVO=Microvascular obstruction. RNM=Remote non-infarcted myocardium. TT=Tissue tracking.

SUPPLEMENTAL FIGURE LEGENDS

Supplemental Fig. 1 Variability in the measurement of LS.

Bland-Altman plots display low inter-observer (a) and intra-observer (b) variability with respect to RNM-LS and infarct-LS.

Abbreviations: LS=Longitudinal strain. RNM=Remote non-infarcted myocardium. SD=Standard deviation.

Supplemental Fig. 2 Characterization and dynamics of infarct-LS on a per patient and on a segmental basis.

a) Percentage of patients and of segments located in the infarcted area with and without reduced infarct-LS at 1-week CMR. b) Percentage of patients and of segments located in the infarcted area with reduced infarct-LS at 1-week CMR that normalize infarct-LS at 6-month CMR. c) Dynamics of infarct-LS (from 1-week to 6-month CMR) in patients with and without reduced infarct-LS at 1-week CMR.

Abbreviations: CMR=Cardiovascular magnetic resonance. LS=Longitudinal strain.

Supplemental Fig. 3 Kaplan Meier curves representing the time to death, time to first re-admission for heart failure and time to first re-admission for infarct in patients included in the study group with and without reduced RNM-LS.

Patients with reduced RNM-LS displayed a higher risk of death and of first re-admission for heart failure but not of first re-admission for infarct than those with preserved RNM-LS.

Abbreviations: LS=Longitudinal strain. RNM=Remote non-infarcted myocardium.

Supplemental Fig. 4 Kaplan Meier curves representing the time to the first MACE in patients included in the study group and in the external validation cohort with and without reduced infarct-LS.

In both the study group (left) and in the validation cohort (right), patients with reduced infarct-LS at 1 week displayed a significant higher risk of MACE during follow-up.

Abbreviations: LS=Longitudinal strain. MACE=Major adverse cardiac events.

Supplemental Fig1

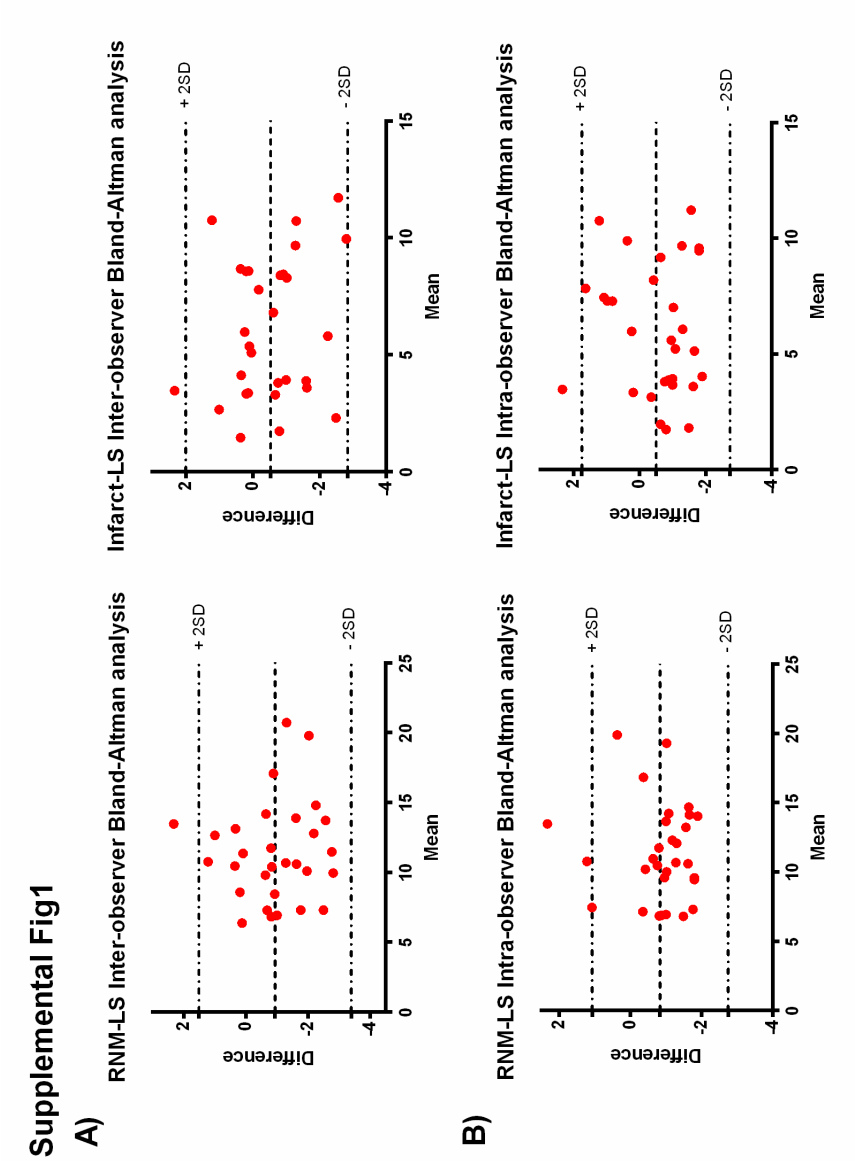

Supplemental Fig2

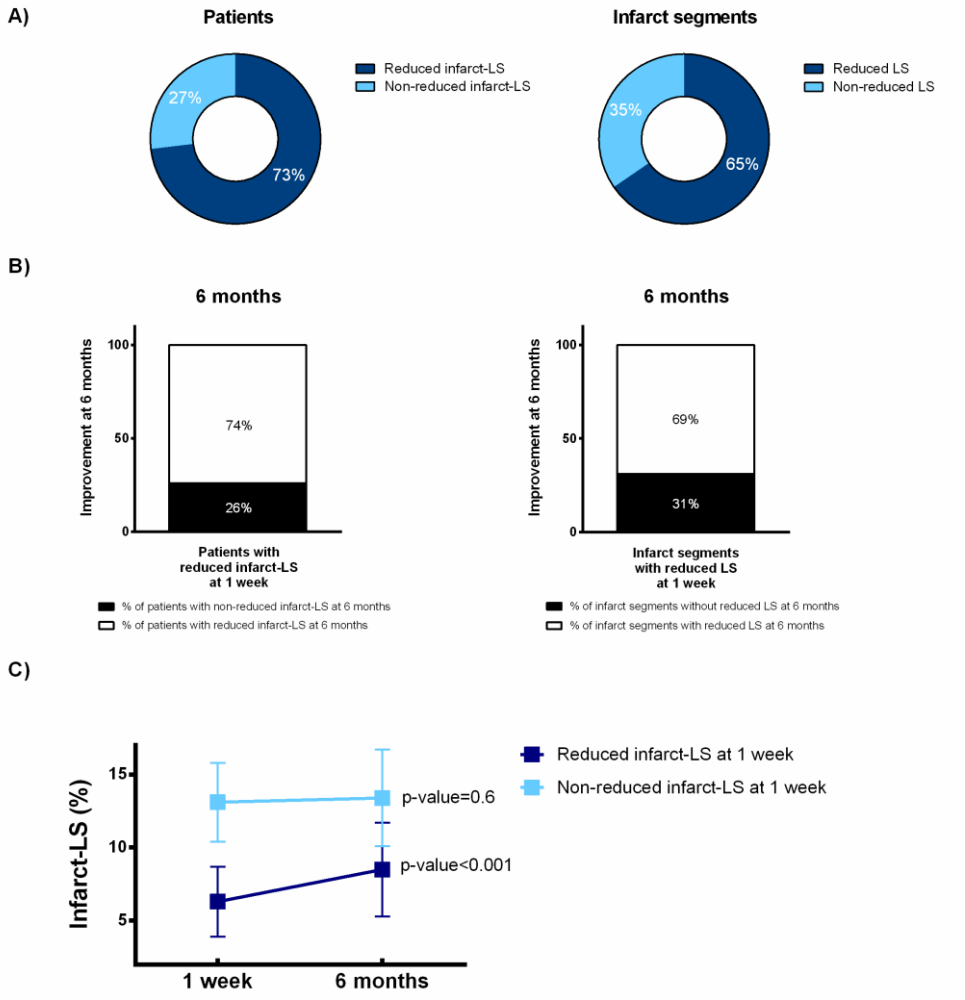

Supplemental Fig3

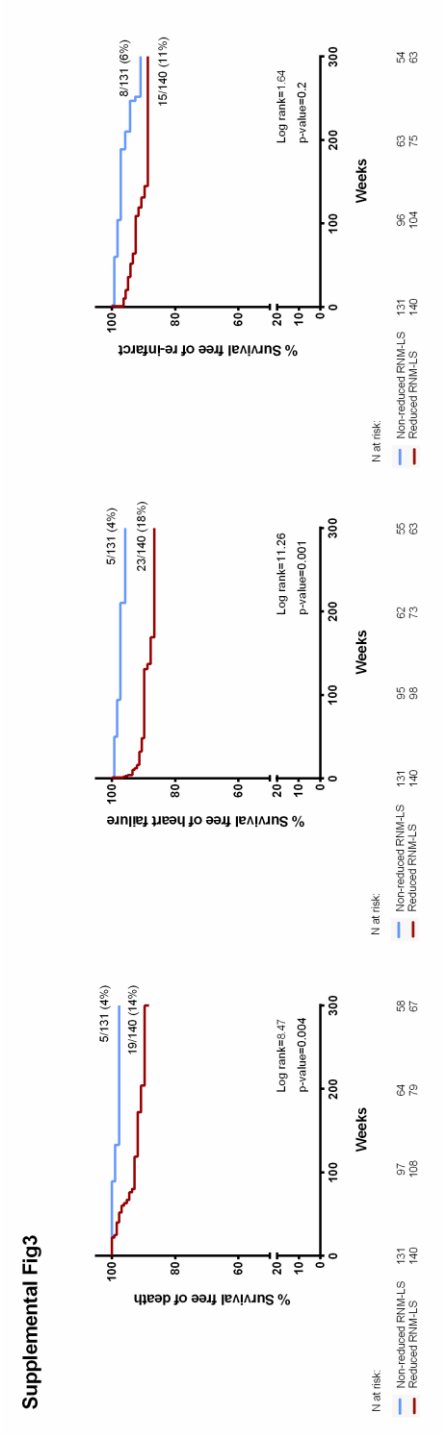

Supplemental Fig4

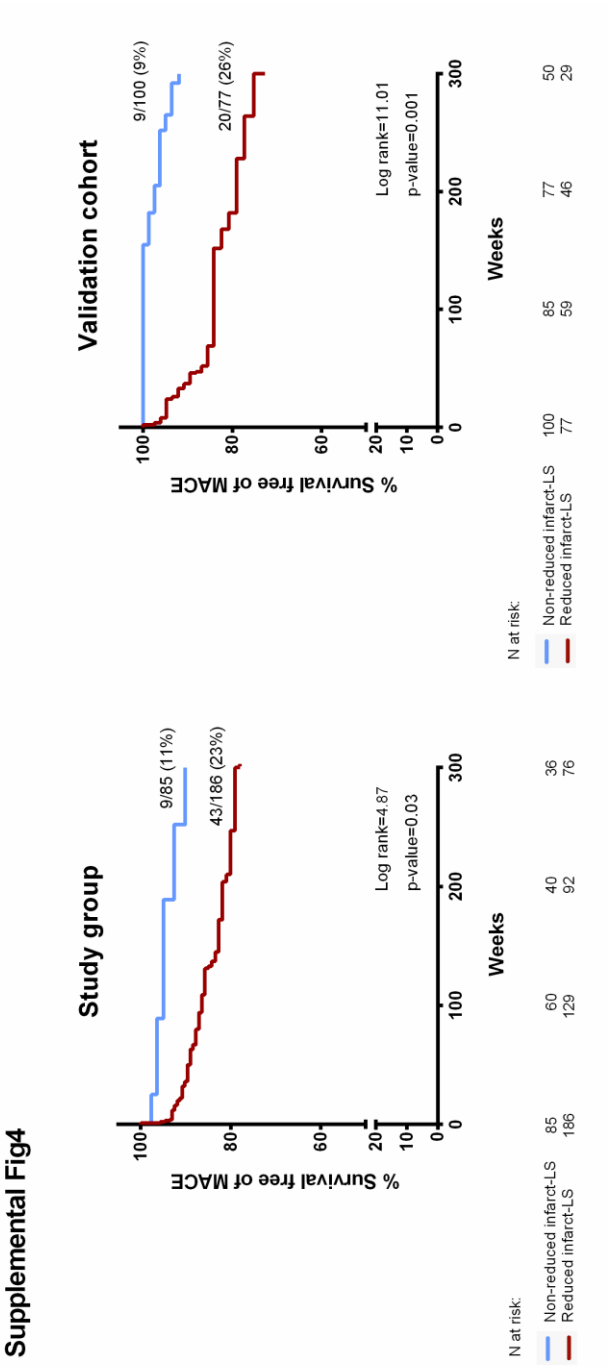

SUPPLEMENTAL VIDEO LEGENDS

Supplemental Video 1. RNM-LS in a control patient and in a patient with a large anterior infarction.

Whereas the control patient displayed preserved LS (left video and panel), severe abnormalities in infarct-LS (anterior area) and RNM-LS (posterior area) can be observed in the infarcted patient (right video and panel). Late gadolinium enhancement images demonstrate absence of infarcted myocardium in the control patient and a large anterior infarction in the infarcted patient.

Abbreviations: I=Infarcted myocardium. LGE=Late gadolinium enhancement. LS=Longitudinal strain. RNM=Remote non-infarcted myocardium.

ANEXO IV: Otras publicaciones y trabajos derivados del desarrollo de la tesis

Publicaciones:

1. Marcos-Garces V*, **Gavara J***, Monmeneu JV, Lopez-Lereu MP, Bosch MJ, Merlos P, Perez N, Rios-Navarro C, De Dios E, Bonanad C, Racugno P, Bellver Navarro A, Ventura Pérez B, Aguilar Botella J, Ventura S, Mainar L, Cánoves J, Pellicer M, Moratal D, Miñana G, Nunez J, Chorro FJ, Bodi V. Vasodilator stress CMR and all-cause mortality in stable ischemic heart disease: a large retrospective registry. J Am Coll Cardiol Img 2020. Doi: 10.1016/j.jcmg.2020.02.027.

2. Marcos-Garces V*, **Gavara J***, Monmeneu JV, Lopez-Lereu MP, Perez N, Rios-Navarro C, De Dios E, Moratal D, Miñana G, Nuñez J, Chorro FJ, Bodi V. A novel clinical and stress cardiac magnetic resonance (C-CMR-10) score to predict long-term all-cause mortality in patients with known or suspected chronic coronary syndrome. J Clin Med 2020;9:1957. Doi: 10.3390/jcm9061957.

3. Perez-Terol I, Rios-Navarro C, de Dios E, Morales JM, **Gavara J**, Perez-Sole N, Diaz A, Minana G, Segura-Sabater R, Bonanad C, Bayés-Genis A, Husser O, Monmeneu JV, Lopez-Lereu MP, Nunez J, Chorro FJ, Ruiz-Sauri A, Bodi V, Monleon D. Magnetic resonance microscopy and correlative histopathology of the infarcted heart. Sci Rep 2019;9:20017.

4. Rios-Navarro C, Ruiz-Sauri A, **Gavara J**, Vidal V, Bonanad C, Miñana G, Chorro FJ, Bodi V. Dinámica de los eosinófilos en sangre y en el tejido cardiaco tras un infarto agudo de miocardio reperfundido. Estudio en un modelo porcino. e-Latido 2019;60–8.

5. Rios-Navarro C, **Gavara J**, Vidal V, Bonanad C, Racugno P, Bayes-Genis A, Miñana G, Husser O, Oltra R, Nuñez J, Chorro FJ, Bodi V, Ruiz-Sauri A. Characterization and implications of the

dynamics of eosinophils in blood and in the infarcted myocardium after coronary reperfusion. PLoS One 2018;13:e0206344.

6. de Gonzalo-Calvo D, Cediel G, Bar C, Núñez J, Revuelta-Lopez E, **Gavara J**. Ríos-Navarro C, Llorente-Cortes V, Bodí V, Thum T, Bayes-Genis A. Circulating miR-1254 predicts ventricular remodeling in patients with ST-segment elevation myocardial infarction: a cardiovascular magnetic resonance study. Sci Rep 2018;8:15115.

7. Larroza A, Lopez-Lereu MP, Monmeneu JV, **Gavara J**, Chorro FJ, Bodí V, Moratal D. Texture analysis of cardiac cine magnetic resonance imaging to detect nonviable segments in patients with chronic myocardial infarction. Med Phys 2018;45:1471–80.

8. Cambronero-Cortinas E, Bonanad C, Monmeneu JV, Lopez-Lereu MP, **Gavara J**, de Dios E, Rios C, Perez N, Racugno P, Paya A, Escribano D, Minana G, Pellicer M, Cànoves J, Nunez J, Chorro FJ, Moratal D, Bodi V. Incidence, outcomes, and predictors of ventricular thrombus after reperfused ST-segment-elevation myocardial infarction by using sequential cardiac MR imaging. Radiology 2017;284:372–80.

9. Ríos-Navarro C, Piqueras L, Hervás A, de Dios E, Ruiz-Saurí A, **Gavara J**, Pérez-Solé N, Miñana G, Chorro FJ, Bodí V. La neoangiogénesis inducida por suero es paralela a la dinámica de la obstrucción microvascular tras un infarto agudo de miocardio reperfundido. Latido 2017;3:29–36.

10.Hervas A, Ruiz-Sauri A, **Gavara J**, Monmeneu JV, de Dios E, Rios-Navarro C, Perez-Sole N, Perez I, Monleon D, Morales JM, Minana G, Nunez J, Bonanad C, Diaz A, Vila JM, Chorro FJ, Bodi V. A multidisciplinary assessment of remote myocardial fibrosis after

reperfused myocardial infarction in swine and patients. J Cardiovasc Transl Res 2016;9:321–33.

11. Hervas A, Ruiz-Sauri A, de Dios E, Forteza MJ, Minana G, Nunez J, Gomez C, Bonanad C, Perez-Sole N, **Gavara J**, Chorro FJ, Bodi V. Inhomogeneity of collagen organization within the fibrotic scar after myocardial infarction: results in a swine model and in human samples. J Anat 2016;228:47–58.

12. Bonanad C, Monmeneu JV, López-Lereu MP, Hervás A, de Dios E, **Gavara J**, Núñez J, Miñana G, Husser O, Payá A, Racugno P, García-Blas S, Chorro FJ, Bodí V. Prediction of long-term major events soon after a first ST-segment elevation myocardial infarction by cardiovascular magnetic resonance. Eur J Radiol 2016;85:585–92.

13. Paya Chaume A, Bonanad Lozano C, Escribano Alarcón D, Racugno P, Monmeneu JV, López MP, **Gavara J**, Núñez J, Chorro FJ, Bodí V. Predicción de eventos cardíacos mayores a largo plazo mediante resonancia magnética cardiaca, tras un infarto agudo de miocardio con elevación del segmento ST. Latido 2016;16:9–18.

Presentaciones en congresos

Nacionales:

1. Ortega M, Ruiz-Sauri A, Rios-Navarro C, **Gavara J**, Marcos-Garces V, Diaz A, Miñana G, Chorro FJ, Bodi V. Morphometric analysis of the dynamic changes of the interstitium after reperfused myocardial infarction. VII Congreso de Investigación Biomédica (CIB 2019). Valencia 2019.

2. Teruel-Sanchís A, Ortega M, Rios-Navarro C, **Gavara J**, Marcos-Garces V, Diaz A, Miñana G, Chorro FJ, Bodi V, Ruiz-Sauri A. Effect of microvascular obstruction on the cellular matrix on a swine model of reperfused myocardial infarction. VII Congreso de Investigación Biomédica (CIB 2019). Valencia 2019.

3. Bondía E, Signes-Costa J, **Gavara J**, Ríos C, Bañuls P, Bodí V, Racugno P, Lopez-Lereu MP, Monmeneu JV, Garrido N, Servera E. Influencia de la hipoxia intermitente en el síndrome de apnea del sueño y su relación con los factores de angiogénesis. 52 Congreso SEPAR. Santiago de Compostela 2019.

4. Bondia E, Signes-Costa J, **Gavara J**, Ríos C, Bañuls P, Bodí V, Racugno P, López-Lereu MP, Monmeneu JV, Garrido N, Servera E. Influencia del sindrome de apnea del sueño sobre las alteraciones estructurales miocárdicas en la cardiopatía isquémica. 52 Congreso SEPAR. Santiago de Compostela 2019.

5. Marcos-Garcés V, González J, **Gavara J**, Pérez-Solé N, Merenciano H, Ríos-Navarro C, Bonanad C, Racugno P, Chorro FJ, López Lereu MP, Monmeneu JV, Bodí V. La fracción de eyección por ecocardiografía como cribado para el uso selectivo de la resonancia magnética cardíaca: estratificación del riesgo tras un IAMCEST.

Congreso de la Sociedad Española de Cardiología (SEC 2019). Barcelona 2019.

6. Marcos-Garcés V, **Gavara J**, López-Lereu MP, Monmeneu JV, Bosch MJ, Pérez-Solé N, Ríos-Navarro C, Bonanad C, Racugno P, Bellver A, Aguilar J, Mainar L, Nuñez J, Chorro FJ, Bodí V. Resonancia magnética cardíaca de estrés con vasodilatador y mortalidad por todas las causas en cardiopatía isquémica estable conocida o sospechada. Congreso de la Sociedad Española de Cardiología (SEC 2019). Barcelona 2019.

7. Marcos-Garcés V, **Gavara J**, Pérez-Solé N, Gabaldón A, Merenciano H, Lorenzo M, Núñez G, Ríos-Navarro C, de Dios E, Bonanad C, Racugno P, López-Lereu MP, Monmeneu JV, Chorro FJ, Bodí V. Contraindicación para una prueba de esfuerzo: peor pronóstico en pacientes con dolor torácico de origen coronario conocido o sospechado. Congreso de la Sociedad Española de Cardiología (SEC 2019). Barcelona 2019.

8. Ruiz-Sauri A, Rios-Navarro C, Ortega M, **Gavara J**, Marcos-Garces V, Chorro FJ, Bodi V. Microscopic study of the infarct-related coronary artery in a swine model of reperfused myocardial infarction. XX Congreso de la Sociedad Española de Histología e Ingeniería Tisular (SEHIT 2019). Murcia 2019.

9. Ruiz-Sauri A, Rios-Navarro C, Ortega M, **Gavara J**, Marcos-Garces V, Chorro FJ, Bodi V. Evaluation of the changes in the extracellular matrix after myocardial infarction by morphometric analysis. XX Congreso de la Sociedad Española de Histología e Ingeniería Tisular (SEHIT 2019). Murcia 2019.

10.Marcos-Garcés V, González J, **Gavara J**, Ríos-Navarro C, Bonanad C, Racugno P, Chorro FJ, López-Lereu MP, Monmeneu JV,

Bodi V. Estratificación del riesgo tras IAMCEST. La fracción de eyección por ecocardiografía como cribado para el uso selectivo de la resonancia magnética cardíaca. XXXVI Congreso de la Sociedad Valenciana de Cardiología 2019 (SVC 2019). Alicante 2019.

11.Marcos-Garcés V, **Gavara J**, Bellvert Navarro A, Aguilar Botella J, Mainar L, Bosch MJ, Lopez-Lereu MP, Monmeneu JV, Chorro FJ, Bodí V. La carga isquémica en RMC de estrés predice la mortalidad y el efecto de la revascularización en pacientes con cardiopatía isquémica conocida o sospechada. XXXVI Congreso de la Sociedad Valenciana de Cardiología 2019 (SVC 2019). Alicante 2019.

12.González D, Miñana G, Núñez Villota J, Bayes-Genis A, de la Espriella R, Ríos Navarro C, **Gavara J**, Marcos Garcés V, Soler Costa M, Bodi Peris V. PSCK9 y fracción de eyección del ventrículo izquierdo a los 6 meses tras un infarto con elevación del segmento ST. Un estudio piloto. XXXVI Congreso de la Sociedad Valenciana de Cardiología 2019 (SVC 2019). Alicante 2019.

13.Ríos-Navarro C, Ruiz-Sauri A, Daghbouche-Rubio N, **Gavara J**, Marcos-Garcés V, Bonanad C, Miñana G, Diaz A, Chorro FJ, Bodí V. Caracterización del daño microscópico en la arteria epicárdica tras un infarto agudo de miocardio en un modelo porcino. XXXVI Congreso de la Sociedad Valenciana de Cardiología 2019 (SVC 2019). Alicante 2019.

14.Ríos-Navarro C, Ruiz-Sauri A, Ortega M, **Gavara J**, Marcos-Garcés V, Bonanad C, Miñana G, Diaz A, Chorro FJ, Bodí V. Análisis morfométrico de los cambios en la matriz extracelular tras un infarto agudo de miocardio. XXXVI Congreso de la Sociedad Valenciana de Cardiología 2019 (SVC 2019). Alicante 2019.

15.Merenciano-González H, Marcos-Garcés V, **Gavara J**, Ríos-Navarro C, López-Lereu MP, Monmeneu JV, Núñez E, Núñez J, Chorro FJ, Bodi V. Fracción de eyección mediante RMC 6 meses tras infarto agudo de miocardio con elevación del segmento ST: Impacto en la estratificación de riesgo en fase crónica. XXXVI Congreso de la Sociedad Valenciana de Cardiología 2019 (SVC 2019). Alicante 2019.

16.Marcos-Garcés V, **Gavara J**, Perez N, Merenciano-González H, Gabaldon-Pérez A, Núñez-Marín G, Lorenzo-Hernández M, Ríos-Navarro C, Chorro FJ, Bodí V. La contraindicación para una prueba de esfuerzo confiere un pronóstico adverso en pacientes con dolor torácico de origen coronario conocido o sospechado. XXXVI Congreso de la Sociedad Valenciana de Cardiología 2019 (SVC 2019). Alicante 2019.

17.Bondía E, Signes-Costa J, **Gavara J**, Ríos C, Bañuls P, Bodí V, Racugno P, Lopez-Lereu MP, Monmeneu JV, Garrido N, Servera E. Relación entre la hipoxia intermitente del síndrome de apnea del sueño con factores angiogénicos. XXVI Congreso de la Sociedad Valenciana de Neumología 2019 (SVN 2019). Peñiscola 2019.

18.Bondía E, Signes-Costa J, **Gavara J**, Ríos C, Bañuls P, Bodí V, Racugno P, Lopez-Lereu MP, Monmeneu JV, Garrido N, Servera E. Alteraciones estructurales miocárdicas en pacientes con síndrome de apnea del sueño y cardiopatía isquémica. XXVI Congreso de la Sociedad Valenciana de Neumología 2019 (SVN 2019). Peñiscola 2019.

19.**Gavara J**, Marcos V, Bonanad C, Monmeneu JV, Lopez-Lereu MP, Rios-Navarro C, Chorro FJ, Bodi V. Estudio del strain miocárdico remoto mediante resonancia magnética cardiaca y su influencia en la evolución de la función en pacientes con infarto de

miocardio. XXXV Congreso de la Sociedad Valenciana de Cardiología 2018 (SVC 2018). Valencia 2018.

20. Rios-Navarro C, Ruiz-Sauri A, **Gavara J**, Vidal V, Bonanad C, Miñana G, Chorro FJ, Bodi V. La eosinopenia tras un infarto de miocardio se asocia con una peor estructura cardíaca y es paralela a la migración de los eosinófilos al tejido infartado. XXXV Congreso de la Sociedad Valenciana de Cardiología 2018 (SVC 2018). Valencia 2018.

21. Marcos-Garces V, **Gavara J**, Perez-Sole N, Rios-Navarro C, de Dios E, Bonanad C, Racugno P, Pellicer M, Nuñez J, Lopez-Lereu MP, Monmeneu JV, Chorro FJ, Bodi V. La resonancia magnética cardiaca de estrés en la predicción de la mortalidad por todas las causas a largo plazo. Exploración de su utilidad en la toma de decisiones. Congreso de la Sociedad Española de Cardiología (SEC 2018). Sevilla 2018.

22. Ruiz-Saurí A, Ríos-Navarro C, **Gavara J**, Hervás A, Perez-Sole N, de Dios E, Daghbouche-Rubio N, Chorro FJ, Bodí V. Implications and mechanistic role of eosinophils after reperfused myocardial infarction. Study in patients and in vivo. XIX Congreso de la Sociedad Española de Histología e Ingeniería Tisular (SEHIT 2017). Santiago de Compostela 2017.

23. Ruiz-Saurí A, Hervás A, Ríos-Navarro C, de Dios E, **Gavara J**, Perez-Sole N, Chorro FJ, Bodí V. Inhomogeneous organization of collagen within the fibrotic scar after myocardial infarction. Results in a swine model and in patients. XIX Congreso de la Sociedad Española de Histología e Ingeniería Tisular (SEHIT 2017). Santiago de Compostela 2017.

24. **Gavara J**, Rios C, Vidal V, Ruiz-Sauri A, de Dios E, Bonanad C, Chorro FJ, Bodi V. Implicaciones clínicas y mecanismos de acción de los eosinófilos tras un infarto de miocardio reperfundido. Estudio en pacientes e in vivo. Congreso de la Sociedad Española de Cardiología (SEC 2017). Madrid 2017.

25. Hervás A, Ríos-Navarro C, Ruiz-Saurí A, de Dios E, **Gavara J**, Perez-Sole N, Bonanad C, Miñana G, Chorro FJ, Bodí V. La cicatrización fibrótica tras un infarto de miocardio muestra una organización heterogénea de las fibras de colágeno. XXXIII Congreso de la Sociedad Valenciana de Cardiología (SVC 2016). Benidorm 2016.

26. Hervás A, Ríos-Navarro C, Ruiz A, **Gavara J**, de Dios E, Miñana G, Chorro FJ, Bodí V. Estudio multidisciplinar de la fibrosis remota tras un infarto de miocardio en un modelo porcino y en muestras humanas. XXXIII Congreso de la Sociedad Valenciana de Cardiología (SVC 2016). Benidorm 2016.

27. Ríos-Navarro C, Piqueras L, Hervás A, de Dios E, Ruiz-Saurí A, **Gavara J**, Perez-Sole N, Miñana G, Chorro FJ, Bodí V. La neoangiogénesis inducida por suero es paralela a la dinámica de la obstrucción microvascular tras un infarto de miocardio reperfundido. XXXIII Congreso de la Sociedad Valenciana de Cardiología (SVC 2016). Benidorm 2016.

28. Gonzalez de Gregorio J, Bodi V, Chorro FJ, Bonanad C, Cardells I, Paya A, Racugno P, Monmeneu JV, **Gavara J**, Lopez-Lereu MP. Comparación de la FEVI calculada por ecocardiografía y por resonancia para estratificación de riesgo y valorar implante de DAI tras IAMEST. XXXIII Congreso de la Sociedad Valenciana de Cardiología (SVC 2016). Benidorm 2016.

29. Hervás A, Ríos-Navarro C, Ruiz-Saurí A, **Gavara J**, de Dios E, Miñana G, Chorro FJ, Bodí V. Estudio multidisciplinar de la fibrosis remota tras un infarto agudo de miocardio reperfundido en un modelo porcino y en muestras humanas. Congreso de la Sociedad Española de Cardiología (SEC 2016). Zaragoza 2016.

30. Ríos-Navarro C, Hervás A, Piqueras L, de Dios E, Ruiz-Saurí A, **Gavara J**, Chorro FJ, Bodí V. La neoangiogénesis inducida por el suero se correlaciona con la resolución de la obstrucción microvascular en un modelo animal de infarto de miocardio. Congreso de la Sociedad Española de Cardiología (SEC 2016). Zaragoza 2016.

31.Hervás A, Ríos-Navarro C, Ruiz-Saurí A, de Dios E, **Gavara J**, Bonanad C, Chorro FJ, Bodí V. Las fibras de colágeno presentan una organización heterogénea en la cicatriz fibrótica tras un infarto de miocardio. Congreso de la Sociedad Española de Cardiología (SEC 2016). Zaragoza 2016.

Internacionales:

1. Merenciano H, Marcos-Garces V, **Gavara J**, Rios-Navarro C, Ortiz JT, Rodríguez J, Mendieta G, Rodríguez-Palomares JF, Valente F, García-Dorado D, Lopez-Lereu MP, Monmeneu JV, Nuñez E, Nuñez J, Bodi V. Ejection fraction by cardiac magnetic resonance 6 months after STEMI: Impact on risk stratification in chronic phase. European Society of Cardiology Congress (ESC 2019). Paris 2019.

2. Marcos-Garces V, **Gavara J**, Rios-Navarro C, Racugno P, Bellver Navarro A, Ventura Pérez B, Aguilar Botella J, Ventura S, Mainar L, Bosch MJ, Merlos P, Lopez-Lereu MP, Monmeneu JV, Chorro FJ, Bodi V. Ischemic burden by vasodilator stress CMR predicts long-term all-cause death and the effect of revascularization in patients with known or suspected stable ischemic heart disease. European Society of Cardiology Congress (ESC 2019). Paris 2019.

3. Marcos-Garces V, Gonzalez J, **Gavara J**, Rios-Navarro C, Bonanad C, Chorro FJ, Ortiz JT, Rodríguez J, Mendieta G, Rodríguez-Palomares JF, Valente F, García-Dorado D, Lopez-Lereu MP, Monmeneu JV, Bodi V. Risk stratification after STEMI. Ejection fraction by echocardiography as the gatekeeper for a selective use of cardiac magnetic resonance. European Society of Cardiology Congress (ESC 2019). Paris 2019.

4. Rios-Navarro C, Ruiz-Sauri A, Daghbouche-Rubio N, **Gavara J**, Marcos-Garces V, Miñana G, Chorro FJ, Bodi V. Histopathological damages in the epicardial coronary artery after ischemia and reperfusion injury in swine. European Society of Cardiology Congress (ESC 2019). Paris 2019..

5. Rios-Navarro C, Ruiz-Sauri A, Ortega M, **Gavara J**, Marcos-Garces V, Miñana G, Chorro FJ, Bodi V. Morphometric analysis of the

dynamic changes of the interstitium after reperfused myocardial infarction. European Society of Cardiology Congress (ESC 2019). Paris 2019.

6. Bondia E, Signes-Costa J, **Gavara J**, Ríos-Navarro C, Bodí V, Racugno P, Lopez-Lereu MP, Monmeneu JV, Bañuls MP, Garrido N, Servera E. Angiogenic factors in patients with myocardial infarction and obstructive sleep apnea. ERS International Congress. Madrid 2019.

7. Bondia E, Signes-Costa J, **Gavara J**, Ríos-Navarro C, Bodí V, Racugno P, Lopez-Lereu MP, Monmeneu JV, Bañuls MP, Garrido N, Servera E. Hypoxic burden and angiogenic factors in patients with myocardial infarction and obstructive sleep apnea. ERS International Congress. Madrid 2019.

8. Bondia E, Signes-Costa Miñana J, **Gavara J**, Ferrer S, Bodi V, Racugno P, Lopez-Lereu MP, Monmeneu JV, Bañuls MP, Servera E. Ventricular structural changes in patients with sleep-disordered breathing (SBD) and myocardial infarction. ERS Internacional Congress 2018. Paris 2018.

9. Marcos V, **Gavara J**, Perez N, Rios-Navarro C, Bonanad C, Racugno P, Lopez-Lereu MP, Monmeneu JV, Chorro FJ, Bodi V. Vasodilator stress cardiovascular magnetic resonance imaging predicts long-term cardiac death and all-cause death in patients with known or suspected coronary artery disease. European Society of Cardiology Congress (ESC 2018). Munich 2018.

10.Rios-Navarro C, Ruiz-Saurí A, Vidal V, de Dios E, Perez-Sole N, **Gavara J**, Daghbouche-Rubio N, Bonanad C, Minana G, Chorro FJ, Bodi V. Clinical implications and mechanistic role of eosinophils after reperfused myocardial infarction. Study in patients and swine.

Póster Oral. European Society of Cardiology Congress (ESC 2017). Barcelona 2017.

11. Rios-Navarro C, Hueso L, Daghbouche-Rubio N, **Gavara J**, de Dios E, Perez-Sole N, Ruiz-Saurí A, Chorro FJ, Bodi V. The pro-angiogenic effect of coronary serum after myocardial infarction on microvascular obstruction repair. Role of hypoxia-inducible factor-1A. Póster Oral. European Society of Cardiology Congress (ESC 2017). Barcelona 2017.

12.Bonanad C, Rodríguez-Palomares JF, **Gavara J**, Valente F, Monmeneu JV, Ferreira I, Lopez-Lereu MP, Rodriguez J, Evangelista A, Chorro FJ, Garcia-Dorado D, Bodi V. Prognostic value of strain assessed by tissue tracking cardiovascular magnetic resonance after a first ST-segment elevation myocardial infarction. European Society of Cardiology Congress (ESC 2017). Barcelona 2017.

13. Hervás A, Ríos-Navarro C, Ruiz-Saurí A, de Dios E, **Gavara J**, Miñana G, Chorro FJ, Bodí V. Fibrotic scar after myocardial infarction presents an inhomogeneous organization of collagen. Results in a swine model and in patients. European Society of Cardiology Congress (ESC 2016). Roma 2016.

14. Ríos-Navarro C, Piqueras L, Hervás A, de Dios E, Ruiz-Saurí A, **Gavara J**, Miñana G, Chorro FJ, Bodí V. Serum-induced neoangiogenesis parallels the dynamics of MVO after reperfused MI in an in vivo model. European Society of Cardiology Congress (ESC 2016). Roma 2016.

ANEXO V: Fuentes de financiación

La presente Tesis Doctoral ha sido realizada bajo los siguientes proyectos de investigación públicos:

1. Proyecto Prometeo para Grupos de Excelencia de la Comunidad Valenciana PROMETEO/2013/007 “Inmunidad y metabolismo: exploración de nuevas vías fisiopatológicas y oportunidades terapéuticas en el infarto agudo de miocardio”. Financiado por la Consellería d´Educació, Generalitat Valenciana. IP: Vicente Bodí Peris. 2013-2016.

2. Proyecto PI14/00271 “Fibrosis miocárdica tras un infarto de miocardio. estudio traslacional para la innovación diagnóstica con resonancia magnética y para el entendimiento de los mecanismos reguladores”. Financiado por Instituto de Salud Carlos III y cofinanciado por los fondos FEDER. IP: Vicente Bodí Peris. 2015-2017.

3. Proyecto PIE15/0013 “A multidisciplinary project to advance in basic mechanisms, diagnosis, prediction, and prevention of cardiac damage in reperfused acute myocardial infarction”. Financiado por Instituto de Salud Carlos III y cofinanciado por los fondos FEDER. IP: Vicente Bodí Peris. 2016-2018.

4. Proyecto PI17/01836 “Estudio multidisciplinar de la obstrucción microvascular y su reparación tras un infarto agudo de miocardio: de la arteria coronaria a la microcirculación. foco en el factor VGFA165b”. Financiado por Instituto de Salud Carlos III y cofinanciado por los fondos FEDER. IP: Vicente Bodí Peris. 2018-2020.

ANEXO VI: Comités de ética

GENERALITAT VALENCIANA

Hospital Clínic Universitari

DEPARTAMENT CLÍNIC MALVA-ROSA

INFORME DEL COMITE ETICO DE INVESTIGACION CLINICA DEL HOSPITAL CLINIC UNIVERSITARI DE VALENCIA

Dña. Cristina Gomis Gozalbo, Secretaria del Comité Ético de Investigación Clínica del Hospital Clínic Universitari de Valencia

CERTIFICA

Que en este Comité, en su reunión de fecha 25 de febrero de 2016, y según consta en el acta de la misma, se han analizado los aspectos éticos y científicos relacionados al proyecto de investigación que lleva por título:

A multidisciplinary project to advance in basic mechanisms, diagnosis, prediction, and prevention of cardiac damage in reperfused acute myocardial infarction.

Mismo que será llevado a cabo en el Servicio de Cardiología y cuyo investigador principal es el Dr. Vicent Bodí Peris, acordando que reúne las características adecuadas referentes a información a los pacientes y cumplimiento de los criterios éticos para la investigación médica y biomédica establecidos en la ***Declaración de Helsinki*** (Junio 1964, Helsinki, Finlandia) de la Asamblea Médica Mundial, y sus revisiones (Octubre 1975, Tokio, Japón), (Octubre 1983, Ve necia, Italia), (Septiembre 1989, Hong Kong), (Octubre 1996, Somerset West, Sudáfrica), (Octubre 2000, Edimburgo), (Octubre 2008 Seúl, Corea) y (Octubre 2013 Fortaleza, Brasil) y en la ***Declaración Universal sobre el Genoma Humano y los Derechos del Hombre de la UNESCO*** y los acuerdos del ***Protocolo Adicional del Consejo de Europa para la protección de los Derechos del Hombre y de la dignidad del ser humano frente a la aplicaciones de la biología y de la medicina*** (París 12-1-1998, ratificado el 23-7-1999).

Lo que certifico a efectos oportunos de la convocatoria de Ayudas a Proyectos en Investigación en Salud del Instituto de Salud Carlos III.

Valencia, 25 de febrero de 2016.

Fdo. : Dra. Dña. Cristina Gomis Gozalbo
Secretaria del Comité Ético de Investigación Clínica

GENERALITAT VALENCIANA

Hospital Clínic Universitari

DEPARTAMENT CLÍNIC MALVA-ROSA

Vicent Bodí Peris
Servicio de CArdiología

Valencia, 1 de marzo de 2016.

Estimado Dr. Bodí,

El motivo de la presente es informarle que en la pasada reunión del Comité de Ética del Hospital Clínico Universitario de Valencia de fecha 25 de febrero de 2016, ha sido evaluado el proyecto titulado "A multidisciplinary project to advance in basic mechanisms, diagnosis, prediction, and prevention of cardiac damage in reperfused acute myocardial infarction." del cual usted es el investigador principal.

En dicha evaluación, se acordó informar favorablemente.

Así mismo, se le informa que la legislación vigente en investigaciones donde se va a proceder a la toma de muestras de pacientes, es la Ley 14/2007 de 3 de julio, de Investigación Biomédica y estas investigaciones deberán cumplir dicha normativa.

En caso de requerir información adicional, no dude en ponerse en contacto con la secretaría del Comité.

Sin otro particular, reciba un cordial saludo.

Dr. Antonio Peláez Hernández
Presidente del Comité Ético de Investigación Clínica

GENERALITAT VALENCIANA
CONSELLERIA DE SANIDAD UNIVERSAL Y SALUD PÚBLICA

Hospital Clínic Universitari

DEPARTAMENT CLÍNIC MALVA-ROSA

INFORME DEL COMITE ETICO DE INVESTIGACION CON MEDICAMENTOS DEL HOSPITAL CLINICO UNIVERSITARIO DE VALENCIA

Doña Marina Soro Domingo, Presidenta del Comité Ético de Investigación con Medicamentos del Hospital Clínico Universitario de Valencia

CERTIFICA

Que este Comité, en su reunión de Comisión Permanente de fecha 29 de agosto de 2019, ha analizado los aspectos éticos y científicos relacionados al proyecto de investigación:

Nº DE ORDEN: 2019/160
TITULO: Caracterización tisular en el infarto de miocardio con elevación del segmento ST: registro multicéntrico de pacientes estudiados con resonancia magnética cardiaca.
PROTOCOLO: Versión: 3 Fecha: 5 de Agosto de 2019
HIP/CI: Aceptada la exención de HIP/CI
INVESTIGADOR: VICENT BODÍ PERIS
GRUPO DE INVESTIGACIÓN/SERVICIO: CARDIOLOGÍA
PETICIÓN DE AYUDA A LA INVESTIGACIÓN: INTERNO-COLABORACIÓN

Emite un **DICTAMEN FAVORABLE** para la realización de dicho proyecto este centro.

Este Comité acepta que dicho estudio sea realizado por el DR. VICENT BODÍ PERIS en el Servicio de Cardiología, como investigador principal, acordando que reúne las características adecuadas referentes a información a los pacientes y cumplimiento de los criterios éticos para la investigación biomédica.

Lo que certifico a efectos oportunos.

Valencia, 29 de agosto de 2019

Fdo. : Doña Marina Soro Domingo